SUPPORTING INFORMATION

Experimental and Theoretical Elucidation of SPAAC Kinetics for Strained Alkyne-Containing Cycloparaphenylenes

Julia M. Fehr,[a] Nathalie Myrthil,[b] Anna L. Garrison,[a] Tavis W. Price,[a] Steven A. Lopez,*[b] and Ramesh Jasti*[a]

[a]Department of Chemistry and Biochemistry, Materials Science Institute, and Knight Campus for Accelerating Scientific Impart, University of Oregon, Eugene, Oregon 97403, United States.
[b]Department of Chemistry and Chemical Biology, Northeastern University, Boston, Massachusetts 02115, United States.

Corresponding authors: s.lopez@northeastern.edu and rjasti@uoregon.edu.

TABLE OF CONTENTS

1. Experimental details

Unless otherwise noted, commercially available materials were used without purification. Compounds **[9+1]CPP**, **[11+1]CPP**, **[11+1]CPP-BnAz**, **3**, **4**, **5**, **7**, and Pd Sphos GIII were prepared according to the literature.[1–3] Moisture and oxygen sensitive reactions were carried out in flame-dried glassware and under an inert atmosphere of purified nitrogen using syringe/septa technique. Tetrahydrofuran (THF), dimethylformamide (DMF), and 1,4-dioxane were dried by filtration through alumina according to the methods described by Grubbs.[4] Thin-layer chromatography (TLC) was performed on aluminium plates coated with 0.20 mm thickness of Silica Gel 60 F254 (Macherey-Nagel). Developing plates were visualized using UV light at wavelengths of 254 and 365 nm. Silica column chromatography was conducted with Zeochem Zeoprep n60 Eco 40-63 μm silica gel. Alumina column chromatography was conducted with SorbTech basic alumina (pH 10), Act. II-III, 50-200 μm. ^{1}H and ^{13}C NMR spectra were recorded on either a Bruker Avance III HD 500 (^{1}H: 500 MHz, ^{13}C: 126 MHz) or Bruker Avance III HD 600 MHz (^{1}H: 600 MHz, ^{13}C: 151 MHz) NMR spectrometer. The samples were measured at 25 °C. The chemical shifts (δ) were reported in parts per million (ppm) and were referenced to the residual protio-solvent (CD$_2$Cl$_2$, ^{1}H: δ = 5.32 ppm and ^{13}C: δ = 53.84 ppm; DMSO-d$_6$, ^{1}H: δ = 2.50 ppm and ^{13}C: δ = 39.52 ppm) or to tetramethylsilane (for CDCl$_3$, TMS, δ = 0.00 ppm). Coupling constants (J) are given in Hz and the apparent resonance multiplicity is reported as s (singlet), d (doublet), t (triplet), q (quartet), dd (doublet of doublets) or m (multiplet). For all [n+1]CPPs and [n+1]CPP-BnAz, ^{1}H NMR spectra were collected in DMSO-d$_6$ as a point of reference for rate experiments, and in some cases an additional ^{1}H spectrum was collected in CD$_2$Cl$_2$. ^{13}C NMRs for these compounds were attempted in DMSO-d$_6$, but in cases of limited solubility, the ^{13}C NMRs were collected in CD$_2$Cl$_2$ instead. The SPAAC reaction yields reported in Scheme 3 of the paper were determined *in-situ* without purification in DMSO-d$_6$ doped with dimethyl sulfone internal standard (14.5 mM, preparation described in section 5 of this document). Infrared absorption (IR) spectra were recorded on a Thermo Scientific Nicolet 6700 spectrometer equipped with a diamond crystal Smart ATR or as a cast film on KCl plates (CH$_2$Cl$_2$ as drop-casting solvent). Characteristic IR absorptions are reported in cm^{-1} and denoted as strong (s), medium (m), and weak (w). UV/Vis absorption and fluorescence spectra were recorded on an Agilant Cary 100 spectrophotometer and a Horiba Jobin Yvon Fluoromax-4 Fluorimeter, respectively. All measurements were carried out under ambient conditions in QS Quartz Suprasil cells (10 mm light path). The absorption maxima (λ_{max}) are reported in nm and the extinction coefficient (ε) in M^{-1} cm^{-1}.

2. Synthesis
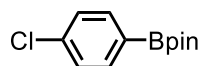
Compound 10. 1-bromo-4-chlorobenzene (7.00 g, 36.6 mmol, 1.00 equiv.) was dissolved in THF (91 mL, 0.4 M) and the solution cooled to −78 °C over the course of 45 minutes. *n*-Butyllithium (2.5 M in hexanes, 15.4 mL, 38.3 mmol, 1.05 equiv.) was added dropwise. After allowing the reaction mixture to stir for 10 minutes, 2-isopropoxy-4,4,5,5-tetramethyl-1,3,2-dioxaborolane (9.70 mL, 47.5 mmol, 1.3 equiv.) was added dropwise. The reaction mixture was allowed to stir for 30 minutes after the addition at −78 °C, at which point it was allowed to warm to room temperature over the course of 30 minutes. Deionized water (25 mL) was added. The resulting mixture was concentrated (ca. 100 mL) *via* rotary evaporator and extracted with EtOAc (3 × 100 mL). The combined organic layers were washed with brine (3 × 100 mL), dried over sodium sulfate, filtered, and concentrated *via* rotary evaporator to yield the crude product as an off-white low-melting solid. The crude product was purified *via* automated column chromatography (SiO$_2$, 0 − 42% CH$_2$Cl$_2$/hexanes) yielding a white solid (3.92 g, 16.4 mmol, 45%). R_f = 0.63 (SiO$_2$, 40% CH$_2$Cl$_2$/hexanes; product slowly decomposes on silica); ^{1}H NMR (500 MHz, Chloroform-*d*) δ 7.73 (d, *J* = 8.1 Hz, 2H), 7.34 (d, *J* = 8.2 Hz, 2H), 1.33 (s, 12H) ppm; ^{13}C NMR (126 MHz, Chloroform-*d*) δ 137.5, 136.1, 128.0, 84.0, 24.9 ppm (5 signals, one signal does not appear); IR (ATR) ṽ 3053 (w), 3007 (w), 2974 (m), 1595 (s), 1564 (w), 1464 (w), 1394 (m), 1357 (s), 1331 (s), 1260 (m), 1138 (s), 1091 (s), 1014 (m), 852 (m), 823 (s), 725 (s), 647 (s); HRMS (ASAP, positive mode) *m/z* calcd for C$_{12}$H$_{17}$BO$_2$Cl: 239.1010 [M+H]$^+$, found 239.1025.
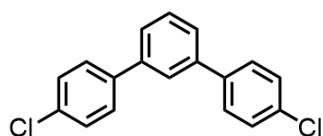
Compound 11. **10** (3.11 g, 13.0 mmol, 2.05 equiv.) and Pd(dppf)Cl$_2$ (0.519 g, 0.64 mmol, 0.1 equiv.) were dissolved in deoxygenated 1,4-dioxane (211 mL, 0.03 M, sparged with N$_2$ for one hour prior to use). 1,3-dibromobenzene (0.77 mL, 6.4 mmol, 1.0 equiv.) was added to the reaction mixture via syringe. The resulting solution was sparged with N$_2$ for an additional 15 minutes. The reaction mixture was heated to 80 °C over the course of 15 minutes. Deoxygenated aqueous K$_3$PO$_4$ solution (21 mL, 2.0 M, sparged with N$_2$ for one hour prior to use) was added via syringe. The reaction mixture was allowed to stir at 80 °C overnight. It was then cooled to room temperature and filtered through a plug of Celite (CH$_2$Cl$_2$). The filtrate was dried over sodium sulfate and concentrated to yield the crude product as a brown solid. The crude product was purified *via* a short plug (SiO$_2$, 2% EtOAc/hexanes), then triturated with methanol to yield a white solid (0.91 g, 3.1 mmol, 48%). R_f = 0.67 (SiO$_2$, 30% CH$_2$Cl$_2$/hexanes); ^{1}H NMR (500 MHz, Chloroform-*d*) δ 7.69 (t, *J* = 1.9 Hz, 1H), 7.56 – 7.47 (m, 7H), 7.42 (d, *J* = 8.5 Hz, 4H) ppm; ^{13}C NMR (126 MHz, Chloroform-*d*) δ 140.66, 139.36, 133.63, 129.41, 128.97, 128.43, 126.21, 125.68 ppm (8 signals); IR (ATR) ṽ 3023 (w), 2911 (w), 1602 (m), 1494 (m), 1465 (m), 1106 (s), 1011 (s), 834 (s), 788 (s), 698 (s); HRMS (ASAP, positive mode) *m/z* calcd for C$_{18}$H$_{12}$Cl$_2$: 298.0316 [M]$^+$, found 298.0321.
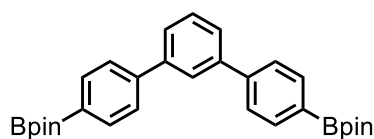
Compound 2. **11** (0.500 g, 1.7 mmol, 1.00 equiv), KOAc (1.08 g, 11 mmol, 6.6 equiv), palladium acetate (0.002 g, 0.008 mmol, 0.005 equiv.), SPhos (0.086 g, 0.21 mmol, 0.125 equiv.), and bis(pinacolato)diboron (1.697 g, 6.7 mmol, 4.0 equiv) were dissolved in 1,4-dioxane (9 mL, 0.19 M) and the resulting reaction mixture was sparged with N_2 for 15 minutes. The reaction mixture was heated to 90 °C and allowed to stir overnight. The reaction mixture was cooled to room temperature. Ethyl acetate was added and the reaction mixture was sonicated. It was then filtered through a plug of Celite (EtOAc). The filtrate was concentrated to yield the crude product as a brown solid. Trituration with methanol yielded the final product as a white solid (0.660 g, 1.36 mmol, 82%). R_f = 0.52 (SiO$_2$, 100% CH$_2$Cl$_2$, product is slowly decomposing on silica); ^{1}H NMR (500 MHz, Chloroform-*d*) δ 7.90 (d, *J* = 7.9 Hz, 4H), 7.83 (t, *J* = 1.9 Hz, 1H), 7.66 (d, *J* = 8.1 Hz, 4H), 7.60 (d, *J* = 7.5 Hz, 2H), 7.51 (t, *J* = 8.1 Hz, 1H), 1.37 (s, 24H) ppm; ^{13}C NMR (126 MHz, Chloroform-*d*) δ 143.80, 141.65, 135.31, 129.22, 126.58, 126.50, 126.25, 83.84, 24.89 ppm (9 signals, one signal does not appear); IR (ATR) ṽ 3043 (w), 3031 (w), 2980 (m), 1608 (m), 1550 (w), 1516 (w), 1465 (w), 1398 (m), 1358 (s), 1322 (s), 1270 (m), 1142 (s), 1091 (s), 1018 (m), 962 (s), 858 (s), 829 (m), 795 (s), 741 (s), 699 (m), 655 (s); HRMS (ASAP, positive mode) *m/z* calcd for C$_{30}$H$_{37}$B$_2$O$_4$: 483.2878 [M+H]$^+$, found 483.2911.
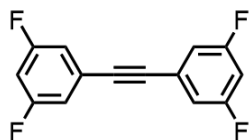

Compound 6. Palladium acetate (0.056 g, 0.25 mmol, 0.02 equiv.), triphenylphosphine (0.164 g, 0.63 mmol, 0.05 equiv.), and copper iodide (0.119 g, 0.63 mmol, 0.05 equiv.) were dissolved in wet acetonitrile (62.5 mL, 0.2 M, sparged with N_2 for 30 minutes prior to use) and the resulting mixture was sparged with nitrogen for an additional 30 minutes. Triethylamine (5.23 mL, 37.5 mmol, 3 equiv.), 3,5-difluoroiodobenzene (1.5 mL, 12.5 mmol, 1 equiv.), and calcium carbide (2.40 g, 37.5 mmol, 3 equiv.) were added in rapid succession. The reaction mixture was stirred at room temperature for 24 hours. Additional portions of calcium carbide (0.200 g, 3.1 mmol, 0.25 equiv.), palladium acetate (0.020 g, 0.09 mmol, 0.007 equiv.), and deionized water (500 μL), were added to drive the reaction to completion. After two additional hours, dichloromethane was added and the reaction mixture was sonicated. It was then filtered through a plug of Celite (CH$_2$Cl$_2$). The filtrate was concentrated to yield the crude product as a dark brown solid. The crude product was purified first *via* a short plug (SiO$_2$, 100% CH$_2$Cl$_2$) and then more vigorously *via* automated column chromatography (SiO$_2$, 100% hexanes) to yield a white solid (1.28 g, 5.13 mmol, 82%). R_f = 0.52 (SiO$_2$, 100% hexanes); ^{1}H NMR (500 MHz, Chloroform-*d*) δ 7.07 – 6.99 (m, 4H), 6.83 (tt, *J* = 8.9, 2.4 Hz, 2H) ppm; ^{13}C NMR (126 MHz, Chloroform-*d*) δ 162.79 (dd, *J* = 249.5, 13.3 Hz), 125.01 (t, *J* = 11.6 Hz), 114.76 (dd, *J* = 19.9, 6.8 Hz), 105.15 (t, *J* = 25.3 Hz), 88.79 (t, *J* = 3.9 Hz) (5 signals); ^{19}F NMR (471 MHz, Chloroform-*d*) δ -109.15 − -109.23 (m) ppm; IR (ATR) ṽ

3091 (w), 1614 (s), 1583 (s), 1507 (w), 1479 (m), 1428 (s), 1366 (s), 1215 (m), 1179 (s), 1121 (s), 989 (s), 850 (s), 666 (s); HRMS (ASAP, positive mode) m/z calcd for $C_{14}H_7F_4$: 251.0484 $[M+H]^+$, found 251.0509.
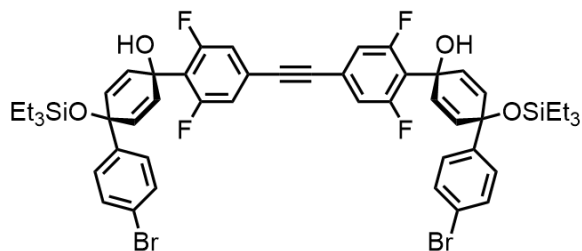
Compound 8. **6** (1.88 g, 7.53 mmol, 1 equiv.) was dissolved in THF (79 mL, 0.2 M) and the solution cooled to −78 °C over the course of 45 minutes. *n*-Butyllithium (2.4 M in hexanes, 6.43 mL, 15.4 mmol, 2.05 equiv.) was added dropwise, turning the solution an opaque gray. The reaction mixture was allowed to stir for ten minutes. Then, **7** (6.00 g, 15.8 mmol, 2.1 equiv., dissolved in 5 mL THF) was added dropwise, turning the solution a cloudy yellow. The reaction mixture was allowed to stir for an additional ten minutes at −78 °C. The reaction mixture was then transferred to a 0 °C bath and allowed to stir for 40 minutes; the mixture turned a clear turquoise over this time period. Deionized water (50 mL) was added. The resulting mixture was concentrated (ca. 75 mL) *via* rotary evaporator and extracted with EtOAc (3 × 100 mL). The combined organic layers were washed with brine (3 × 100 mL), dried over sodium sulfate, filtered, and concentrated *via* rotary evaporator to yield the crude product as an orange low-melting solid. The crude product was purified *via* automated column chromatography (40 − 80% CH_2Cl_2/hexanes), followed by recrystallization in minimal CH_2Cl_2 and hexanes to yield a white crystalline solid (2.34 g, 2.3 mmol, 31%). R_f = 0.33 (SiO$_2$, 80% CH_2Cl_2/hexanes); ^{1}H NMR (500 MHz, Methylene Chloride-d_2) δ 7.39 (d, J = 8.2 Hz, 4H), 7.25 (d, J = 8.2 Hz, 4H), 7.15 − 7.07 (m, 4H), 6.33 (dt, J = 10.4, 2.9 Hz, 4H), 5.96 (d, J = 9.8 Hz, 4H), 2.74 (t, J = 2.6 Hz, 2H), 1.00 (t, J = 7.9 Hz, 18H), 0.71 (q, J = 7.9 Hz, 12H) ppm; ^{13}C NMR (126 MHz, Methylene Chloride-d_2) δ 160.85 (dd, J = 250.7, 9.2 Hz), 144.97, 133.42, 131.49, 128.87 (t, J = 2.3 Hz), 127.87, 124.29 (t, J = 13.5 Hz), 121.95 (t, J = 13.8 Hz), 121.26, 116.49 (dd, J = 22.0, 7.3 Hz), 89.25 (t, J = 3.5 Hz), 71.56, 67.86 (t, J = 1.9 Hz), 7.22, 6.74 ppm (15 signals); ^{19}F NMR (471 MHz, Chloroform-d) δ -106.97 − -107.06 (m) ppm; IR (ATR) ṽ 3596 (w), 3091 (w), 3039 (w), 2953 (m), 2910 (w), 2874 (m), 1625 (m), 1585 (w), 1550 m), 1456 (m), 1417 (m), 1194 (m), 1164 (m), 1107 (w), 1075 (m), 1004 (s), 970 (m), 937 (m), 856 (s), 709 (s), 601 (s); HRMS (ASAP, positive mode) m/z calcd for $C_{50}H_{52}O_4F_4Si_2Br_2$: 1006.1707 $[M]^+$, found 1006.1714.
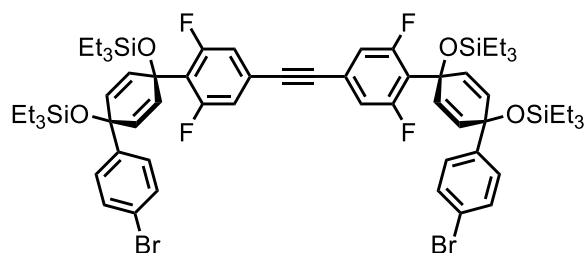
Compound 1. **8** (2.70 g, 2.67 mmol, 1.0 equiv.) and imidazole (0.820 g, 12 mmol, 4.5 equiv.) were dissolved in *N,N*-dimethylformamide (46.8 mL, 0.2 M). Chlorotriethylsilane (1.57 mL, 9.36 mmol, 3.5 equiv.) was added *via* syringe. The reaction mixture was heated to 40 °C and allowed to stir overnight. It was then cooled to room temperature and saturated aqueous solution of sodium bicarbonate (150 mL) was added. The reaction was extracted with ethyl acetate (3 × 100 mL). The combined organic layers were then washed with aqueous 5% LiCl (5 × 100 mL), washed with brine (3 × 100 mL), dried over sodium sulfate, filtered, and concentrated *via* rotary evaporator to yield the crude product as a white solid. The crude product was purified *via* automated column chromatography (SiO$_2$, 0 – 20% CH$_2$Cl$_2$/hexanes) to yield a white solid (2.73 g, 2.22 mmol, 83%). R_f = 0.48 (20% CH$_2$Cl$_2$/hexanes); ^{1}H NMR (500 MHz, Chloroform-*d*) δ 7.32 (d, *J* = 8.6 Hz, 4H), 7.14 (d, *J* = 8.6 Hz, 4H), 7.04 – 6.96 (m, 4H), 6.39 (dt, *J* = 10.3, 3.2 Hz, 4H), 5.89 (d, *J* = 10.1 Hz, 4H), 0.96 (t, *J* = 7.9 Hz, 18H), 0.90 (t, *J* = 7.9 Hz, 18H), 0.66 (q, *J* = 7.9 Hz, 12H), 0.56 (q, *J* = 7.9 Hz, 12H) ppm; ^{13}C NMR (126 MHz, Chloroform-*d*) δ 160.44 (dd, *J* = 252.6, 9.3 Hz), 144.77, 131.96, 131.10, 129.63 (t, *J* = 2.8 Hz), 127.29, 123.64 (t, *J* = 13.2 Hz), 123.00 (t, *J* = 13.7 Hz), 120.90, 115.95 (dd, *J* = 20.9, 7.1 Hz), 89.02 (t, *J* = 3.1 Hz), 71.15, 69.35 (t, *J* = 2.7 Hz), 7.04, 6.80, 6.38, 6.18 ppm (17 signals); ^{19}F NMR (471 MHz, Chloroform-*d*) δ -104.72 (d, *J* = 10.2 Hz) ppm; IR (ATR) ṽ 3041 (w), 2951 (m), 2909 (w), 2873 (m), 1622 (m), 1549 (m), 1476 (m), 1455 (m), 1414 (m), 1238 (m), 1193 (m), 1173 (w), 1161 (w), 1108 (m), 1071 (s), 1017 (s), 953 (s), 855 (s), 829 (m), 733 (s), 711 (s), 603 (s); HRMS (ASAP, positive mode) *m/z* calcd for C$_{62}$H$_{80}$O$_4$F$_4$Si$_4$Br$_2$: 1234.3437 [M]$^+$, found 1234.3463.
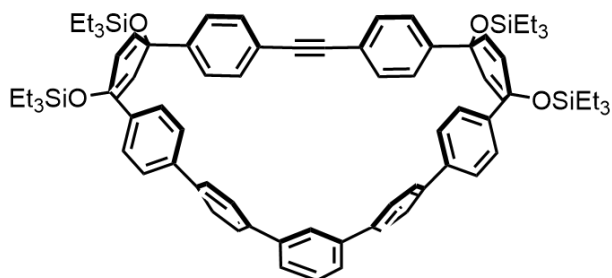

Compound 12. **2** (0.150 g, 0.311 mmol, 1.1 equiv.), **3** (0.33 g, 0.283 mmol, 1.0 equiv.), and Pd SPhos Gen III (0.023 g, 0.028 mmol, 0.1 equiv.) were dissolved in 1,4-dioxane (445 mL, 0.0007 M, sparged with N$_2$ for one hour prior to use). The resulting solution was sparged with N$_2$ for an additional 15 minutes. The reaction mixture was heated to 80 °C over the course of 15 minutes. Deoxygenated aqueous K$_3$PO$_4$ solution (45 mL, 2.0 M, sparged with N$_2$ for one hour prior to use) was added via syringe. The reaction mixture was allowed to stir at 80 °C overnight. It was then cooled to room temperature and the aqueous layer was removed. Concentration *via* rotary evaporator yielded the crude product as a brown solid, which was redissolved in CH$_2$Cl$_2$, dried over sodium sulfate, and reconcentrated. The crude product was purified *via* automated column chromatography (SiO$_2$, 0 – 30% CH$_2$Cl$_2$/hexanes). This was followed by sonication in ethanol and vacuum filtration to yield the final product as a white solid (0.0892 g, 0.072 mmol, 26%). R_f = 0.34 (30% CH$_2$Cl$_2$/hexanes); ^{1}H NMR (500 MHz, Methylene Chloride-*d$_2$*) δ 7.59 – 7.52 (m, 6H), 7.51 – 7.45 (m, 5H), 7.42 (d, *J* = 8.4 Hz, 4H), 7.30 (d, *J* = 8.4 Hz, 4H), 7.23 (d, *J* = 8.4 Hz, 4H), 7.14 (d, *J* = 8.4 Hz, 4H), 7.10 (t, *J* = 1.9 Hz, 1H), 6.01 (d, *J* = 10.1 Hz, 4H), 5.90 (d, *J* = 10.1 Hz, 4H), 0.93 – 0.83 (m, 36H), 0.63 – 0.51 (m, 24H); ^{13}C NMR (126 MHz, CD$_2$Cl$_2$) δ 146.52, 145.06, 142.59, 141.72, 140.14, 140.12, 134.08, 132.51, 131.64, 131.54, 129.58, 128.74, 127.61, 127.29, 126.78, 126.58,

124.41, 122.41, 89.46, 72.07, 72.00, 7.24, 7.21, 6.86, 6.80 (25 signals); IR (ATR) ṽ 3029 (w), 2951 (m), 2910 (w), 2873 (m), 1600 (w), 1558 (w), 1505 (w), 1456 (w), 1238 (w), 1172 (w), 1111 (m), 1074 (s), 1003 (m), 960 (s), 859 (m), 820 (m), 792 (m), 719 (s); HRMS (ASAP, positive mode) m/z calcd for $C_{80}H_{96}O_4Si_4$: 1232.6386 [M]$^+$, found 1232.6281.
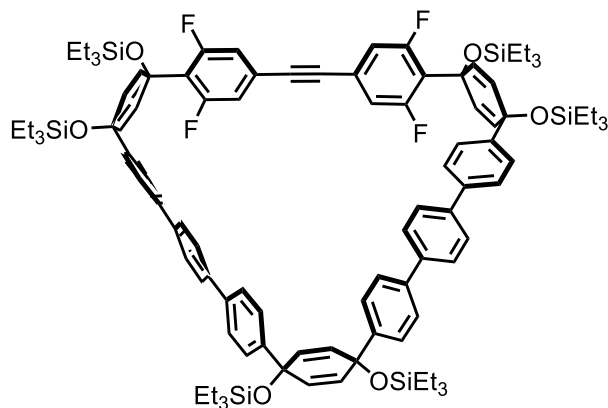

Compound 9. **1** (0.460 g, 0.371 mmol, 1.0 equiv.), **5** (0.367 g, 0.408 mmol, 1.1 equiv.), and Pd SPhos Gen III (0.029 g, 0.037 mmol, 0.1 equiv.) were dissolved in 1,4-dioxane (464 mL, 0.0008 M, sparged with N_2 for one hour prior to use). The resulting solution was sparged with N_2 for an additional 15 minutes. The reaction mixture was heated to 80 °C over the course of 15 minutes. Deoxygenated aqueous K_3PO_4 solution (46.4 mL, 2.0 M, sparged with N_2 for one hour prior to use) was added via syringe. The reaction mixture was allowed to stir at 80 °C for 2 hours. It was then cooled to room temperature and filtered through a plug of Celite (CH_2Cl_2) and dried over sodium sulfate. Concentration *via* rotary evaporator yielded the crude product as a brown solid. The crude product was purified *via* automated column chromatography (0 − 33% CH_2Cl_2/hexanes). The resultant solid was washed with pentanes and ethanol to yield the final product as a white solid (0.239 g, 0.139 mmol, 37%). R_f = 0.57 (40% CH_2Cl_2/hexanes); ^{1}H NMR (500 MHz, Chloroform-*d*) δ 7.64 (d, *J* = 8.2 Hz, 4H), 7.61 (d, *J* = 8.2 Hz, 4H), 7.55 (d, *J* = 8.1 Hz, 4H), 7.50 (d, *J* = 8.1 Hz, 4H), 7.40 (dd, *J* = 13.1, 8.1 Hz, 8H), 7.08 − 7.00 (m, 4H), 6.42 (dt, *J* = 10.3, 3.1 Hz, 4H), 6.04 (s, 4H), 5.96 (d, *J* = 9.8 Hz, 4H), 1.04 − 0.94 (m, 36H), 0.91 (t, *J* = 7.9 Hz, 18H), 0.75 − 0.61 (m, 24H), 0.57 (q, *J* = 7.9 Hz, 12H); ^{13}C NMR (126 MHz, Chloroform-*d*) δ 160.53 (dd, *J* = 252.6, 9.1 Hz), 145.01, 144.81, 139.66, 139.39, 139.30, 139.14, 132.31, 131.56, 129.14 (t, *J* = 3.1 Hz), 127.31, 127.21, 126.65, 126.52, 126.47, 125.93, 123.58 (t, *J* = 13.2 Hz), 123.28 (t, *J* = 13.7 Hz), 116.04 (dd, *J* = 21.4, 6.6 Hz), 89.02 (t, *J* = 2.7 Hz), 71.69, 71.36, 69.43 (t, *J* = 2.7 Hz), 7.11, 7.08, 6.81, 6.52, 6.45, 6.20; ^{19}F NMR (471 MHz, Chloroform-*d*) δ -104.52 (d, *J* = 10.4 Hz); IR (ATR) ṽ 3028 (w), 2951 (m), 2909 (w), 2874 (m), 1619 (m), 1550 (m), 1485 (m), 1456 (m), 1412 (m), 1237 (m), 1193 (m), 1173 (m), 1114 (m), 1066 (s), 1004 (s), 952 (s), 857 (s), 812 (s), 716 (s); HRMS (ASAP, positive mode) m/z calcd for $C_{104}H_{130}O_6 F_4Si_6$: 1718.8419 [M]$^+$, found 1718.8438.
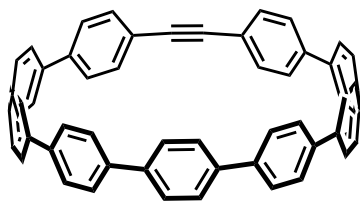
[9+1]CPP. The synthesis of [9+1]CPP has been described previously.[2] As our kinetics experiments were performed in *d*-DMSO, we include here NMR information for this compound in *d*-DMSO; ^{1}H NMR (600 MHz, DMSO-d_6) δ 7.70 – 7.63 (m, 32H), 7.39 (d, *J* = 8.2 Hz, 4H); ^{13}C NMR (126 MHz, DMSO) δ 139.16, 137.79, 137.36, 137.27, 137.15, 136.99, 136.84, 131.00, 127.21, 127.17, 127.15, 126.68, 122.17, 98.76 (14 signals, five unaccounted for).
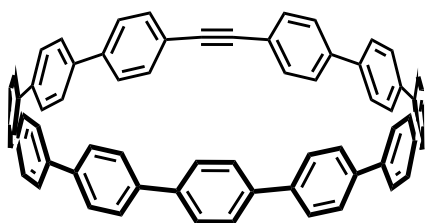

[11+1]CPP. The synthesis of [11+1]CPP has been described previously.[2] As our kinetics experiments were performed in *d*-DMSO, we include here NMR information for this compound in *d*-DMSO; ^{1}H NMR (500 MHz, DMSO-d_6) δ 7.76 – 7.69 (m, 40H), 7.48 (d, *J* = 8.2 Hz, 4H); ^{13}C NMR (126 MHz, DMSO) δ 139.24, 138.10, 137.71, 137.55, 137.45, 137.42, 137.19, 131.29, 127.14, 127.10, 126.70, 121.96, 96.75 (13 signals, 10 unaccounted for).
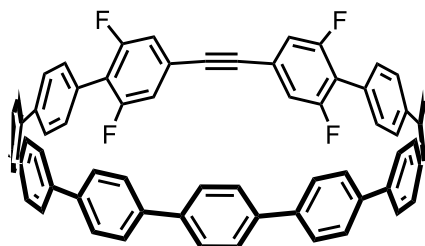

fluor[11+1]CPP. *Deprotection of silyl ether groups.* **9** (0.100 g, 0.0581 mmol, 1.0 equiv.) was dissolved in tetrahydrofuran (7.3 mL, 0.008 M) at room temperature. Acetic acid (0.17 mL, 2.91 mmol, 50 equiv.) was added dropwise, closely followed by dropwise addition of tetra-*n*-butylammonium fluoride (1 M solution in tetrahydrofuran, 1.45 mL, 1.45 mmol, 25 equiv.). The reaction mixture was allowed to stir for 18 hours at room temperature. Deionized water (15 mL) was added. The organic layer was almost completely removed *via* rotary evaporator, and the resultant white suspension was vigorously sonicated. The now-deprotected intermediate (a white solid) was isolated *via* vacuum filtration and thorough washing with DI water and dichloromethane. *Reductive aromatization*. SnCl₂·2H₂O (0.181 g, 0.8 mmol, 1.0 equiv. with respect to HCl) was dissolved in tetrahydrofuran (20 mL, 0.040 M). HCl (0.13 mL, 1.6 mmol, 2.0 equiv with respect to SnCl₂·2H₂O) was added and the reaction was allowed to stir for 30 minutes. Concurrently in a separate flask, the deprotected macrocycle (0.060, 0.0581 mmol, 1.0 equiv.)

was dissolved in tetrahydrofuran (8 mL, 0.0073 M). After the 30 minutes had elapsed, prepared H_2SnCl_4 solution (8.72 mL, 0.349 mmol, 0.040 M, 6 equiv.) was added to the solution of deprotected macrocycle. The reaction was allowed to stir for 1.5 hours. The reaction was diluted with hexanes (15 mL) then subjected directly to purification *via* a short plug (basic AlO_x, 50% CH_2Cl_2/hexanes). Subsequent sonication in acetone and vacuum filtration yielded the final product as a white solid (0.030 g, 0.032 mmol, 55% over two steps); R_f = 0.60 (50% CH_2Cl_2/hexanes, compound is slowly decaying on silica). ^1H NMR (500 MHz, Methylene Chloride-d_2) δ 7.72 – 7.58 (m, 34H), 7.52 (d, J = 8.2 Hz, 4H), 7.04 (d, J = 8.4 Hz, 4H); ^1H NMR (500 MHz, DMSO-d_6) δ 7.76 (td, J = 15.9, 13.8, 8.2 Hz, 34H), 7.50 (d, J = 8.1 Hz, 4H), 7.41 (d, J = 8.6 Hz, 4H); ^{19}F NMR (471 MHz, Methylene Chloride-d_2) δ -114.18 (d, J = 9.9 Hz); ^{19}F NMR (471 MHz, DMSO-d_6) δ -113.88 (d, J = 6.1 Hz); ^{13}C NMR (126 MHz, Methylene Chloride-d_2) δ 160.30 (dd, J = 249.9, 8.5 Hz), 141.05, 139.17, 139.14, 139.12, 138.96, 138.86, 138.79, 138.56, 131.33 (t, J = 2.8 Hz), 128.14, 127.96, 127.87, 127.83, 127.75, 127.71, 127.63, 127.55, 127.32, 125.00 (t, J = 12.8 Hz), 119.00 (t, J = 17.6 Hz), 115.35 (dd, J = 20.2, 7.3 Hz), 96.76 (t, J = 3.5 Hz) (23 signals); IR (ATR) ṽ 3025 (w), 1617 (w), 1597 (w), 1556 (w), 1483 (s), 1393 (w), 1363 (w), 1195 (m), 1177 (m), 1021 (m), 1001 (m), 809 (s), 747 (s); HRMS (ESI, positive mode) *m/z* calcd for $C_{68}H_{40}F_4$: 932.3066 $[M]^+$, found 932.3083.
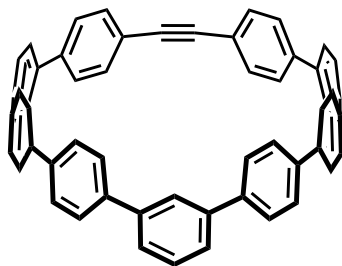
m[9+1]CPP. *Deprotection of silyl ether groups.* **12** (0.060 g, 0.0486 mmol, 1.0 equiv.) was dissolved in tetrahydrofuran (6.1 mL, 0.008 M) at room temperature. Tetra-*n*-butylammonium fluoride (1 M solution in tetrahydrofuran, 0.21 mL, 0.21 mmol, 4.4 equiv.) was added dropwise to the solution. The reaction mixture was allowed to stir for 1 hour at room temperature. Deionized water (5 mL) was added. The organic layer was almost completely removed *via* rotary evaporator, and the resultant white suspension was vigorously sonicated. The now-deprotected intermediate (a white solid) was isolated *via* vacuum filtration and thorough washing with DI water and dichloromethane. *Reductive aromatization*. $SnCl_2 \cdot 2H_2O$ (0.181 g, 0.8 mmol, 1.0 equiv. with respect to HCl) was dissolved in tetrahydrofuran (20 mL, 0.040 M). HCl (0.13 mL, 1.6 mmol, 2.0 equiv with respect to $SnCl_2 \cdot 2H_2O$) was added and the reaction was allowed to stir for 30 minutes. Concurrently in a separate flask, deprotected OH-*m*[9+1]macrocycle (0.038 g, 0.0486 mmol, 1.0 equiv.) was dissolved in tetrahydrofuran (8 mL, 0.006 M). After the 30 minutes had elapsed, prepared H_2SnCl_4 solution (2.7 mL, 0.11 mmol, 0.040 M, 2.2 equiv.) was added to the solution of deprotected OH-*m*[9+1]macrocycle. The reaction was allowed to stir for 1 hour. The reaction was diluted with hexanes (20 mL) then subjected directly to purification *via* a short plug (basic AlO_x, 45% CH_2Cl_2/hexanes). Subsequent sonication in ether and vacuum filtration yielded the final product as a light yellow solid (0.014 g, 0.020 mmol, 41% over two steps); R_f = 0.43 (45% CH_2Cl_2/hexanes); ^1H NMR (500 MHz, Methylene Chloride-d_2) δ 7.66 – 7.51 (m, 27H), 7.43 (d, J =

8.1 Hz, 4H), 7.38 (d, J = 8.3 Hz, 4H), 6.71 (t, J = 2.0 Hz, 1H); ^{1}H NMR (600 MHz, DMSO-d_6) δ 7.76 (dd, J = 8.7, 7.1 Hz, 8H), 7.73 − 7.62 (m, 20H), 7.58 (t, J = 7.6 Hz, 1H), 7.50 (d, J = 8.4 Hz, 3H), 7.41 (d, J = 8.6 Hz, 4H), 6.70 (t, J = 1.9 Hz, 1H); ^{13}C NMR (126 MHz, CD$_2$Cl$_2$) δ 142.82, 141.60, 140.48, 139.75, 139.66, 139.03, 138.76, 138.51, 135.00, 131.18, 129.54, 129.05, 127.97, 127.78, 127.70, 127.65, 127.19, 124.36, 123.76, 101.44 (20 signals, one unaccounted for); IR (ATR) ṽ 3025 (w), 1592 (m), 1480 (s), 1391 (w), 1107 (w), 1000 (m), 909 (w), 858 (m), 830 (s), 806 (s), 797 (s), 746 (s), 726 (m), 708 (m); HRMS (ESI, positive mode) m/z calcd for C$_{56}$H$_{36}$: 708.2812 [M]$^+$, found 708.2835.
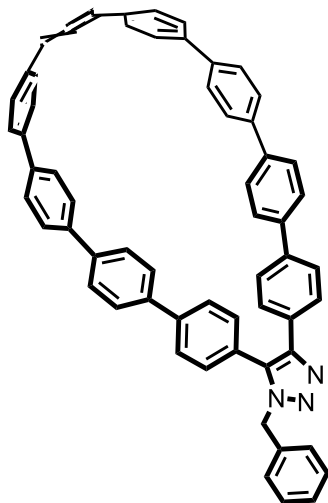
[9+1]CPP-BnAz. **[9+1]CPP** (0.013 g, 0.0181 mmol, 1 equiv.) was dissolved in toluene (2.0 mL, 0.009 M). Benzyl azide (0.0125 mL, 0.100 mmol, 5.5 equiv.) was added and the reaction was allowed to proceed for 4 hours at 50 °C. The toluene was removed *via* rotary evaporator. The crude product was purified *via* a short plug (basic AlO$_x$, 100% CH$_2$Cl$_2$). The resultant solid was sonicated in ethanol and vacuum filtered to yield the final product as a yellow solid (0.008 g, 0.010 mmol, 55%); R_f = 0.52 (SiO$_2$ 4% MeOH/CH$_2$Cl$_2$); ^{1}H NMR (500 MHz, DMSO-d_6) δ 7.75 − 7.61 (m, 28H), 7.51 (d, J = 8.5 Hz, 2H), 7.44 (d, J = 8.4 Hz, 2H), 7.37 − 7.25 (m, 7H), 7.12 (d, J = 6.5 Hz, 2H), 5.62 (s, 2H); ^{13}C NMR (126 MHz, DMSO) δ 144.82, 140.19, 139.38, 138.57, 138.41, 138.10, 137.83, 137.62, 137.28, 137.23, 137.11, 136.78, 136.75, 136.70, 136.68, 136.65, 135.81, 134.49, 130.71, 129.77, 128.71, 128.08, 127.93, 127.46, 127.41, 127.38, 127.36, 127.26, 127.24, 127.21, 127.06, 126.95, 126.91, 126.88, 125.81, 51.36 (36 signals, 7 unaccounted for); IR (ATR) ṽ 3025 (m), 2923 (w), 1590 (m), 1479 (s), 1392 (w), 1351 (w), 1263 (m), 1002 (m), 816 (s), 738 (s); HRMS (ASAP, positive mode) m/z calcd for C$_{63}$H$_{43}$N$_3$: 841.3457 [M]$^+$, found 841.3365.
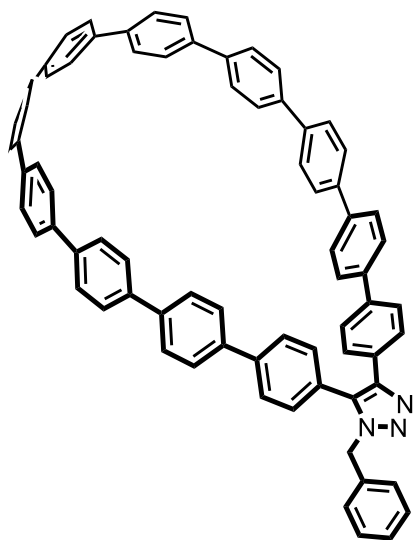
[11+1]CPP-BnAz. The synthesis of **[11+1]CPP-BnAz** conjugate has been described previously.[2] As our kinetics experiments were performed in *d*-DMSO, we include here NMR information for this compound in *d*-DMSO. ^{1}H NMR (500 MHz, DMSO-d_6) δ 7.85 − 7.64 (m, 36H), 7.59 (d, *J* = 8.1 Hz, 2H), 7.53 (d, *J* = 8.0 Hz, 2H), 7.38 − 7.29 (m, 7H), 7.13 (d, *J* = 7.3 Hz, 2H), 5.63 (s, 2H); ^{13}C NMR (126 MHz, DMSO) δ 144.44, 140.14, 139.16, 138.64, 138.59, 138.35, 138.09, 137.98, 137.91, 137.76, 137.72, 137.59, 137.44, 137.40, 137.35, 137.29, 137.08, 137.05, 137.02, 135.82, 134.32, 130.76, 129.88, 128.72, 127.94, 127.68, 127.31, 127.26, 127.18, 127.14, 126.99, 126.94, 126.88, 126.04, 51.34 (35 signals, 16 unaccounted for).
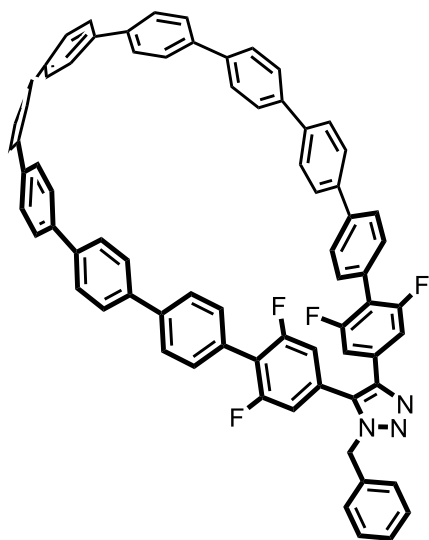
fluor[11+1]CPP-BnAz. **fluor[11+1]CPP** (0.016 g, 0.017 mmol, 1.0 equiv.) was dissolved in toluene (5.7 mL, 0.003 M). Benzyl azide (0.015 mL, 0.12 mmol, 7.0 equiv.) was added and the reaction was allowed to proceed for 18 hours at 45 °C. The toluene was removed *via* rotary evaporator. The crude product was purified *via* a short plug (basic AlO$_x$, 100% CH$_2$Cl$_2$). The resultant solid was

sonicated in ether and vacuum filtered to yield the final product as a light yellow solid (0.013 g, 0.012 mmol, 69%); R_f = 0.35 (SiO$_2$, 100% CH$_2$Cl$_2$); ^{1}H NMR (500 MHz, Methylene Chloride-d_2) δ 7.69 – 7.62 (m, 32H), 7.56 (d, J = 8.1 Hz, 2H), 7.43 (d, J = 8.0 Hz, 2H), 7.39 – 7.33 (m, 3H), 7.20 – 7.15 (m, 2H), 7.03 (d, J = 8.1 Hz, 2H), 6.81 (d, J = 7.1 Hz, 2H), 5.58 (s, 2H); ^{1}H NMR (500 MHz, DMSO-d_6) δ 7.79 – 7.71 (m, 32H), 7.55 (d, J = 8.0 Hz, 2H), 7.44 (d, J = 8.0 Hz, 2H), 7.40 – 7.30 (m, 5H), 7.17 (d, 2H), 7.07 (d, J = 8.5 Hz, 2H), 5.70 (s, 2H); ^{19}F NMR (471 MHz, Methylene Chloride-d_2) δ -111.86 (d, J = 7.4 Hz), -113.99 (d, J = 8.4 Hz); ^{19}F NMR (471 MHz, DMSO-d_6) δ -112.66 (d, J = 7.0 Hz), -113.61 (d, J = 7.8 Hz); ^{13}C NMR (126 MHz, Methylene Chloride-d_2) δ 160.75 (dd, J = 251.5, 8.1 Hz), 160.43 (d, J = 248.2, 8.1 Hz), 144.05 (t, J = 1.9 Hz), 141.40, 140.53, 139.71, 139.62, 139.26, 139.10, 139.02, 138.82, 138.79, 138.64, 138.59, 138.53, 138.51, 138.47, 133.04 (t, J = 2.4 Hz), 132.23 (t, J = 11.1 Hz), 131.21 (t, J = 2.5 Hz), 131.08 (t, J = 1.8 Hz), 129.38, 128.98, 128.31 (t, J = 11.2 Hz), 128.09, 127.99, 127.92, 127.90, 127.88, 127.86, 127.84, 127.81, 127.79, 127.77, 127.75, 127.73, 127.70, 127.65, 127.30, 127.18, 126.96, 120.14 (t, J = 17.7 Hz), 117.96 (t, J = 18.9 Hz), 114.32 (dd, J = 19.3, 8.0 Hz), 110.63 (dd, J = 20.4, 7.6 Hz), 52.95 (46 signals, 5 unaccounted for); IR (ATR) ṽ 3024 (w), 1907 (w), 1630 (w), 1557 (w), 1485 (m), 1395 (m), 1365 (m), 1199 (m), 1111 (w) 1022 (m), 1002 (m), 867 (m), 808 (s), 726 (m); HRMS (ASAP, positive mode) m/z calcd for C$_{75}$H$_{48}$N$_3$F$_4$: 1066.3784 [M+H]$^+$, found 1066.3641.
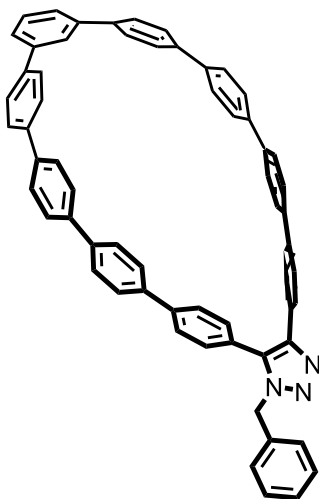
***m*[9+1]CPP-BnAz**. ***m*[9+1]CPP** (0.014 g, 0.020 mmol, 1.0 equiv.) was dissolved in tetrahydrofuran (3.0 mL, 0.0065 M). Benzyl azide (0.040 mL, 0.32 mmol, 16 equiv.) was added and the reaction was allowed to stir for 2 hours. The tetrahydrofuran was removed *via* rotary evaporator. The crude product was purified *via* a short plug (basic AlO$_x$, 50-100% CH$_2$Cl$_2$/hexanes). The resultant solid was sonicated in ether and vacuum filtered to yield the final product as a yellow solid (0.0047 g, 0.0056 mmol, 28%); R_f = 0.58 (SiO$_2$, 5% MeOH/CH$_2$Cl$_2$); ^{1}H NMR (500 MHz, DMSO-d_6) δ 7.73 – 7.63 (m, 22H), 7.61 – 7.53 (m, 3H), 7.47 – 7.40 (m, 6H), 7.39 – 7.28 (m, 3H), 7.26 (d, J = 8.3 Hz, 2H), 7.22 (d, J = 8.0 Hz, 2H), 7.16 (d, J = 6.7 Hz, 2H), 6.28 (t, J = 1.9 Hz, 1H), 5.66 (s, 2H); ^{1}H NMR (600 MHz, Methylene Chloride-d_2) δ 7.65 – 7.51 (m, 23H), 7.48 (d, J = 8.1 Hz, 2H), 7.41 – 7.31 (m, 9H), 7.23 (d, J = 8.4 Hz, 4H), 7.11 (d, J = 8.1 Hz, 2H), 6.31 (d, J = 1.9 Hz, 1H), 5.61 (s, 2H); ^{13}C NMR (151 MHz, CD$_2$Cl$_2$) δ 146.95, 143.11, 143.02, 142.41, 142.36, 141.84, 140.54, 140.03,

139.79, 139.58, 139.56, 139.52, 139.32, 138.85, 138.73, 138.51, 138.48, 136.15, 135.39, 131.33, 130.32, 129.61, 129.48, 129.45, 129.21, 129.01, 128.63, 128.02, 127.98, 127.87, 127.83, 127.81, 127.68, 127.50, 127.48, 127.46, 127.37, 126.59, 123.51, 52.57 (40 signals, 5 unaccounted for); IR (ATR) $\tilde{v}$ 3026 (m), 1596 (m), 1478 (s), 1391 (w), 1352 (w), 1263 (m), 1110 (w), 1002 (m), 831 (s), 811 (s), 736 (s), 714 (s); HRMS (ASAP, positive mode) m/z calcd for $C_{63}H_{44}N_3$: 842.3535 [M+H]$^+$, found 842.3501.

3. Nuclear magnetic resonance spectra
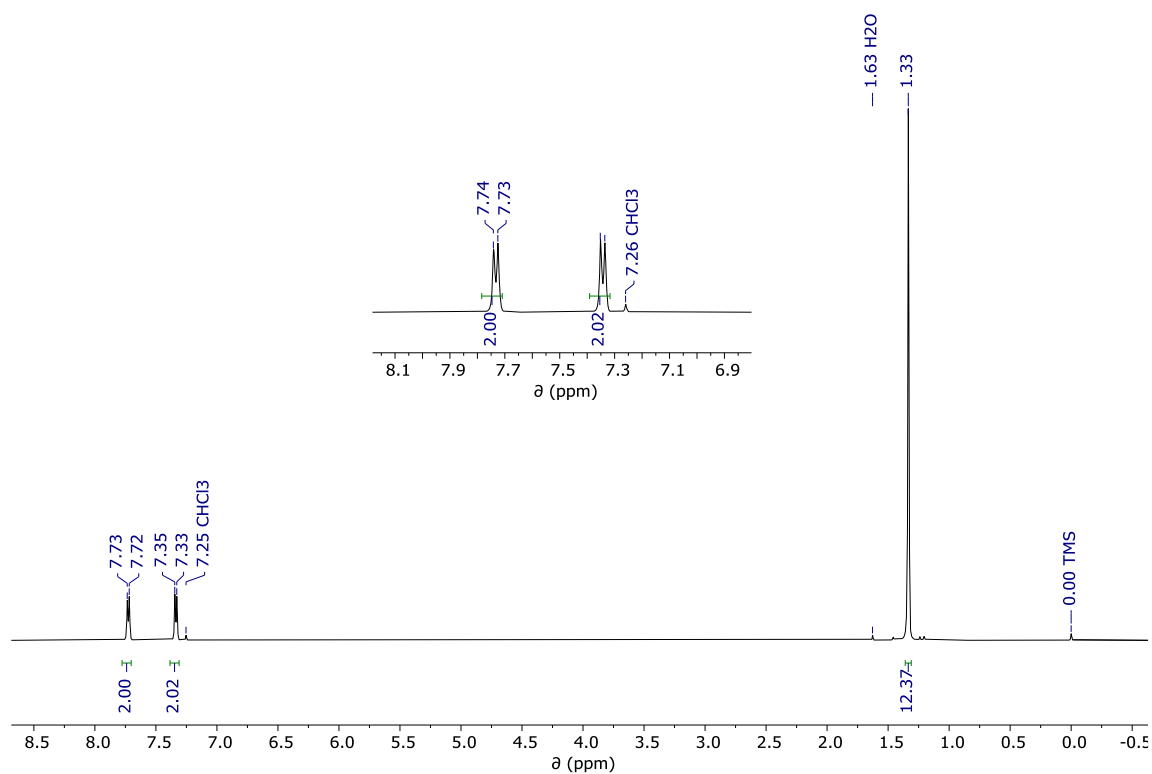
Figure S1: ^{1}H NMR spectrum (500 MHz) of **10** in CDCl$_3$ at room temperature.
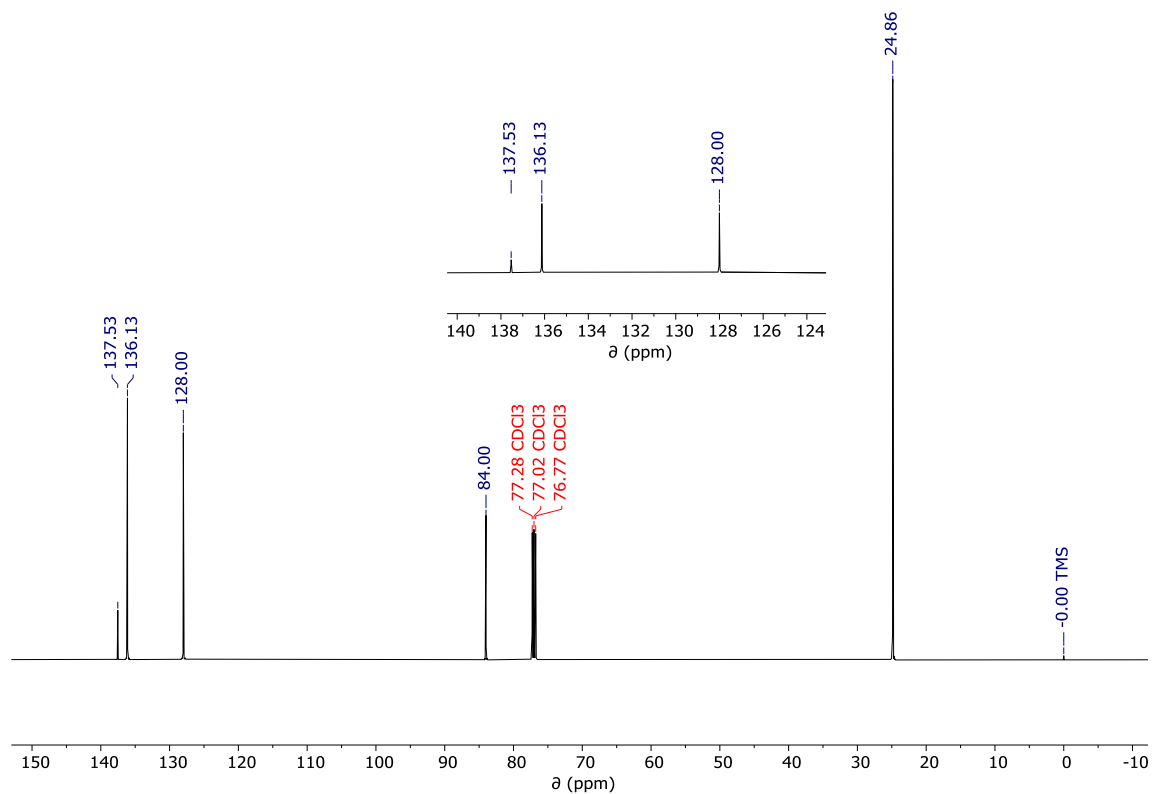
Figure S2: ^{13}C NMR spectrum (126 MHz) of **10** in CDCl$_3$ at room temperature.
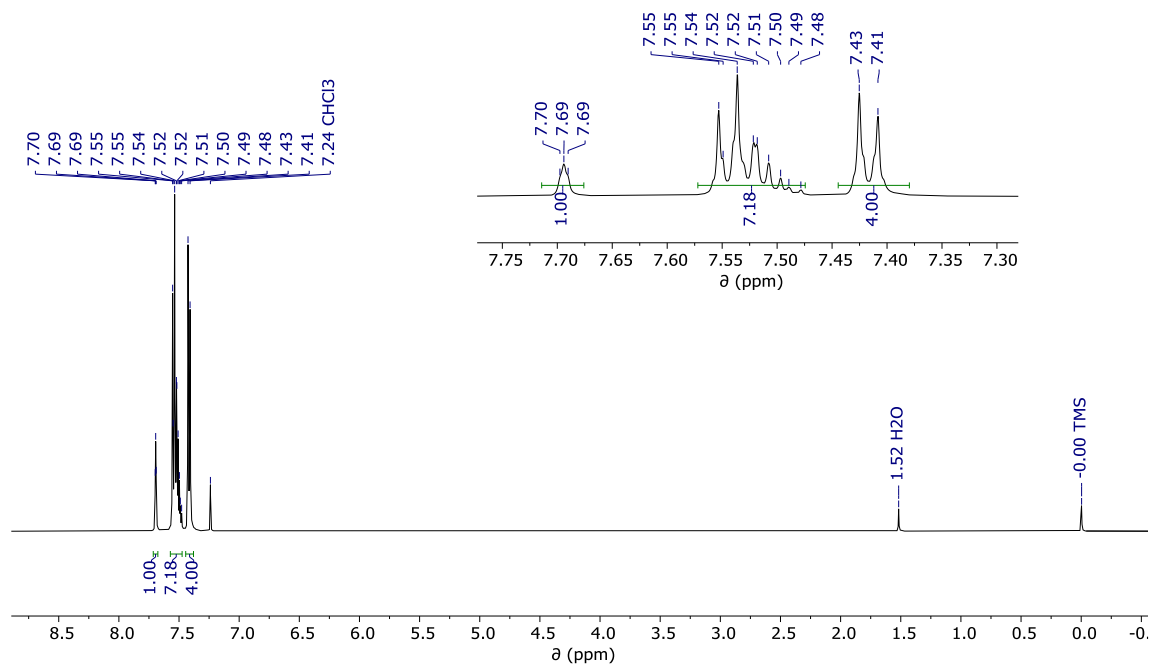
Figure S3: ^{1}H NMR spectrum (500 MHz) of **11** in CDCl$_3$ at room temperature.
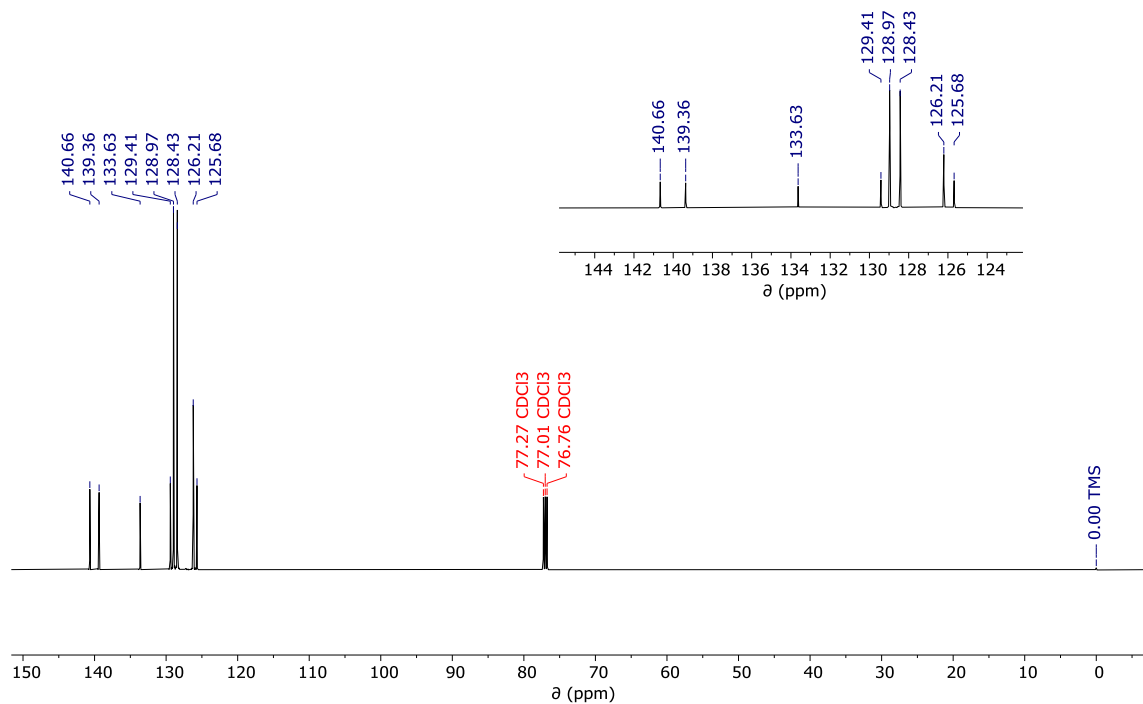
Figure S4: ^{13}C NMR spectrum (126 MHz) of **11** in CDCl$_3$ at room temperature.
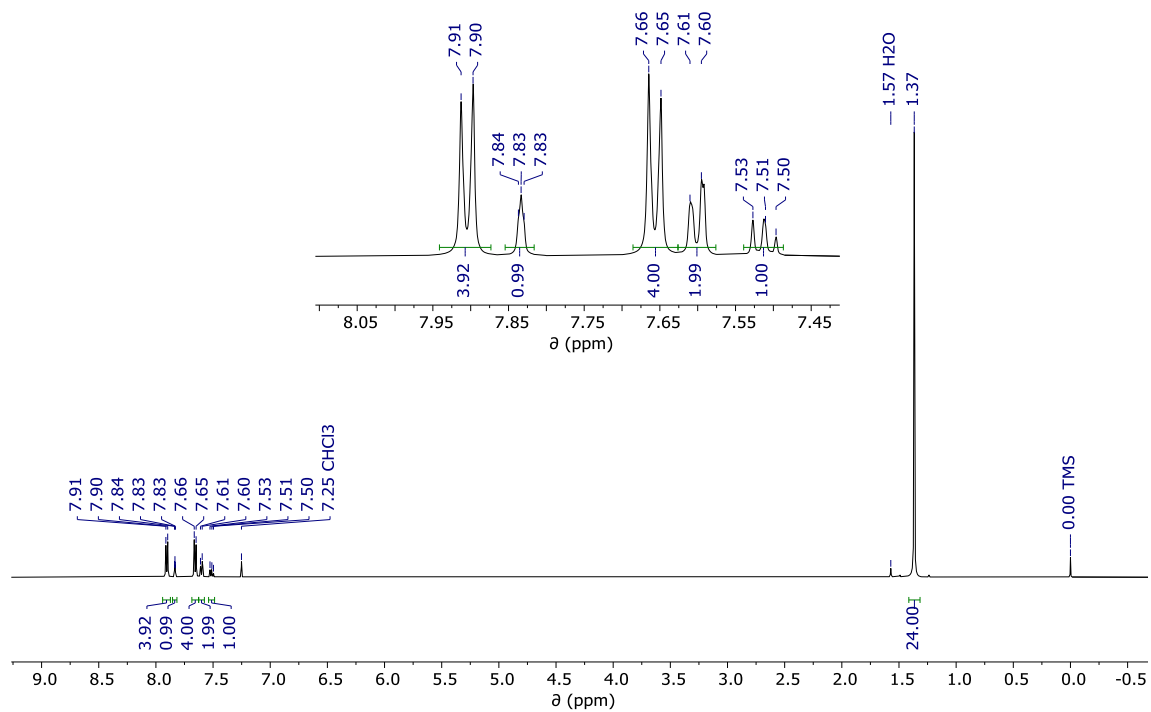
Figure S5: ^{1}H NMR spectrum (500 MHz) of **2** in CDCl$_3$ at room temperature.
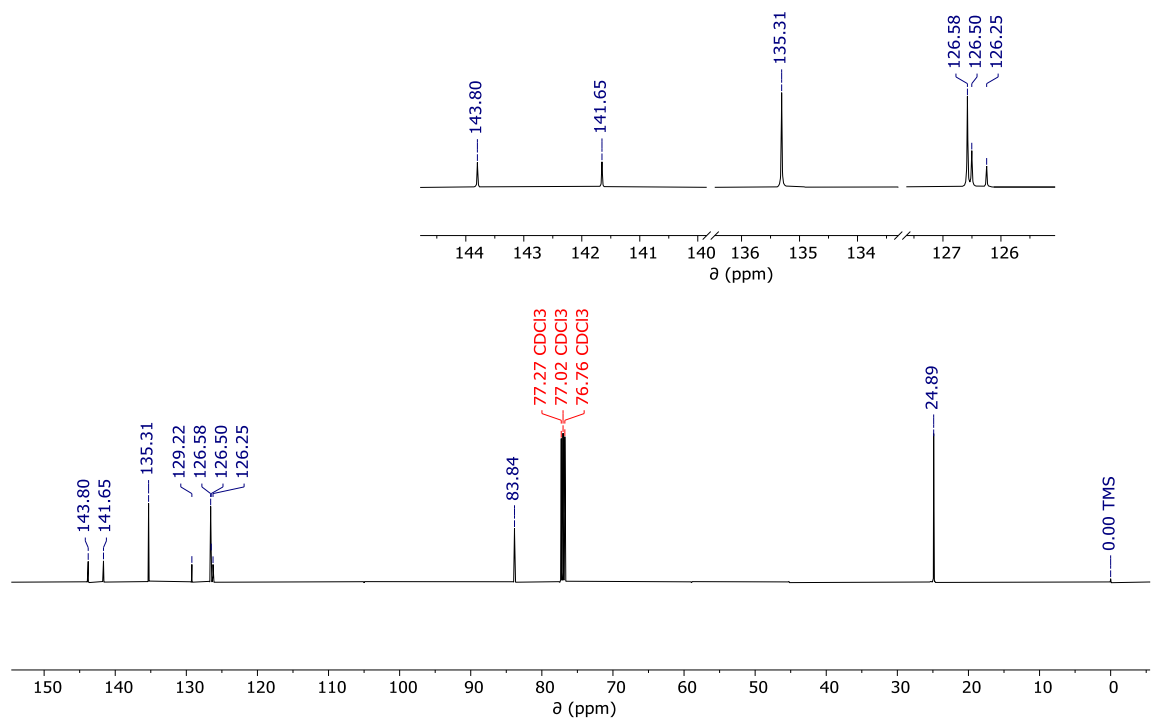
Figure S6: ^{13}C NMR spectrum (126 MHz) of **2** in CDCl$_3$ at room temperature.
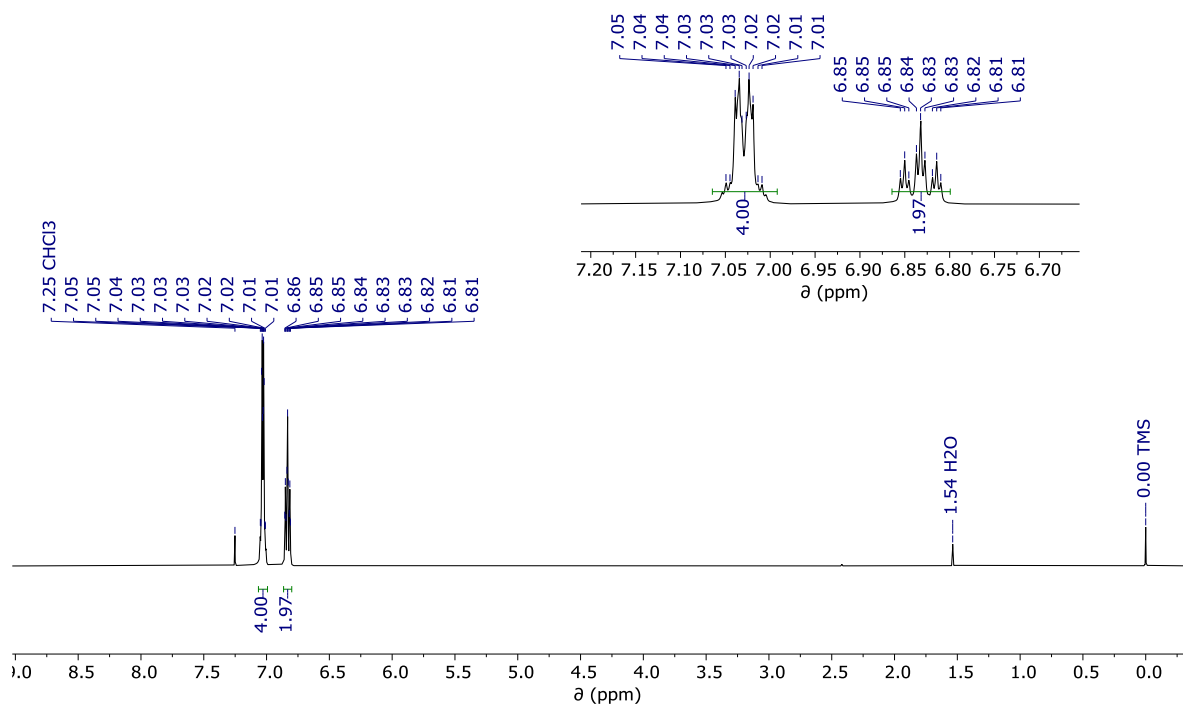
Figure S7: ^{1}H NMR spectrum (500 MHz) of **6** in CDCl$_3$ at room temperature.
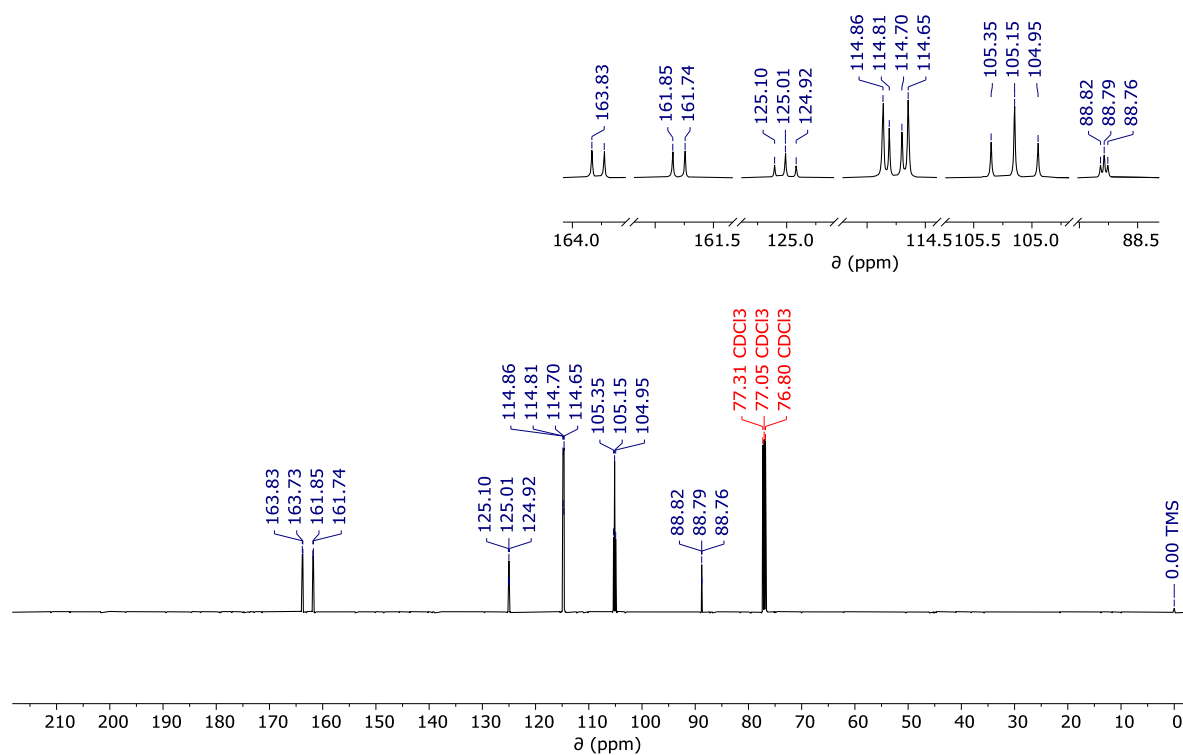
Figure S8: ^{13}C NMR spectrum (126 MHz) of **6** in CDCl$_3$ at room temperature.
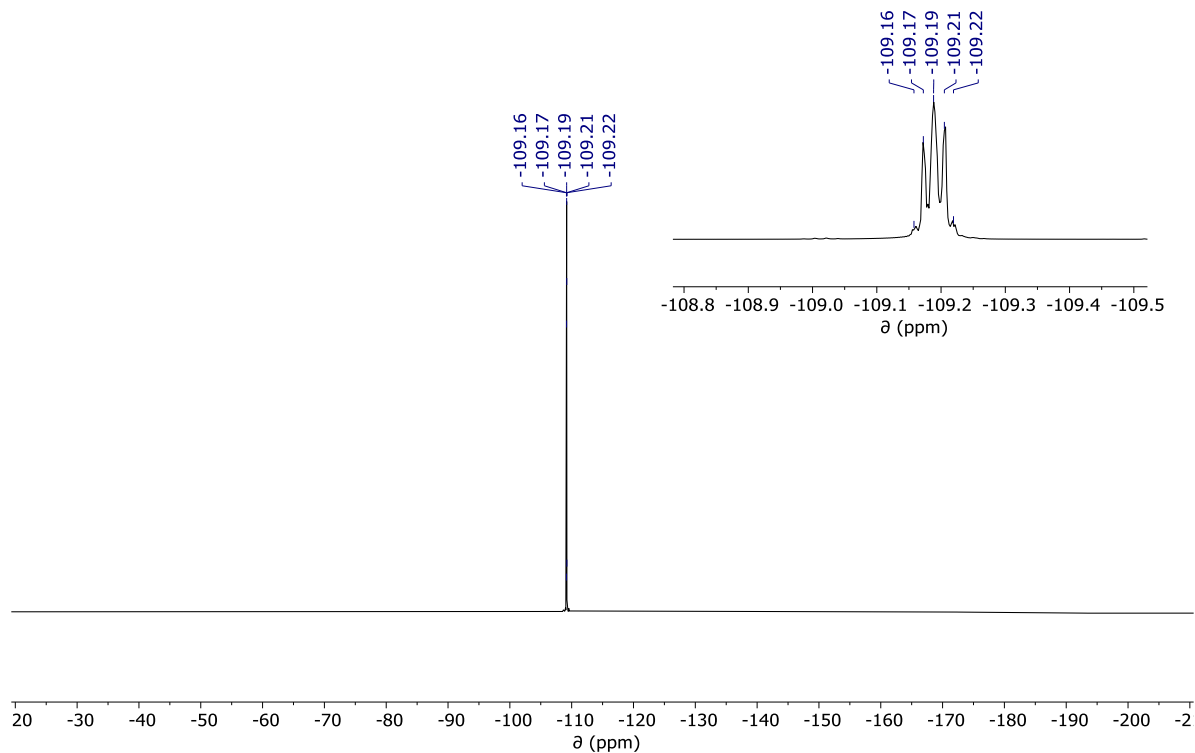
Figure S9: ^{19}F NMR (471 MHz) of **6** in $CDCl_3$ at room temperature.
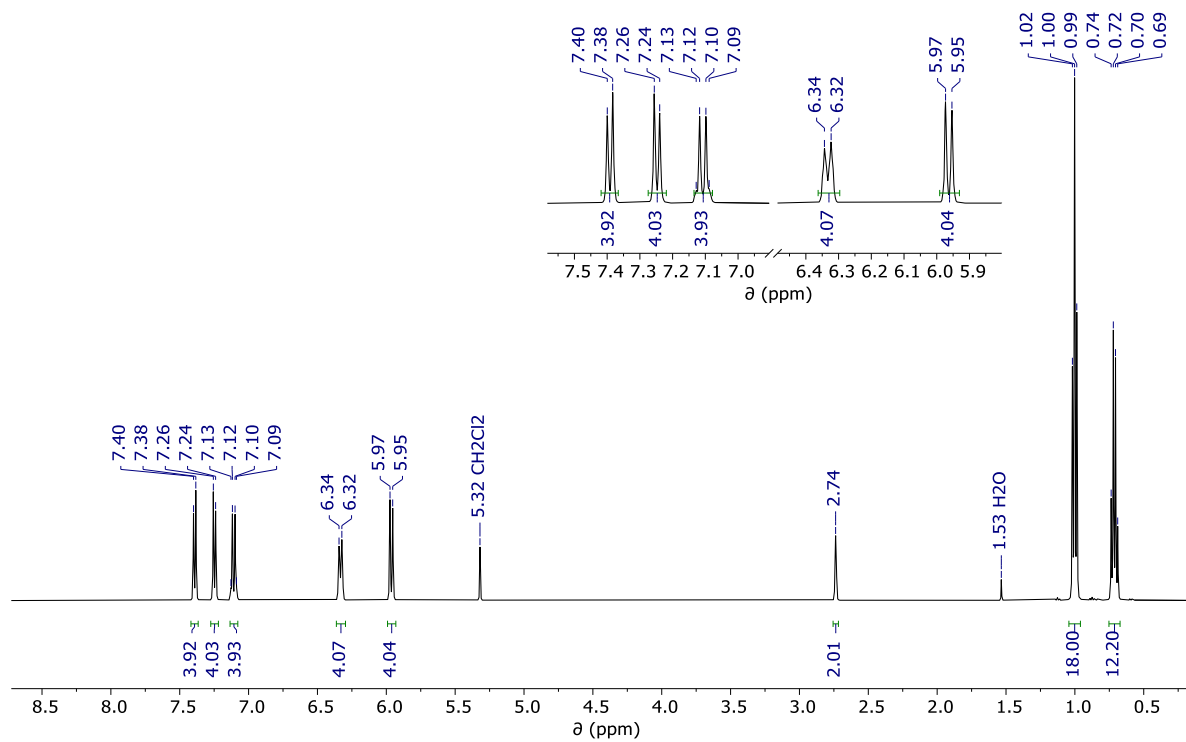
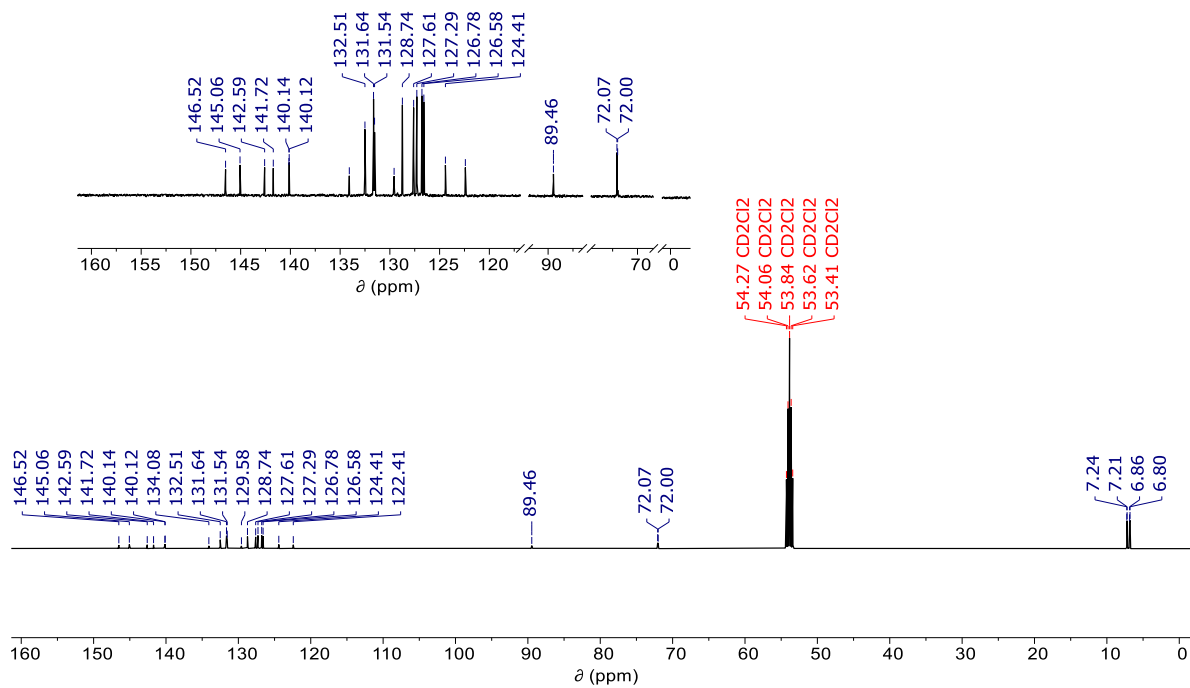**Figure S10**: ^1H NMR (500 MHz) of **8** in CD_2Cl_2 at room temperature.
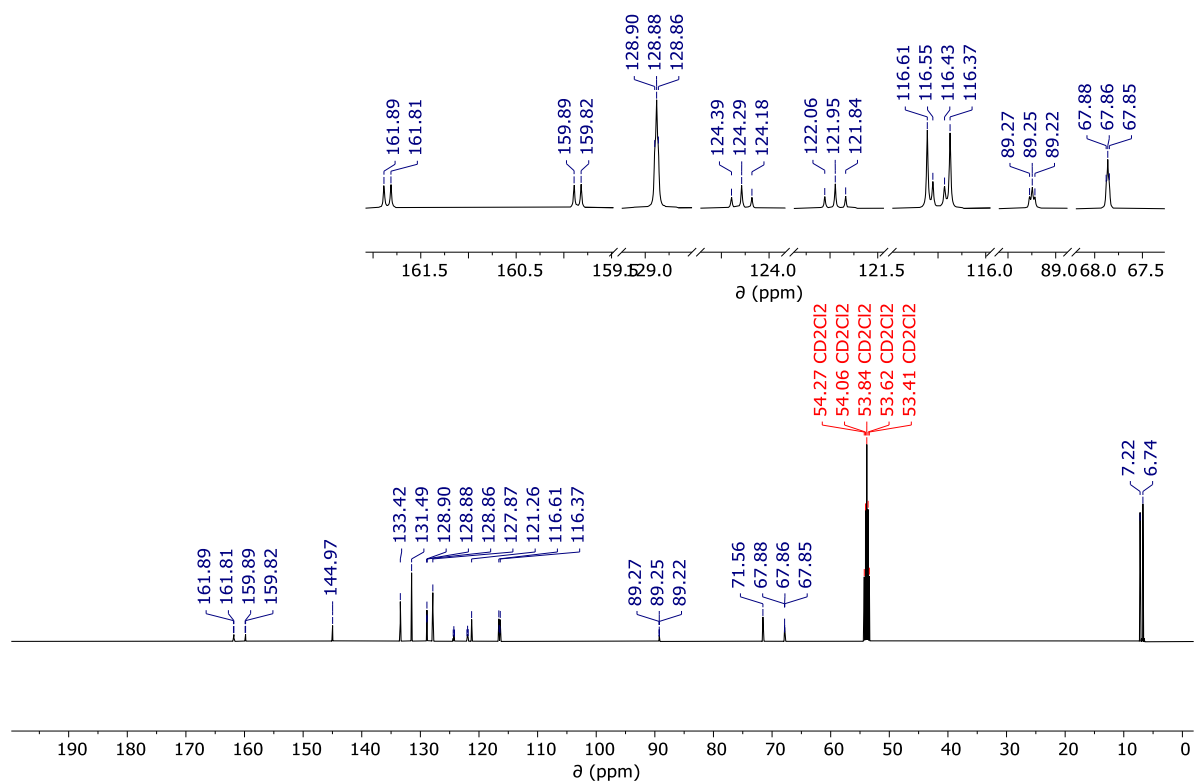
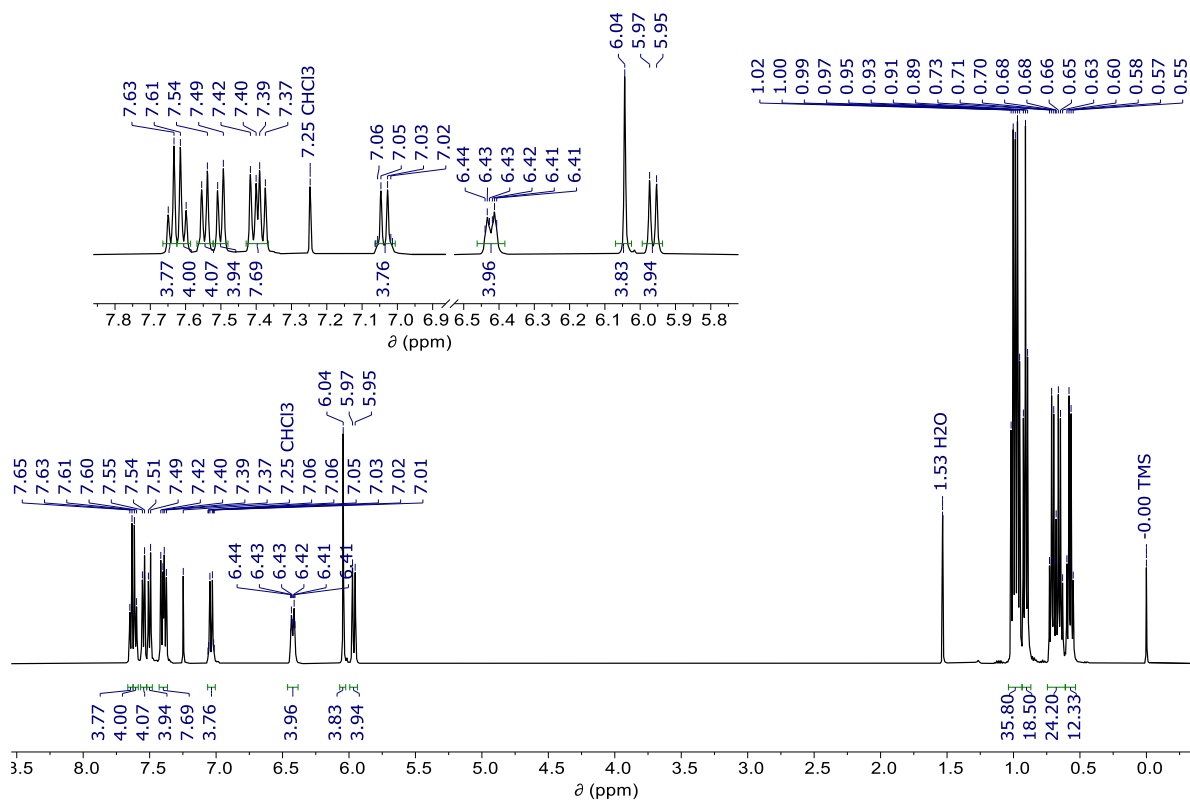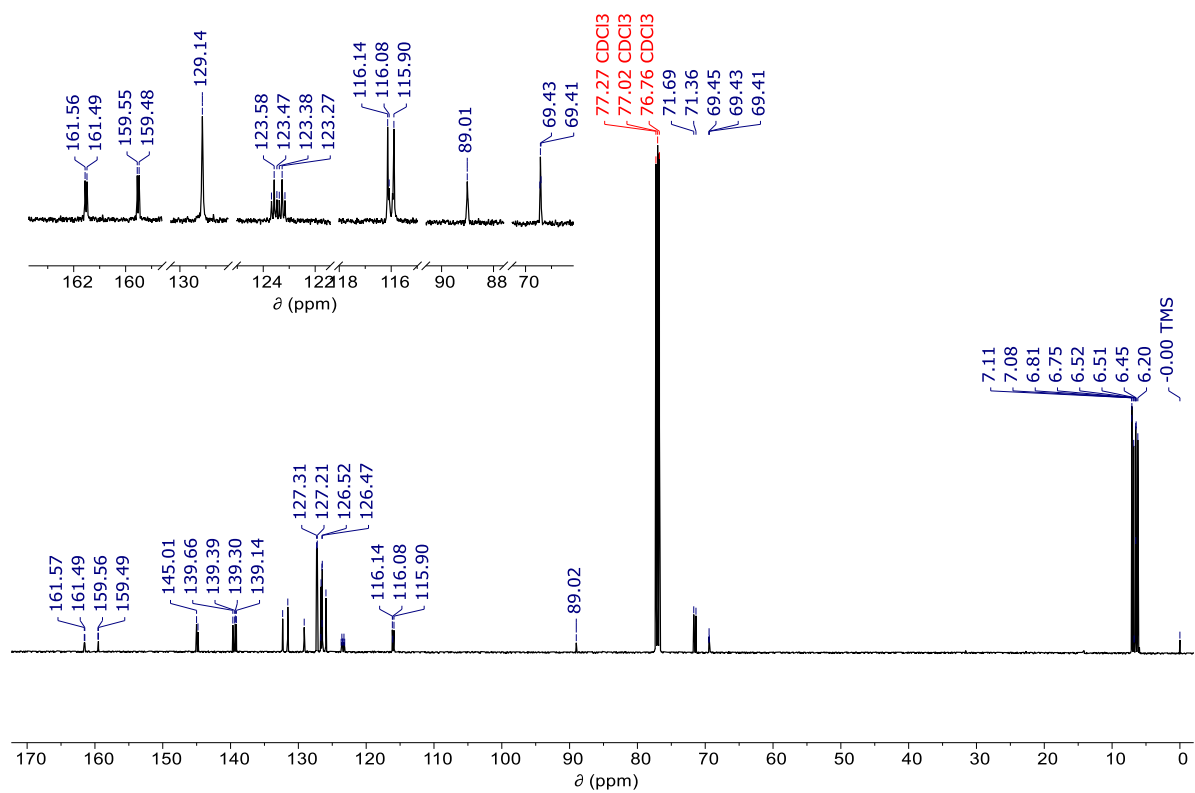**Figure S11**: ^{13}C NMR (126 MHz) of **8** in CD$_2$Cl$_2$ at room temperature.
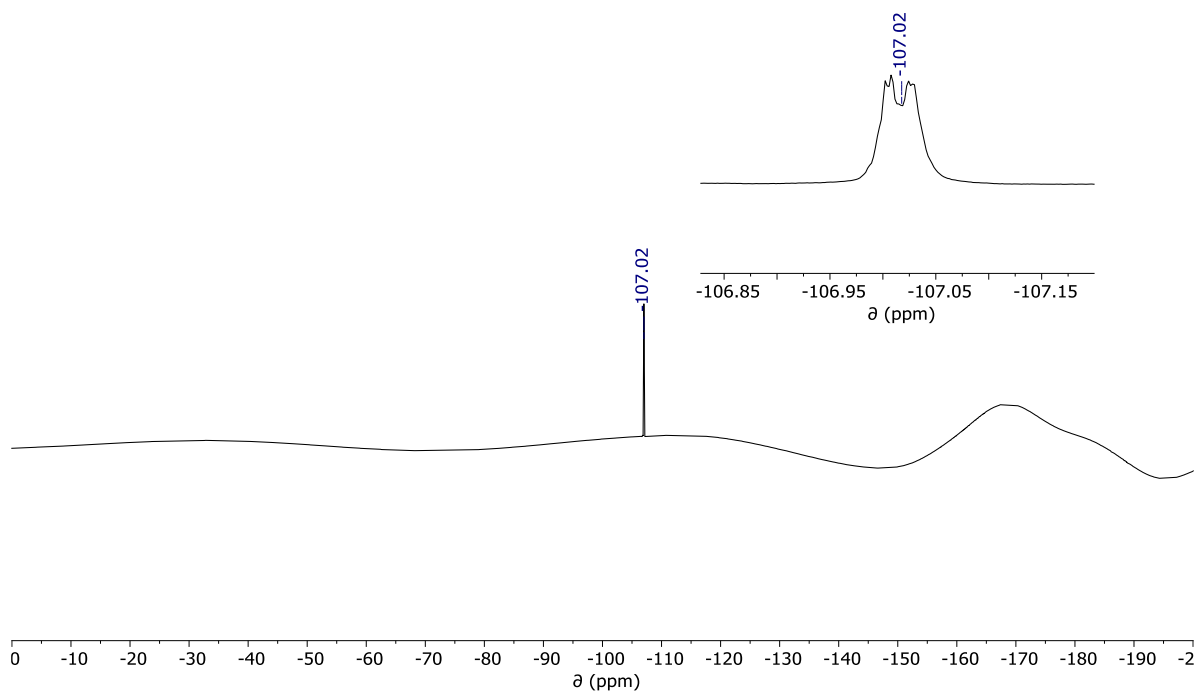
Figure S12: ^{19}F NMR (471 MHz) of **8** in CDCl$_3$ at room temperature.

20
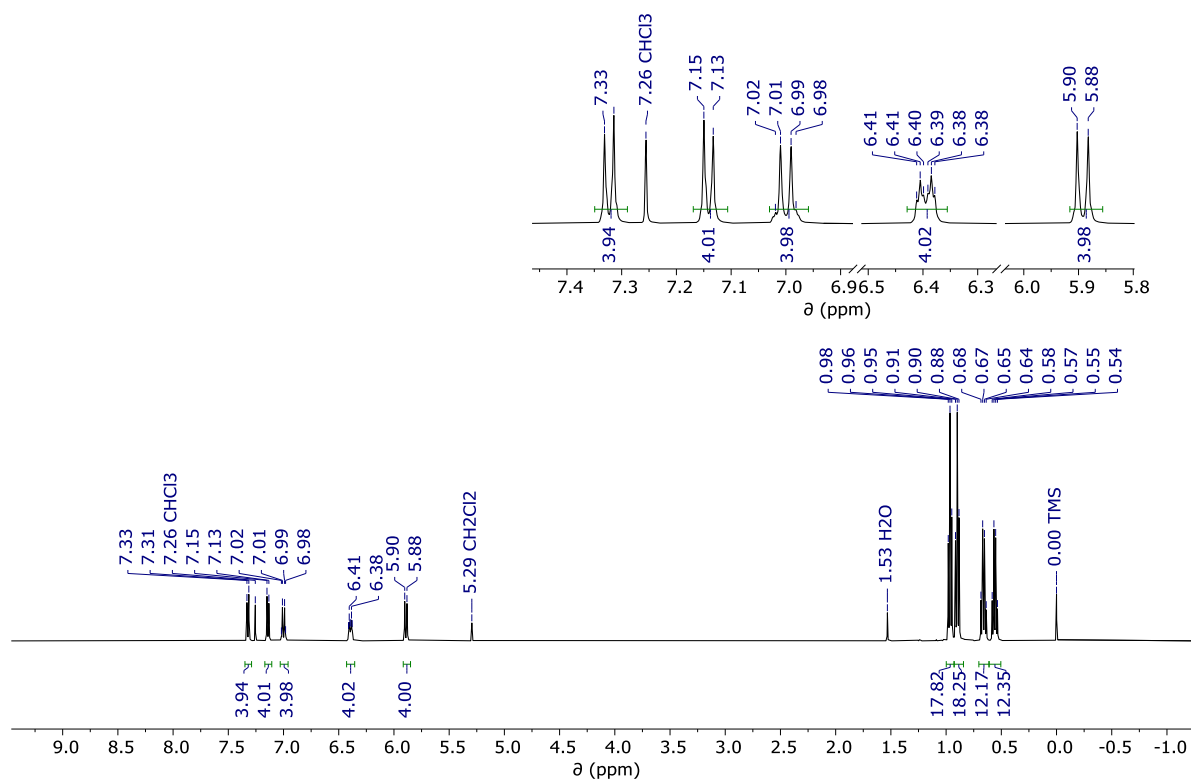
Figure S13: ^{1}H NMR (500 MHz) of **1** in CDCl$_3$ at room temperature.
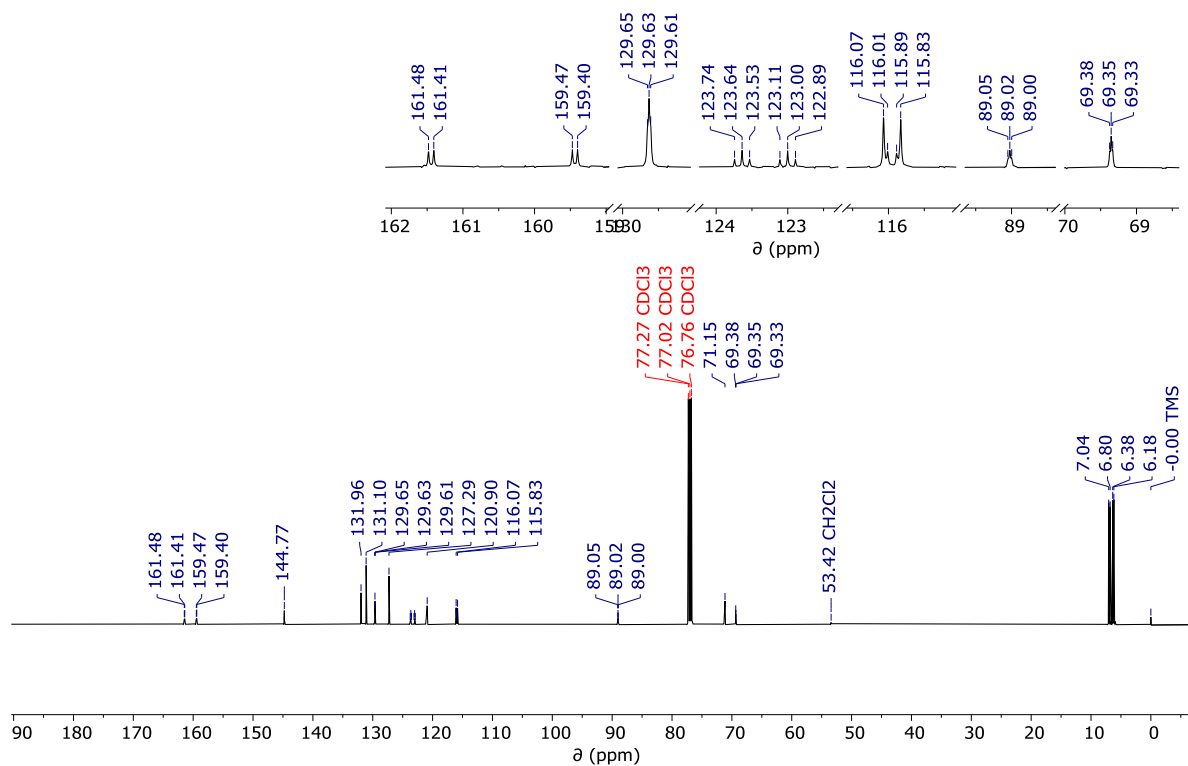
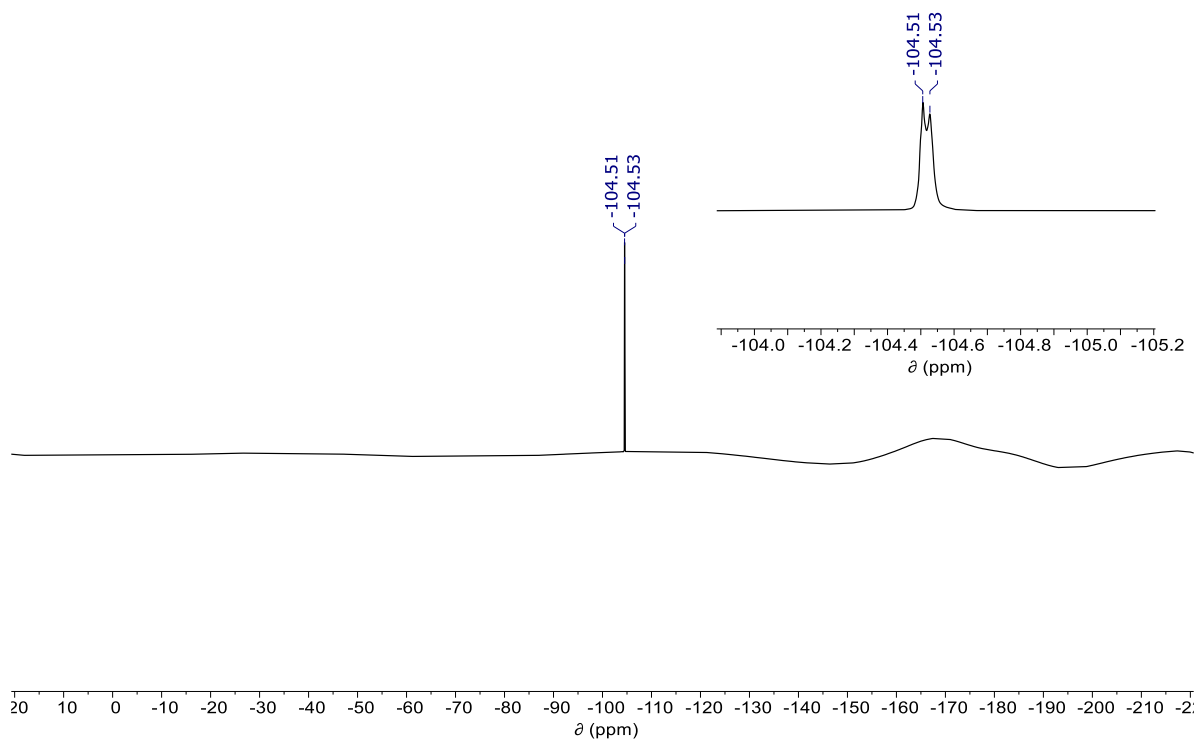**Figure S14**: ^{13}C NMR (126 MHz) of **1** in CDCl$_3$ at room temperature.

21
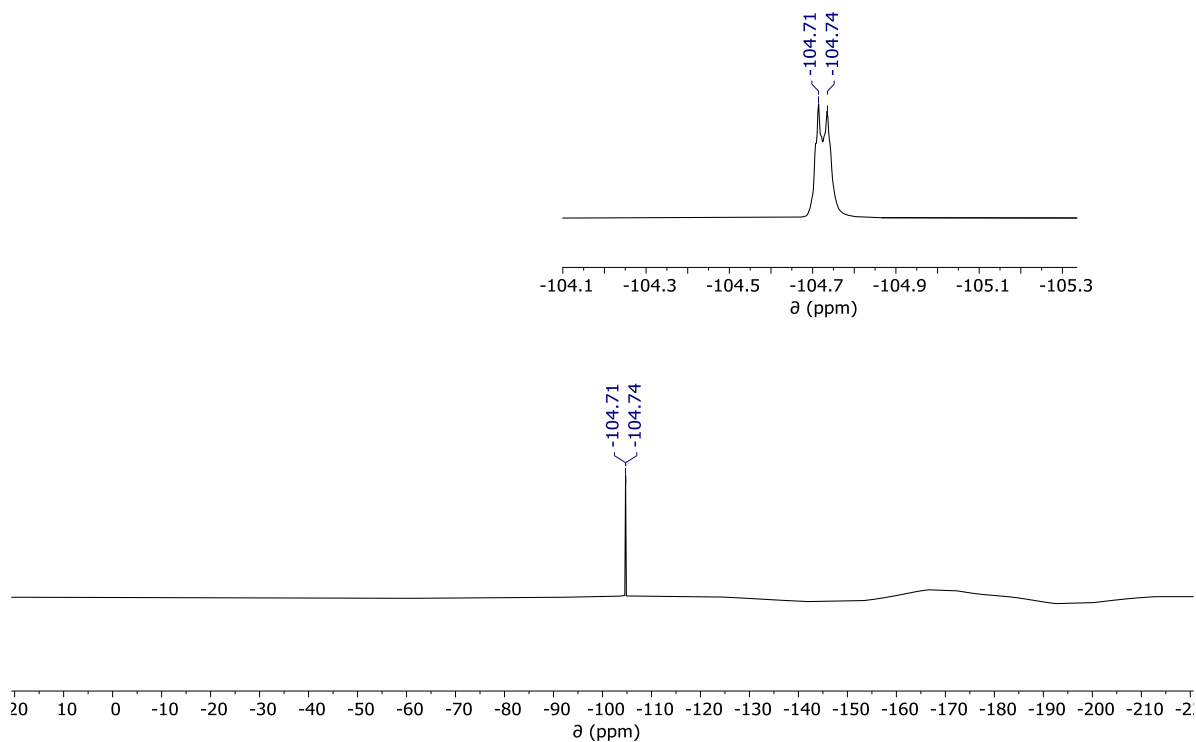
Figure S15: ^{19}F NMR (471 MHz) of **1** in CDCl$_3$ at room temperature.
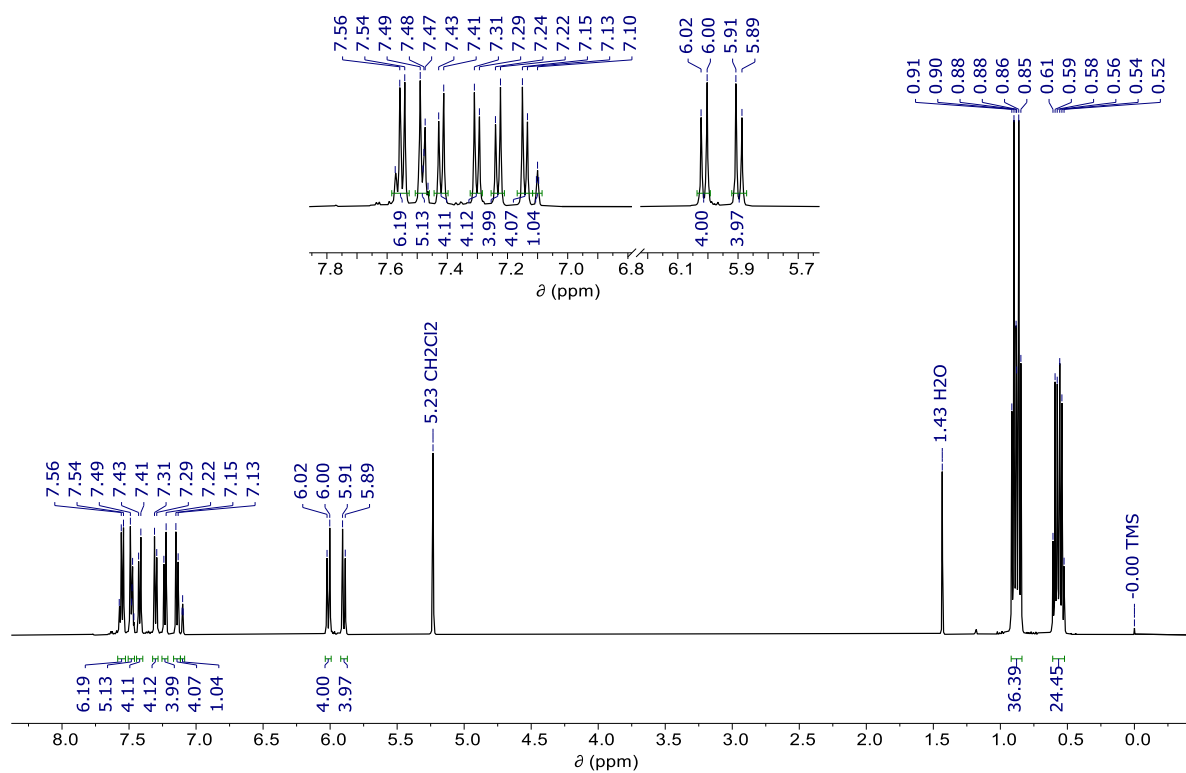
Figure S16: ^{1}H NMR (500 MHz) of **12** in CD$_2$Cl$_2$ at room temperature.

Figure S17: ^{13}C NMR (126 MHz) of **12** in CD_2Cl_2 at room temperature.

Figure S18: ^1H NMR (500 MHz) of **9** in $CDCl_3$ at room temperature.

Figure S19: ^{13}C NMR (126 MHz) of **9** in CDCl$_3$ at room temperature.

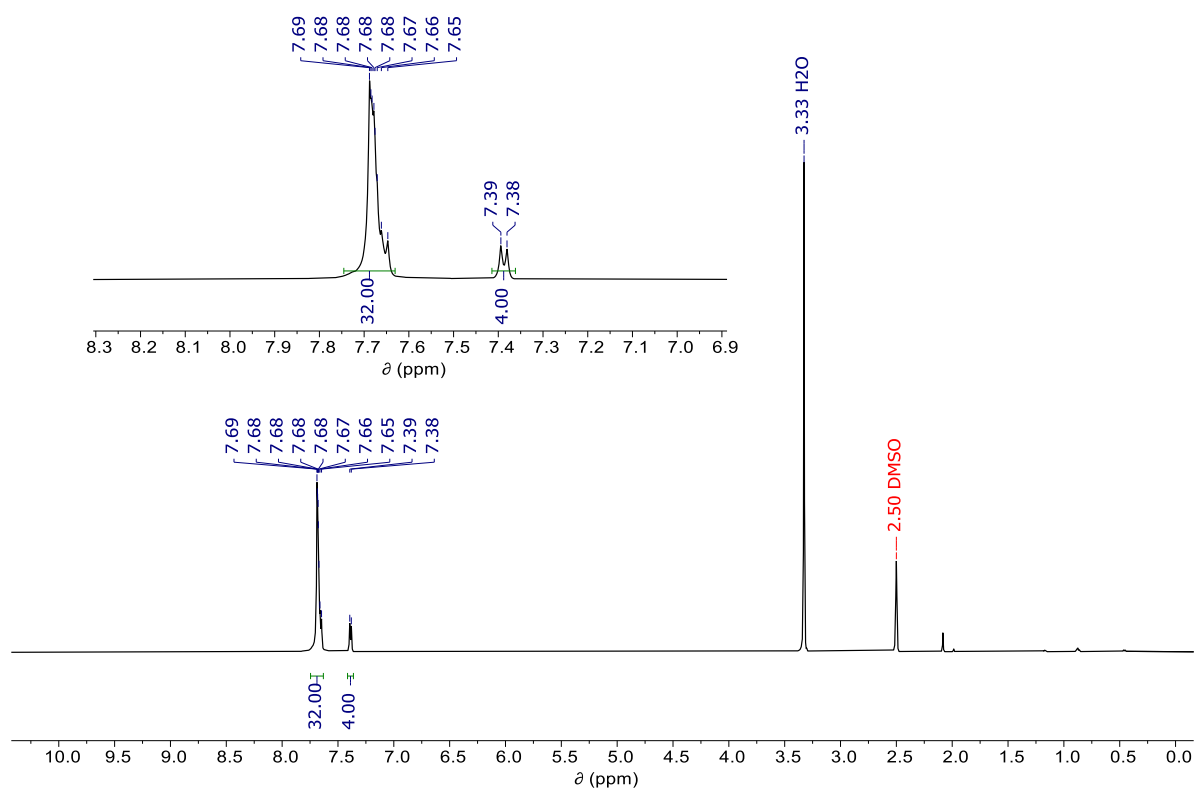**Figure S20**: ^{19}F NMR (471 MHz) of **9** in CDCl$_3$ at room temperature.

Figure S21: ^{1}H NMR (600 MHz) of **[9+1]CPP** in *d*-DMSO at room temperature.
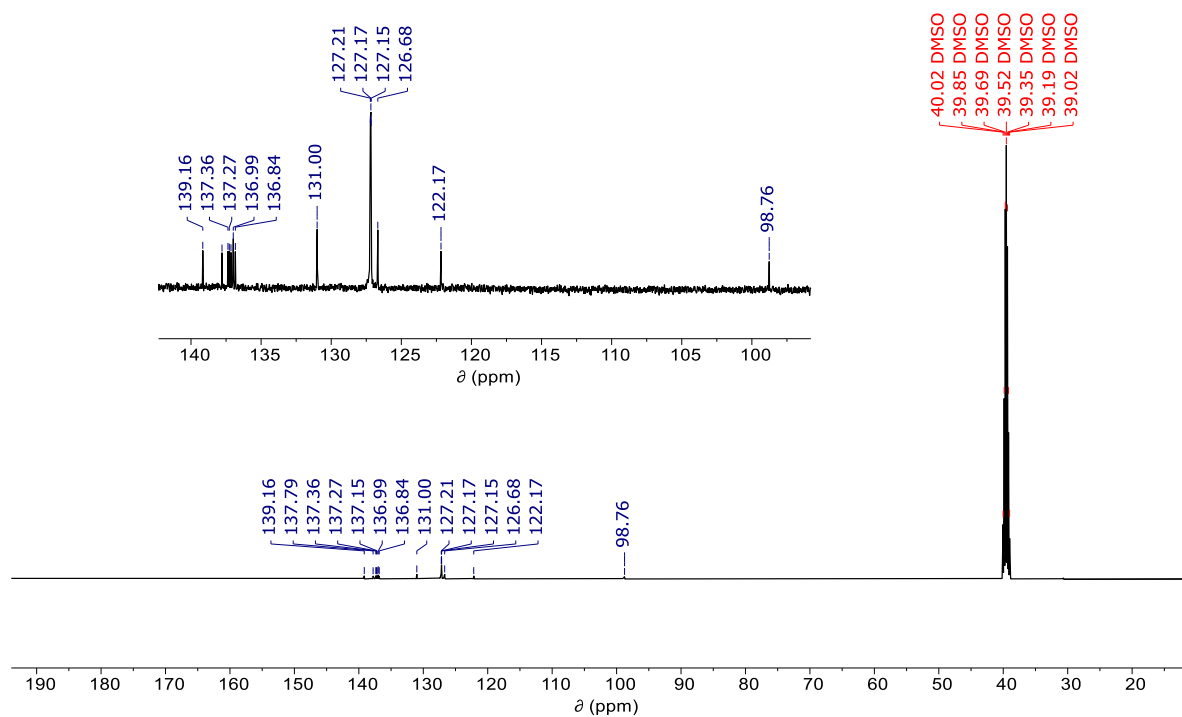

Figure S22: ^{13}C NMR (126 MHz) of **[9+1]CPP** in *d*-DMSO at room temperature.
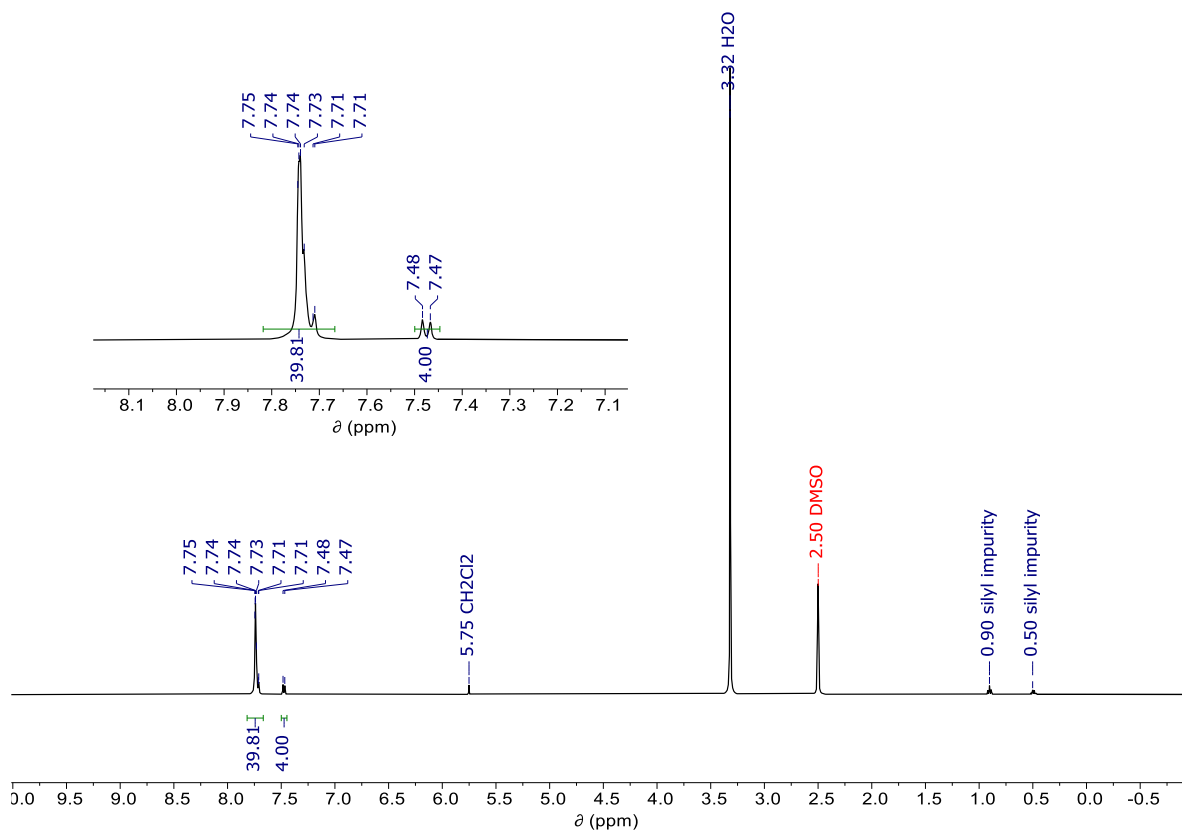
Figure S23: ^{1}H NMR (500 MHz) of **[11+1]CPP** in *d*-DMSO at room temperature.
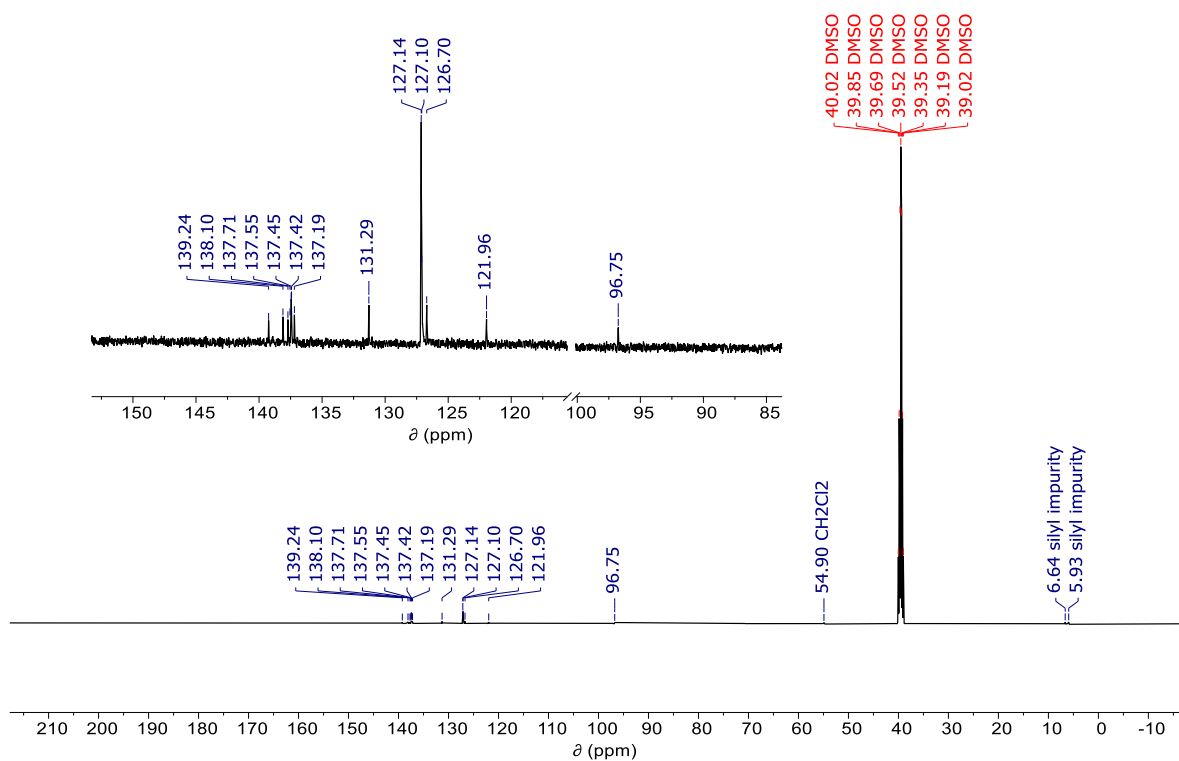

Figure S24: ^{13}C NMR (126 MHz) of **[11+1]CPP** in *d*-DMSO at room temperature.
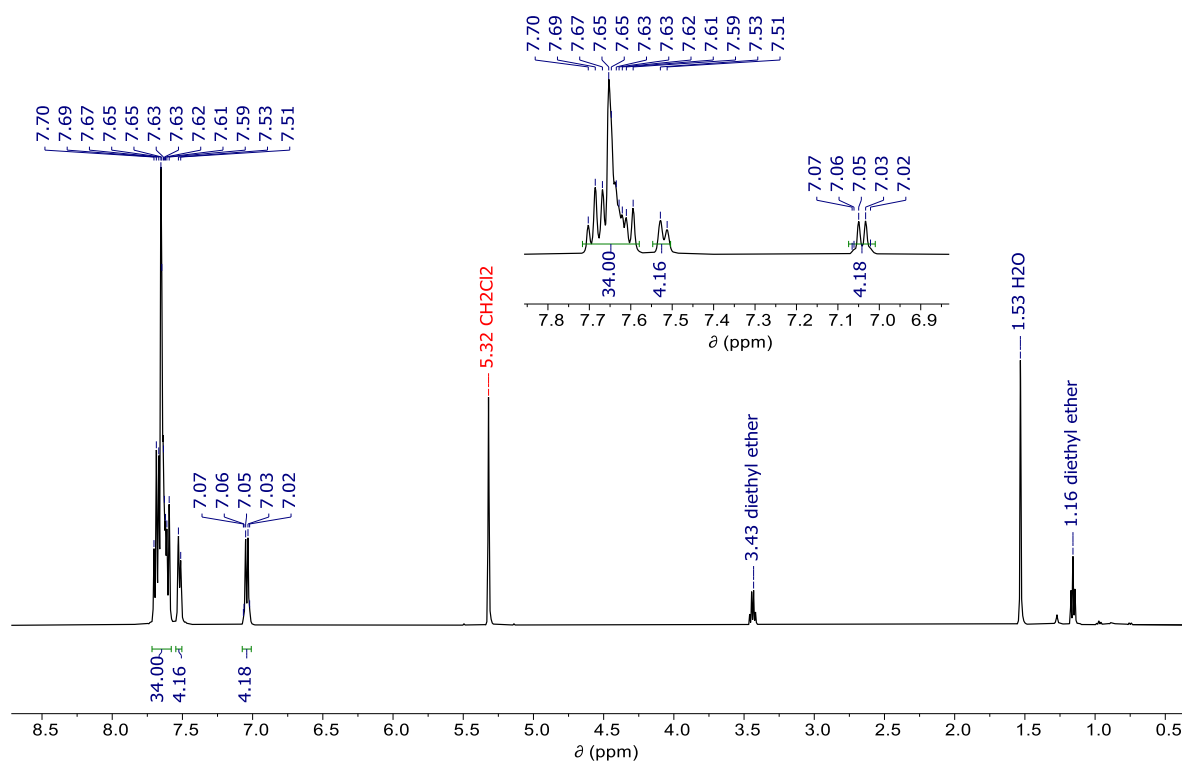
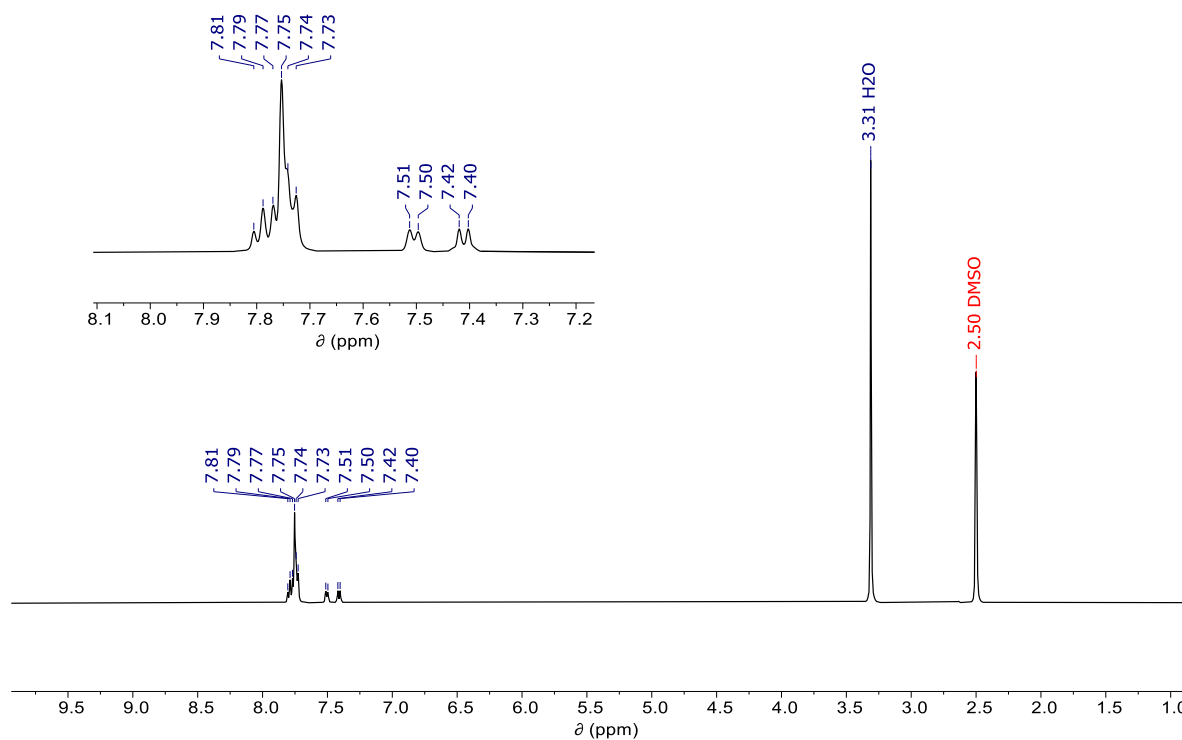**Figure S25**: ^{1}H NMR (500 MHz) of **fluor[11+1]CPP** in CD$_2$Cl$_2$ at room temperature.

Figure S26: ^{1}H NMR (500 MHz) of **fluor[11+1]CPP** in *d*-DMSO at room temperature.
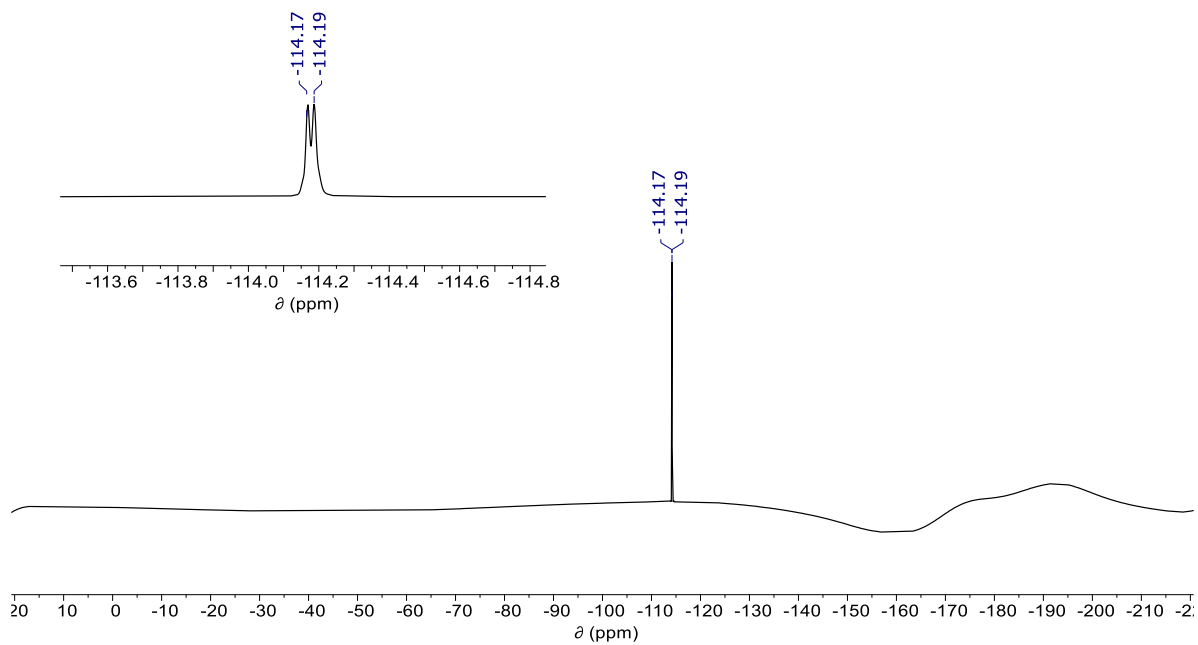
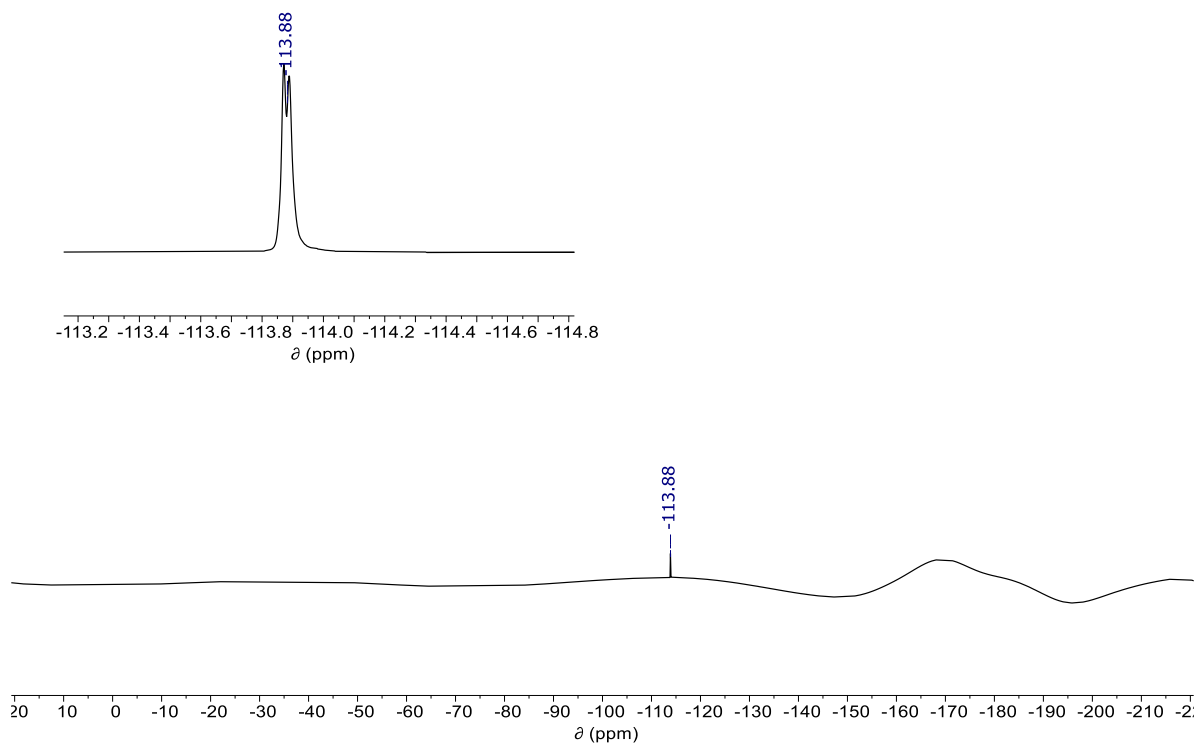**Figure S27**: ^{19}F NMR (471 MHz) of **fluor[11+1]CPP** in CD$_2$Cl$_2$ at room temperature.

Figure S28: ^{19}F NMR (471 MHz) of **fluor[11+1]CPP** in *d*-DMSO at room temperature.
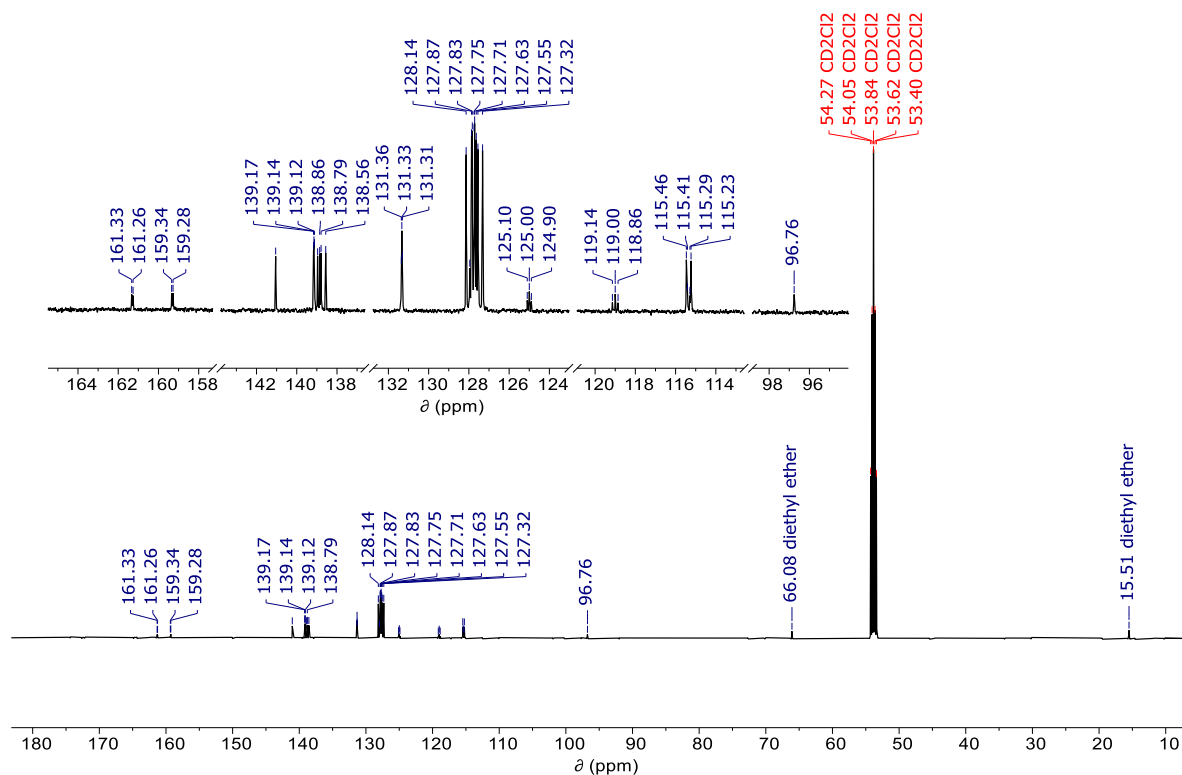
Figure S29: ^{13}C NMR (126 MHz) of **fluor[11+1]CPP** in CD$_2$Cl$_2$ at room temperature.
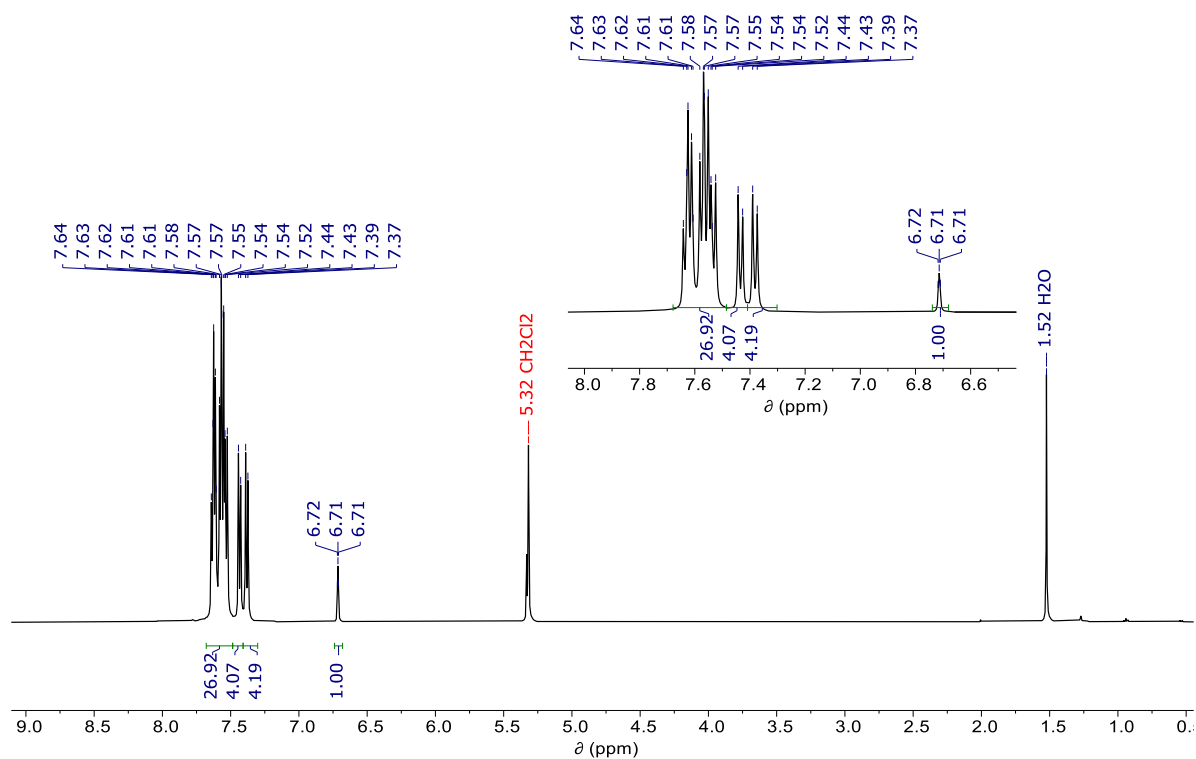
Figure S30: ^{1}H NMR (500 MHz) of *m*[9+1]CPP in CD$_2$Cl$_2$ at room temperature.
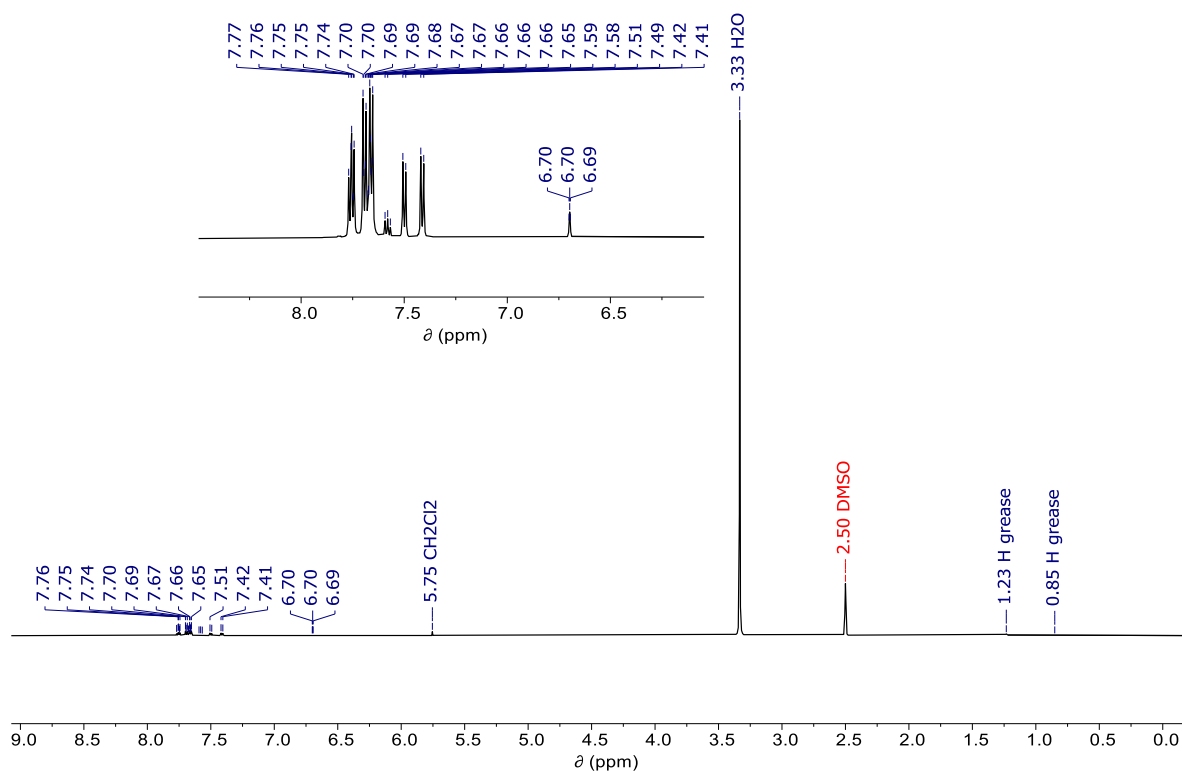
Figure S31: ^{1}H NMR (600 MHz) of *m*[9+1]CPP in *d*-DMSO at room temperature.
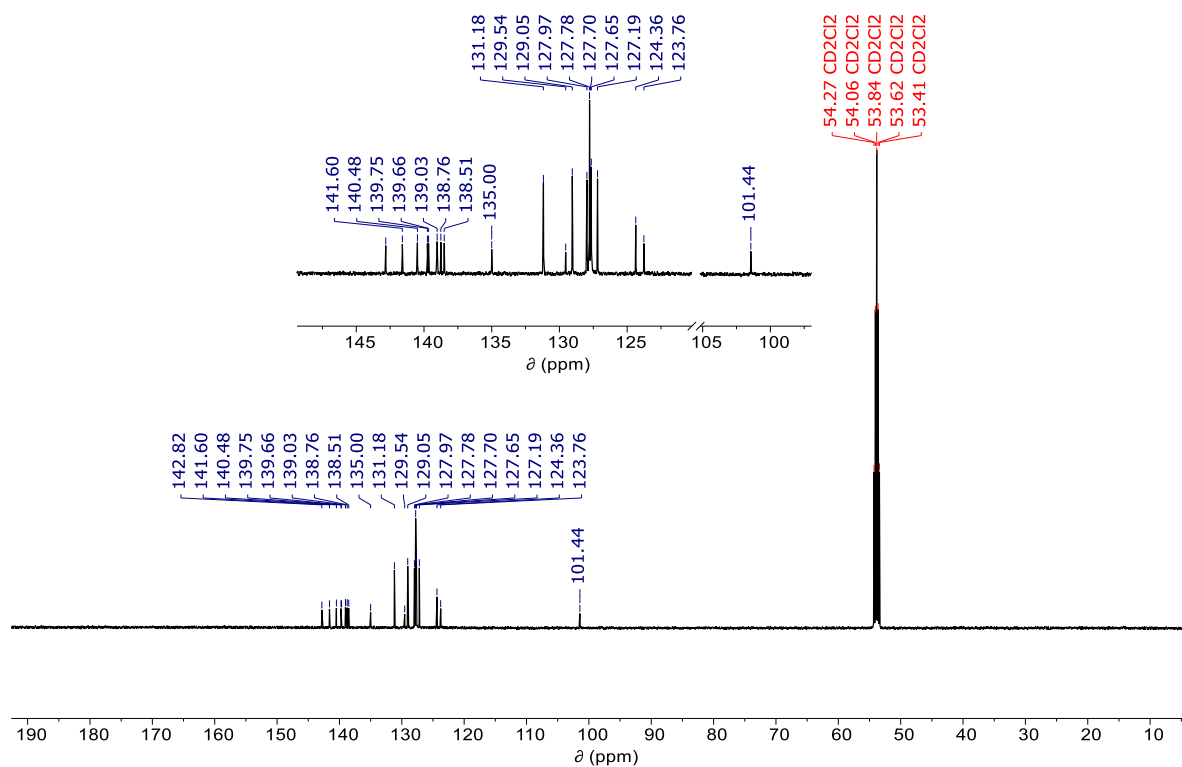
Figure S32: ^{13}C NMR (126 MHz) of *m*[9+1]CPP in CD$_2$Cl$_2$ at room temperature.

30
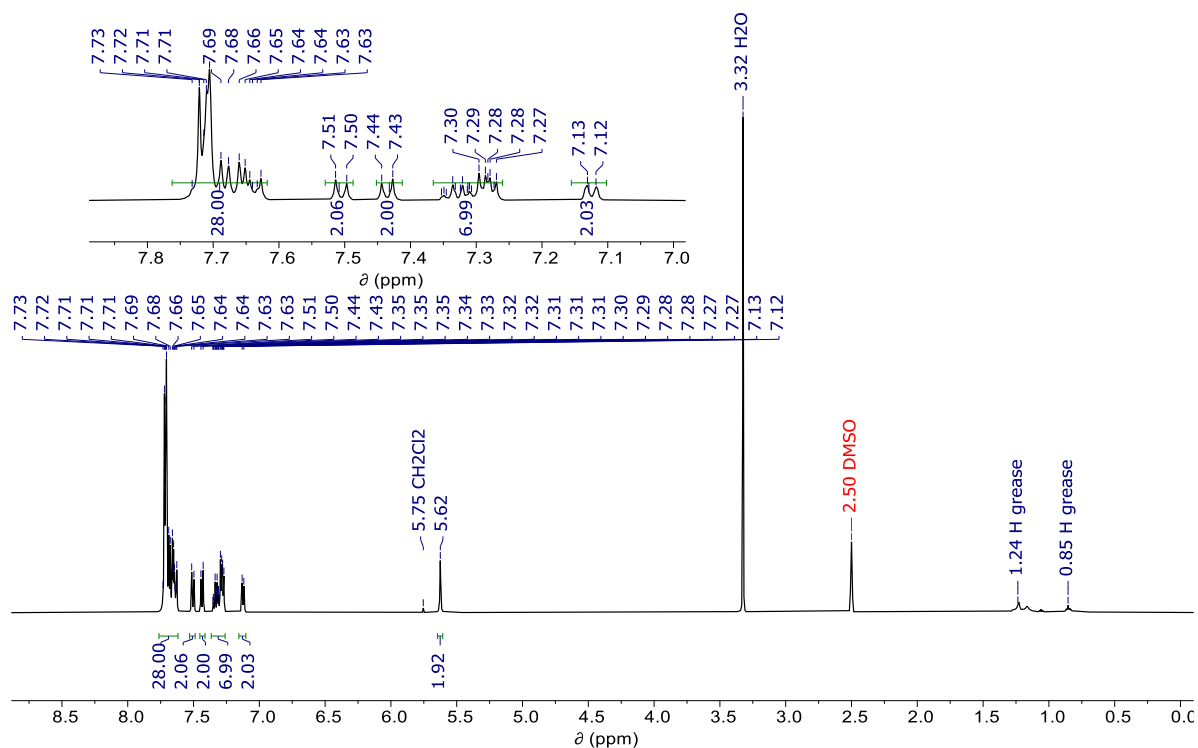
Figure S33: ^{1}H NMR (500 MHz) of **[9+1]CPP-BnAz** in *d*-DMSO at room temperature.

Figure S34: ^{13}C NMR (126 MHz) of **[9+1]CPP-BnAz** in *d*-DMSO at room temperature.

31

Figure S35: ¹H NMR (500 MHz) of **[11+1]CPP-BnAz** in *d*-DMSO at room temperature.

Figure S36: ¹³C NMR (126 MHz) of **[11+1]CPP-BnAz** in *d*-DMSO at room temperature.
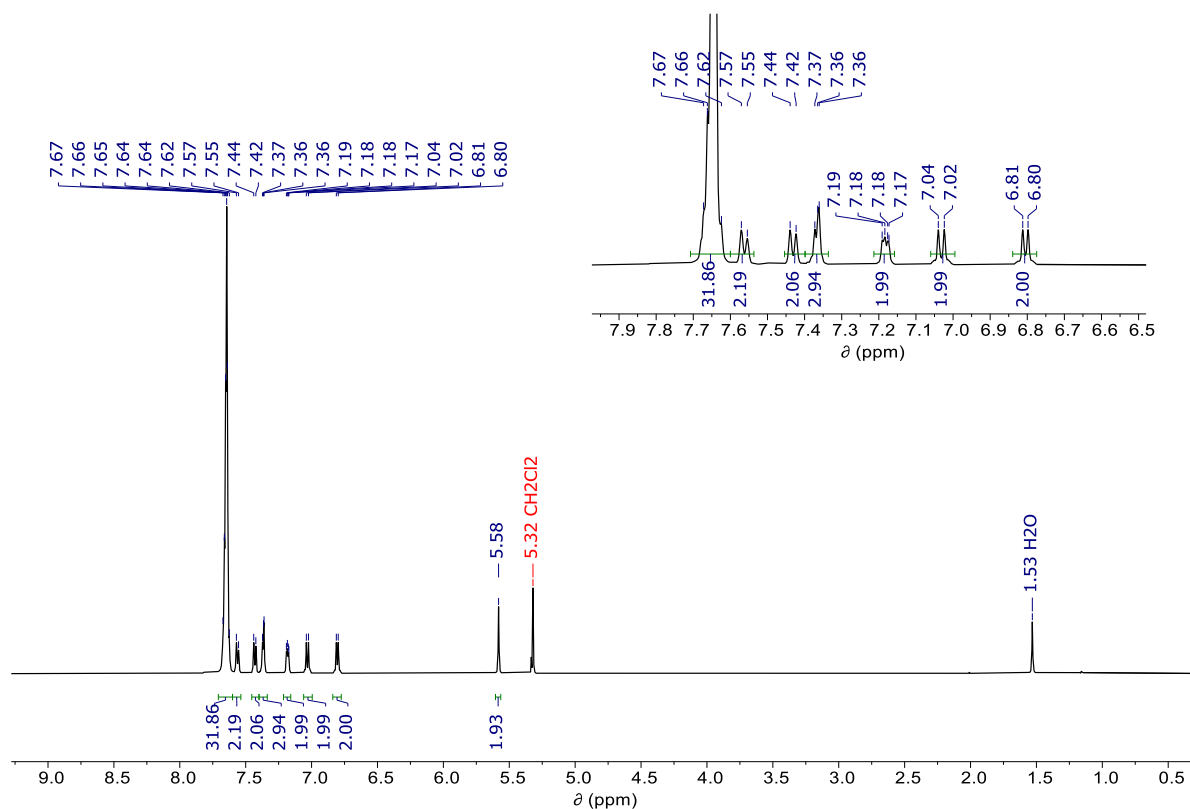
Figure S37: ^{1}H NMR (500 MHz) of **fluor[11+1]CPP-BnAz** in CD$_2$Cl$_2$ at room temperature.
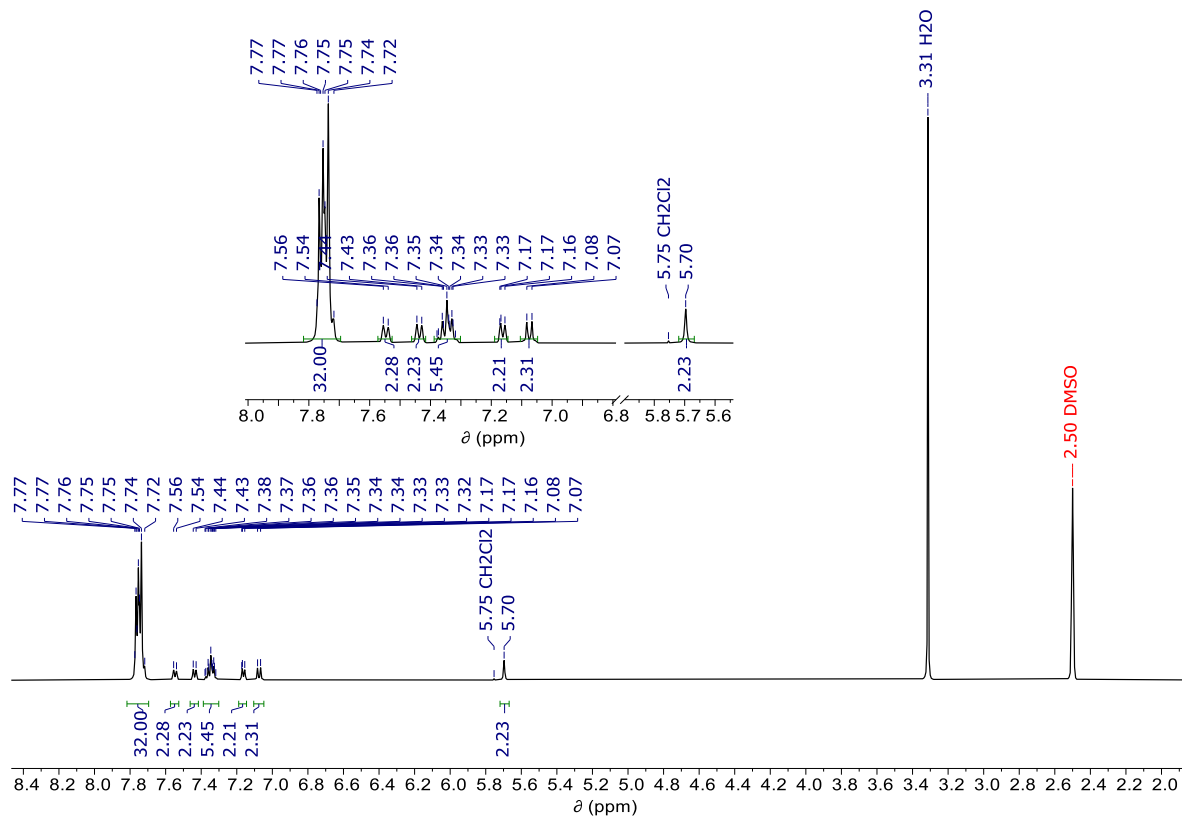
Figure S38: ^{1}H NMR (500 MHz) of **fluor[11+1]CPP-BnAz** in *d*-DMSO at room temperature.
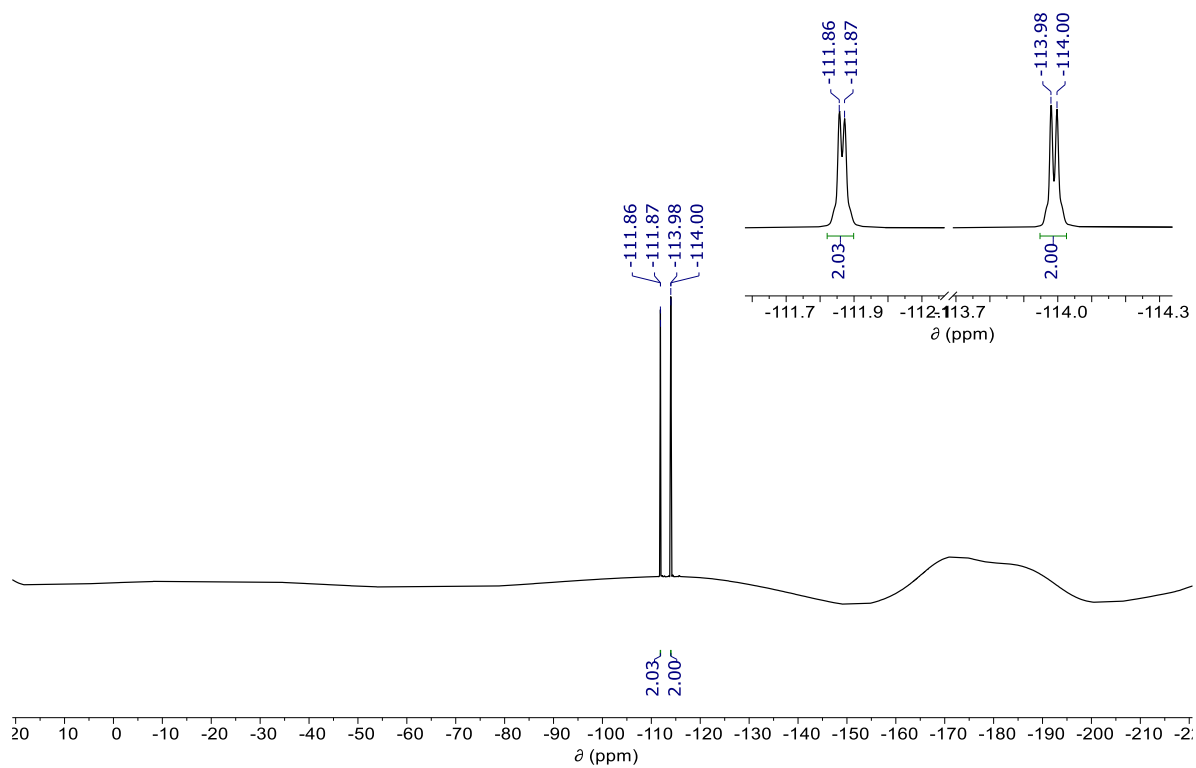
Figure S39: ^{19}F NMR (471 MHz) of **fluor[11+1]CPP-BnAz** in CD$_2$Cl$_2$ at room temperature.
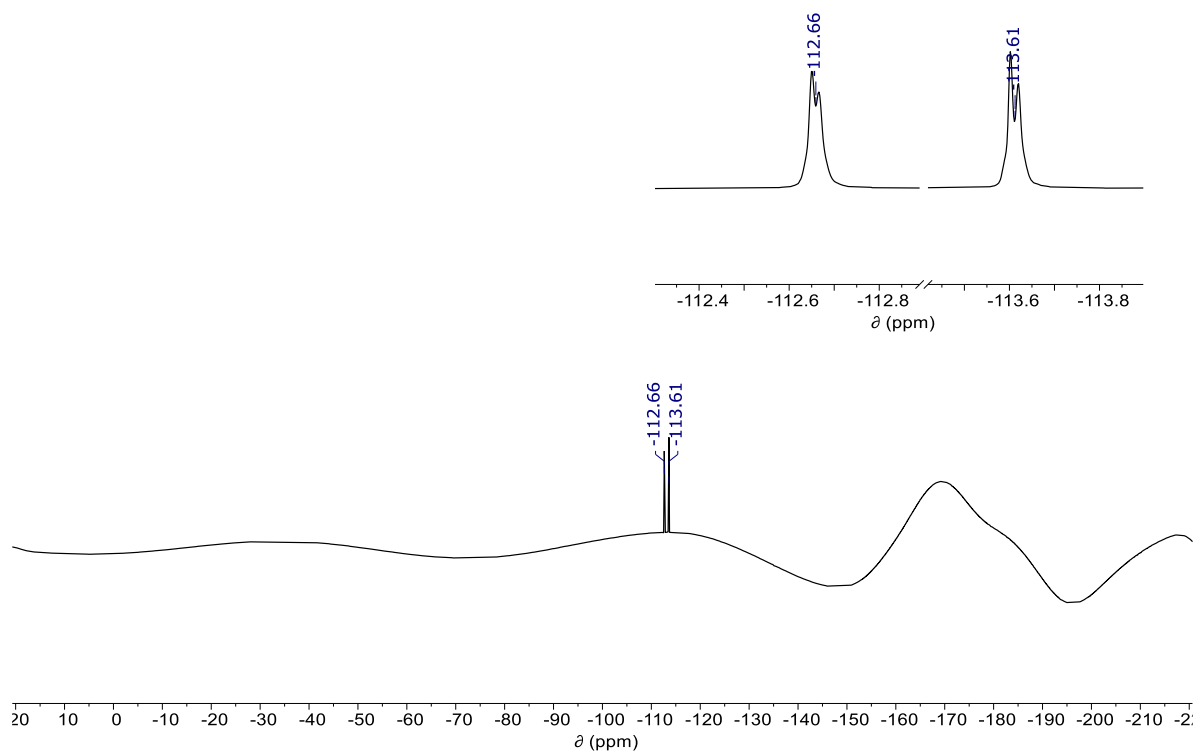
Figure S40: ^{19}F NMR (471 MHz) of **fluor[11+1]CPP-BnAz** in *d*-DMSO at room temperature.
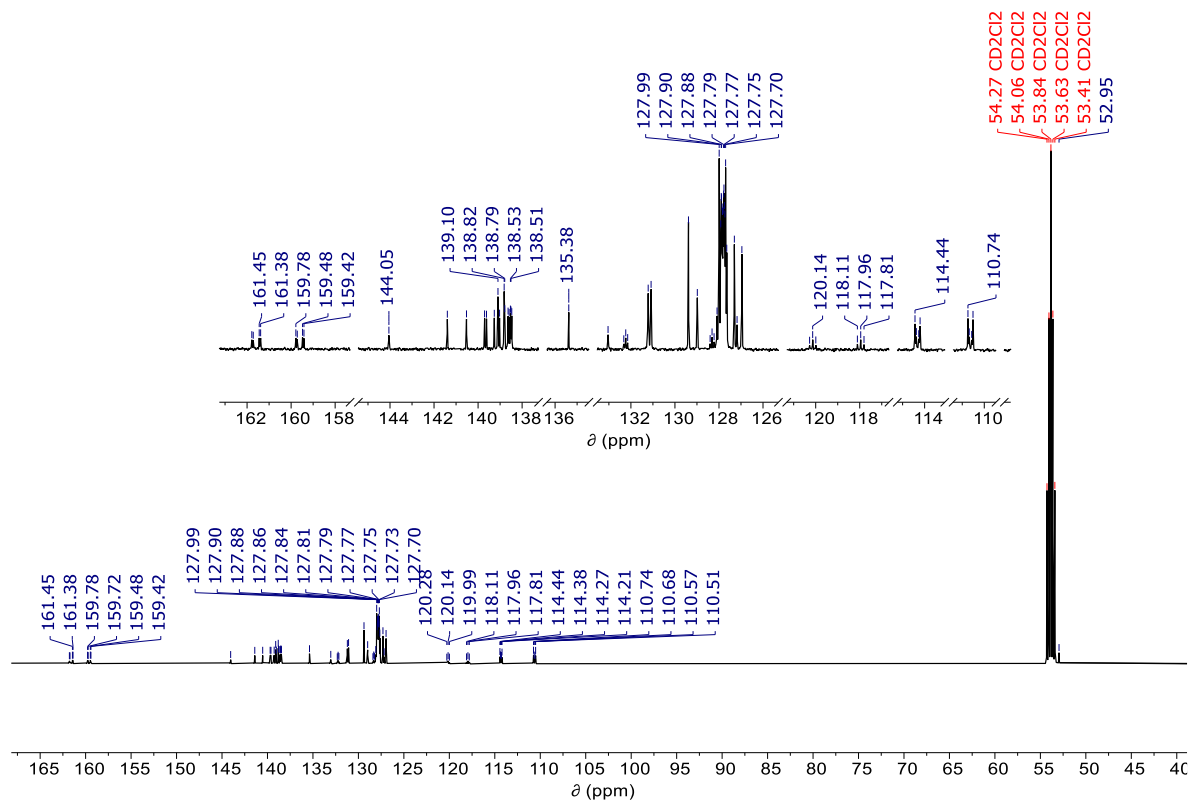
Figure S41: ^{13}C NMR (126 MHz) of **fluor[11+1]CPP-BnAz** in CD_2Cl_2 at room temperature.
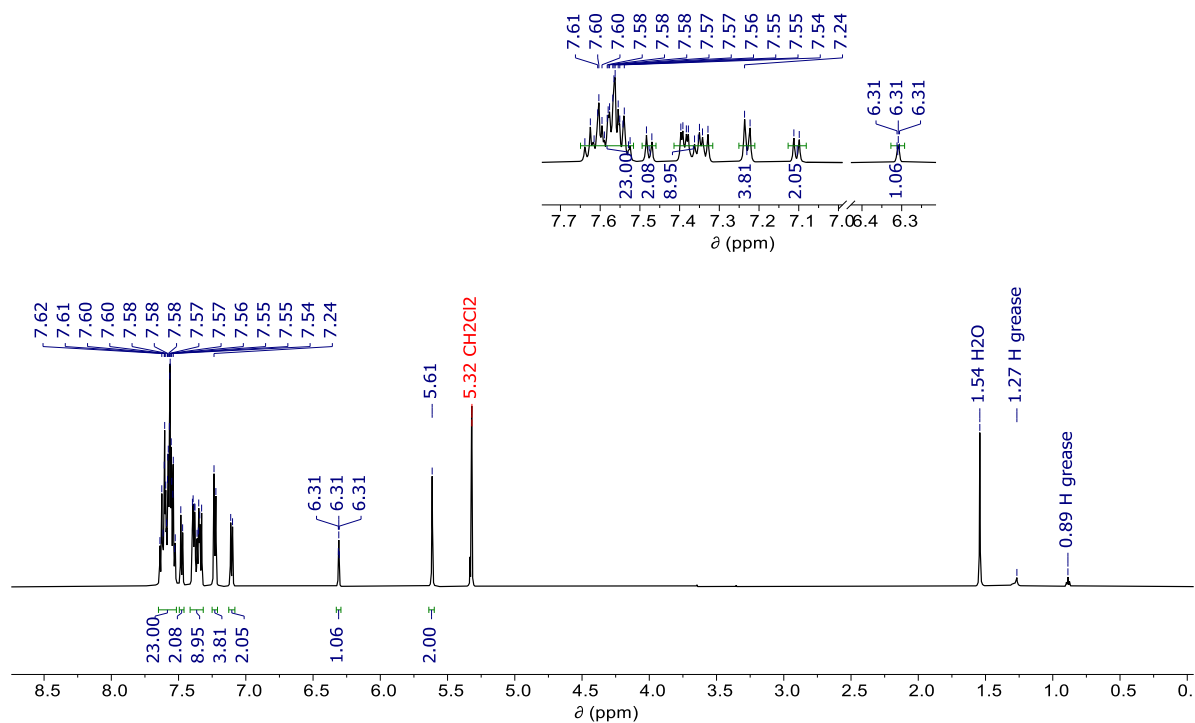
Figure S42: ^{1}H NMR (600 MHz) of *m*[9+1]CPP-BnAz in CD_2Cl_2 at room temperature.
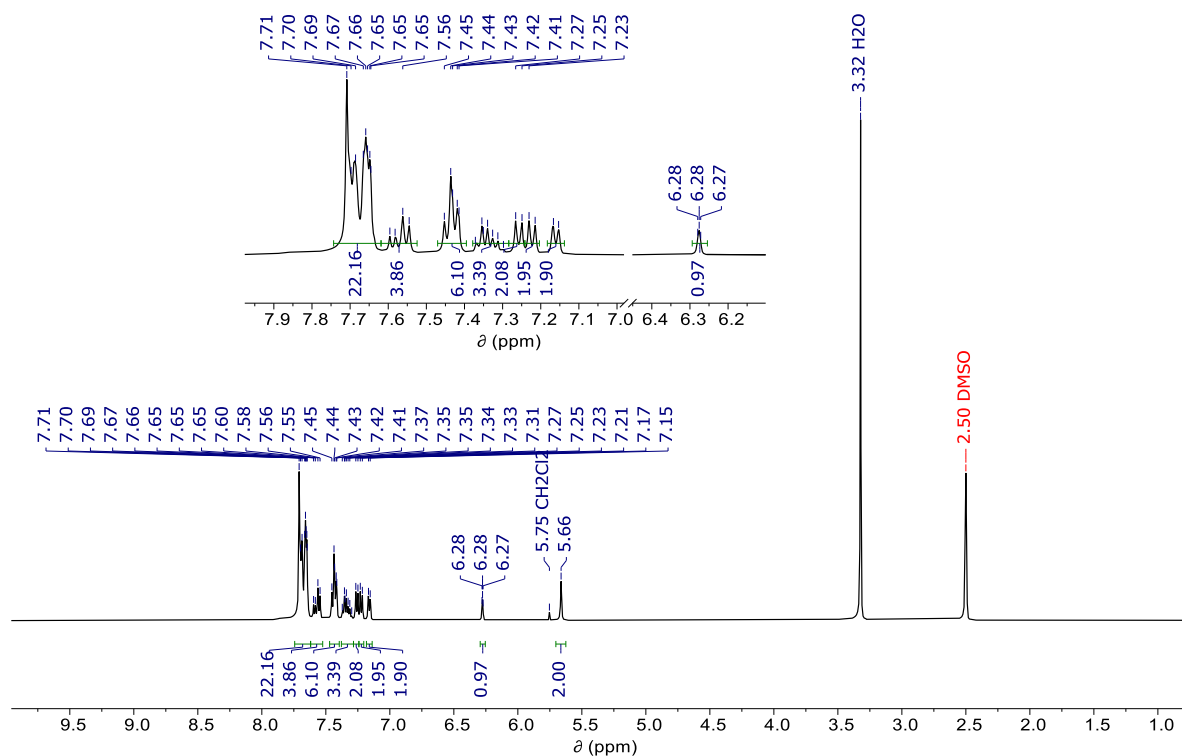
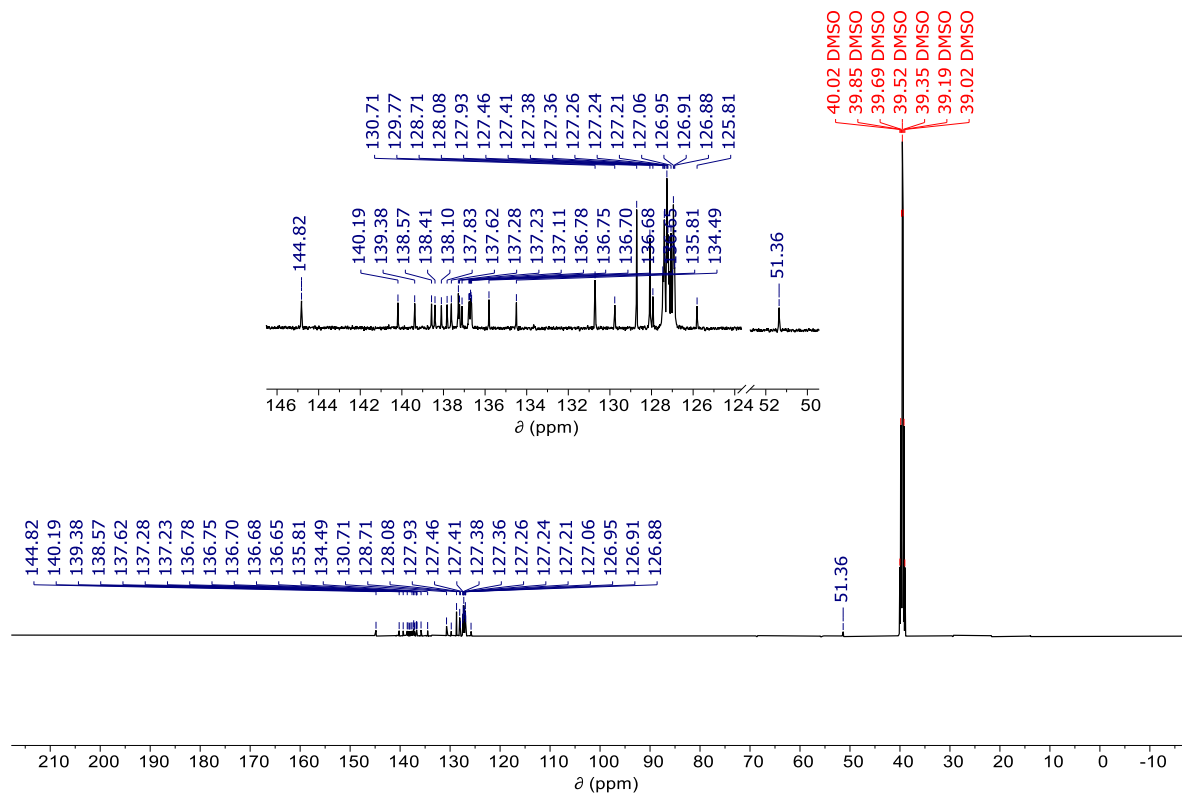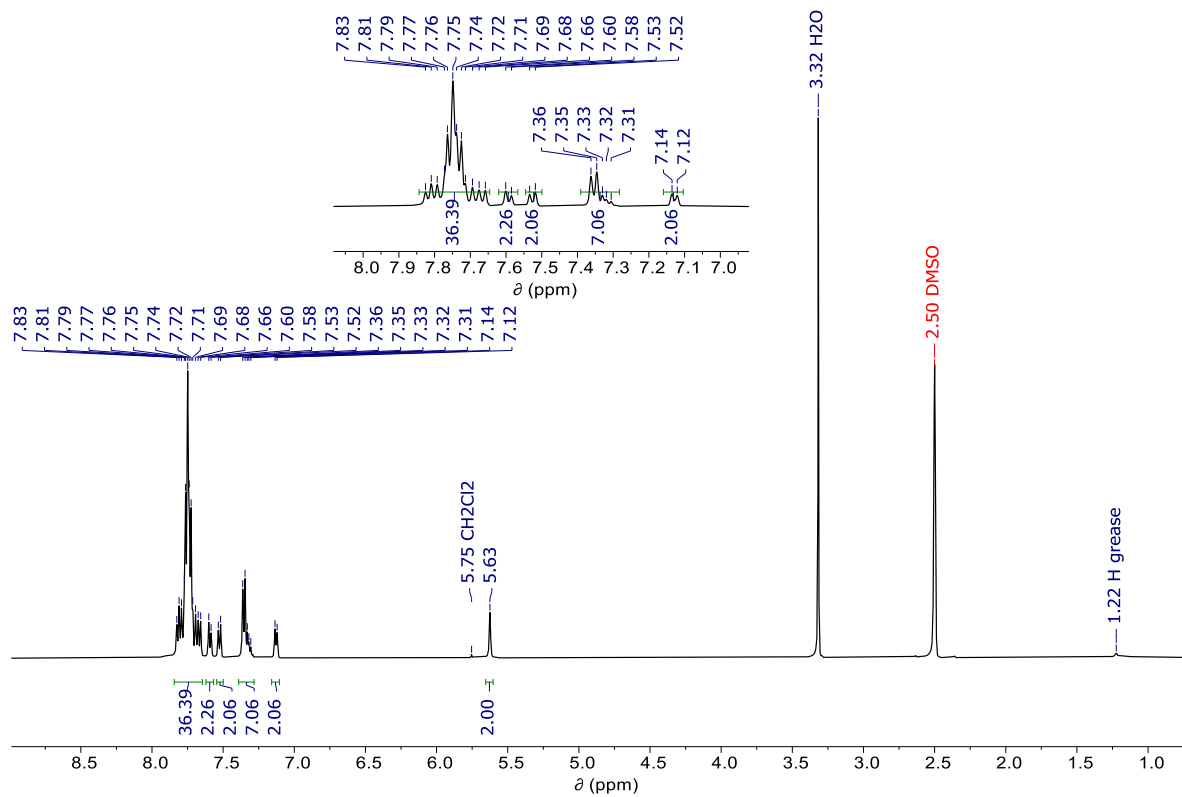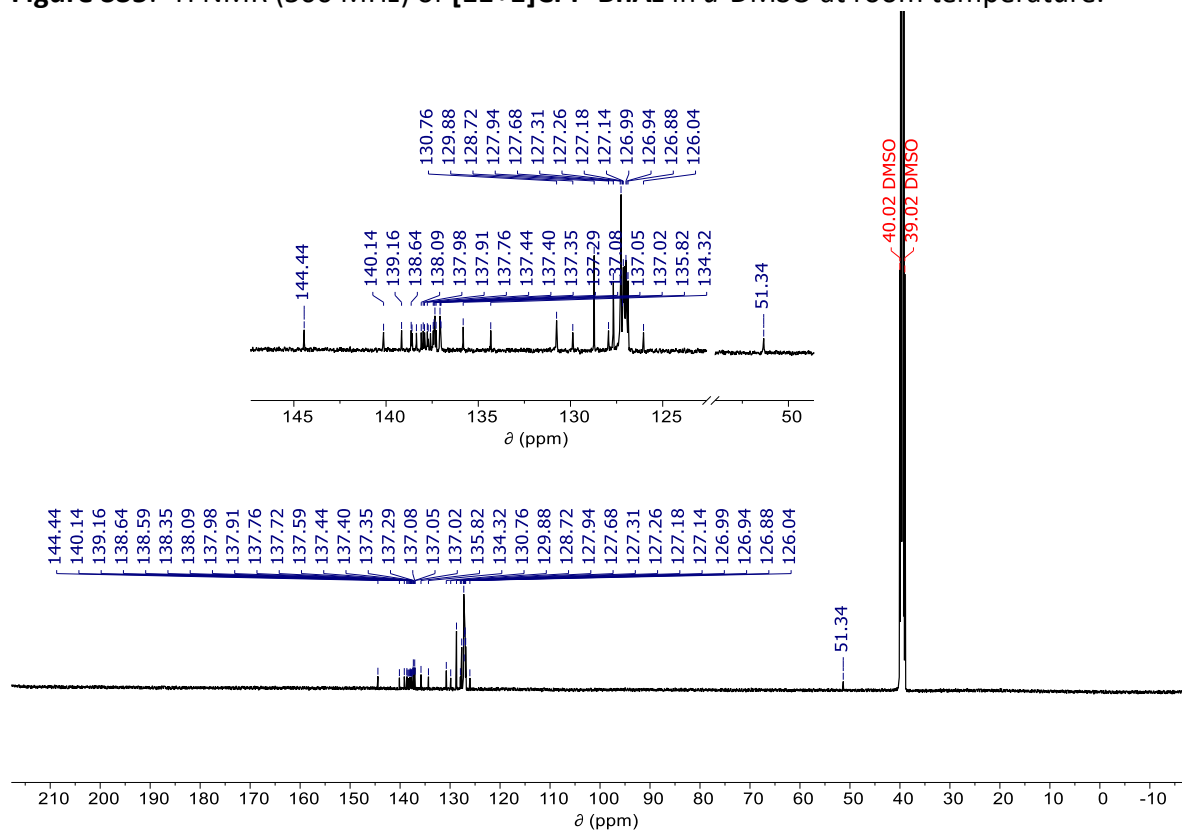**Figure S43**: ^{1}H NMR (500 MHz) of *m*[9+1]CPP-BnAz in *d*-DMSO at room temperature.
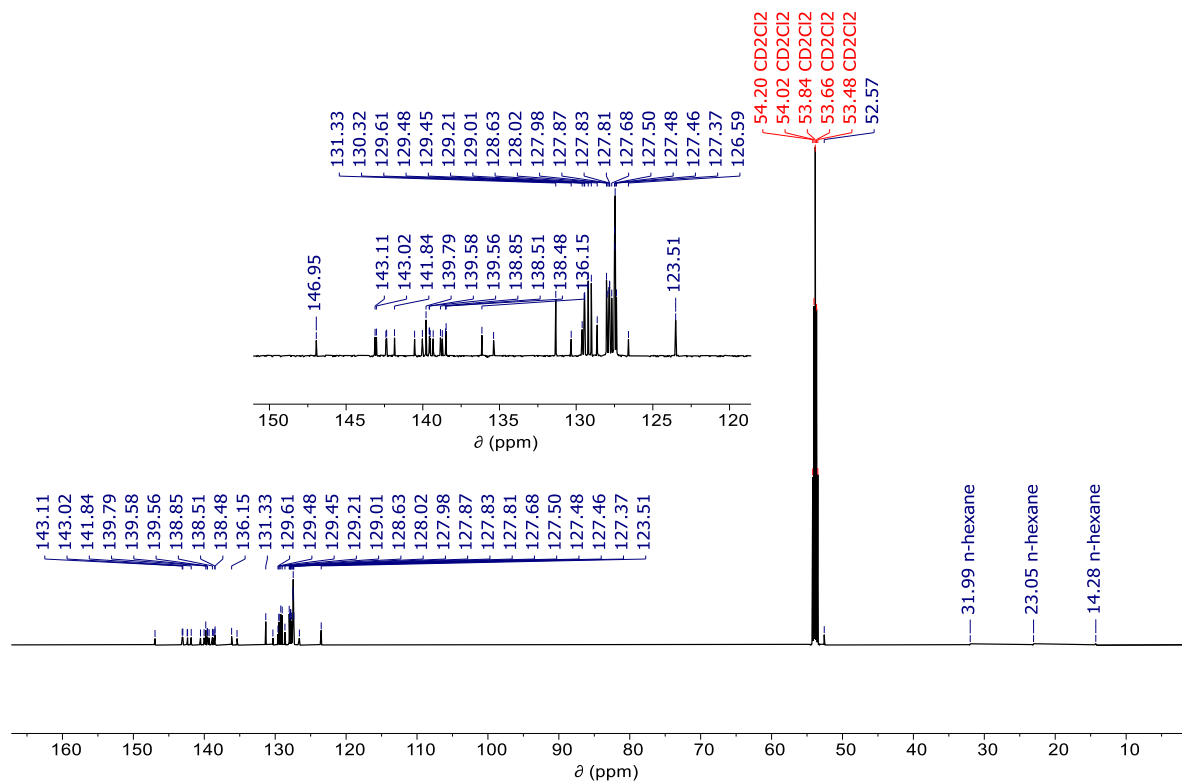
Figure S44: ^{13}C NMR (151 MHz) of *m*[9+1]CPP-BnAz in CD$_2$Cl$_2$ at room temperature.

4. Photophysical characterization

For molar absorptivity measurements, the compound of interest was first dissolved at known concentration using volumetric glassware. This solution was then added incrementally to a cuvette containing a known amount of solvent and absorbance measurements were taken after each addition. Three trials were performed for each compound.

[9+1]CPP molar absorptivity / DMSO

$\lambda_{max,abs}$ = 351 nm	
trial	**slope ($M^{-1} cm^{-1}$)**
1	1.3×10^5
2	1.2×10^5
3	1.2×10^5
avg.	1.2×10^5
std. dev.	0.0087×10^5
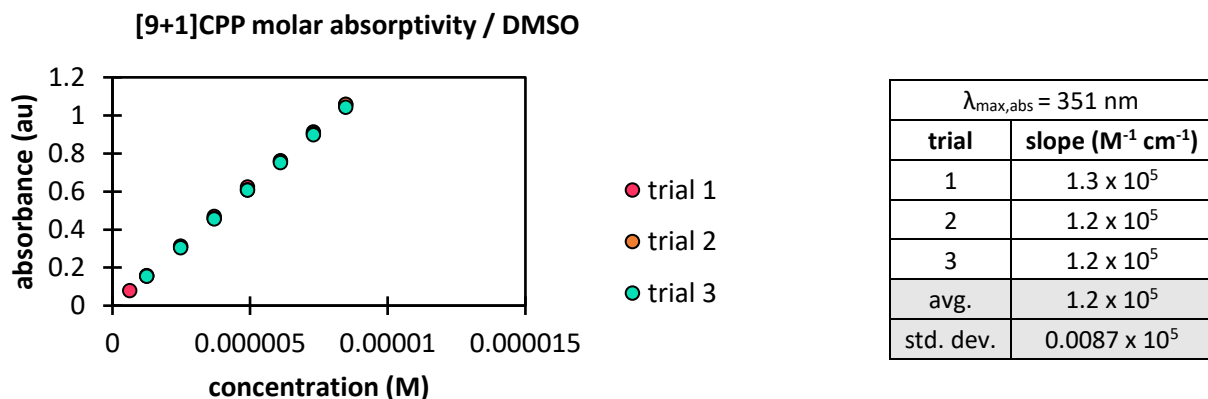
Figure S45. Beer's law plot for **[9+1]CPP** in DMSO.

[9+1]CPP-BnAz molar absorptivity / DMSO

$\lambda_{max,abs}$ = 335 nm	
trial	**slope ($M^{-1} cm^{-1}$)**
1	9.0×10^4
2	9.1×10^4
3	9.1×10^4
avg.	9.1×10^4
std. dev.	0.069×10^4
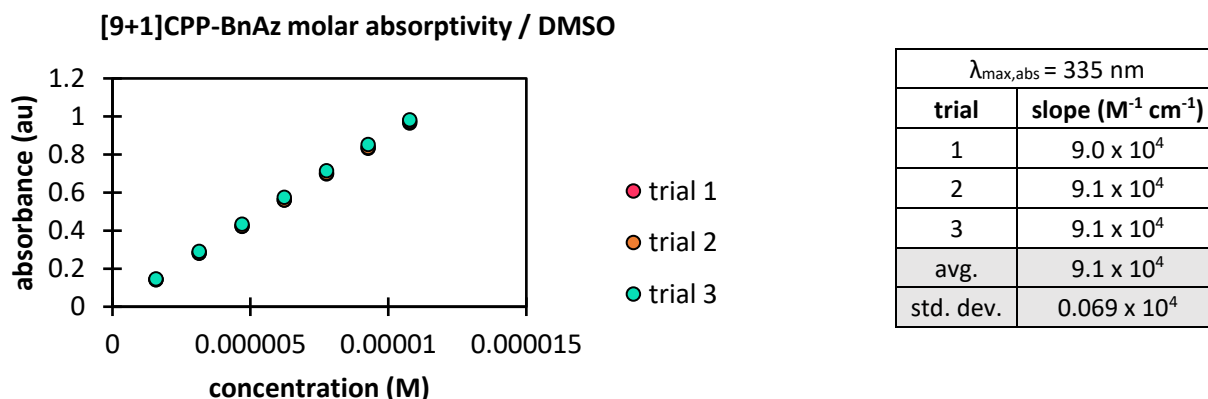
Figure S46. Beer's law plot for **[9+1]CPP-BnAz** in DMSO.

[11+1]CPP molar absorptivity / DMSO

$\lambda_{max,abs}$ = 350 nm	
trial	**slope ($M^{-1} cm^{-1}$)**
1	1.7×10^5
2	1.7×10^5
3	1.7×10^5
avg.	1.7×10^5
std. dev.	0.0023×10^5
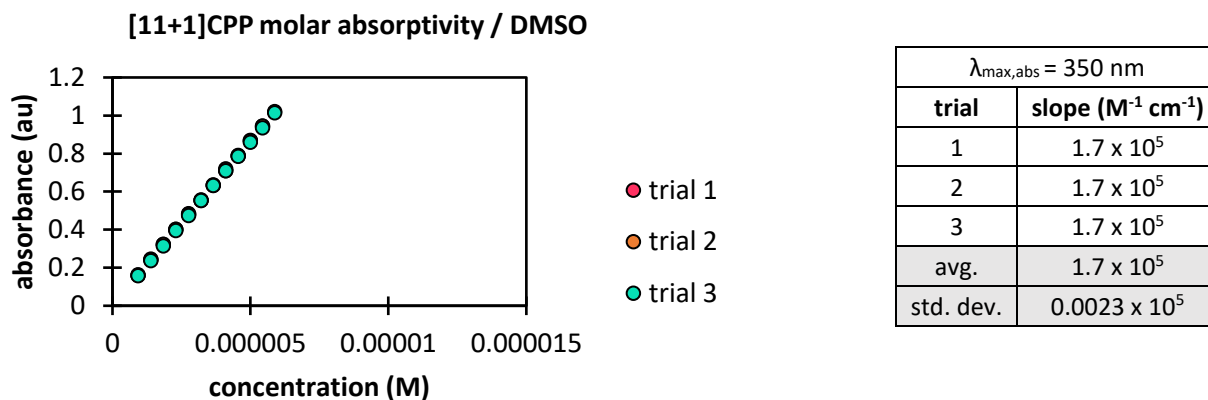
Figure S47. Beer's law plot for **[11+1]CPP** in DMSO.

[11+1]CPP-BnAz molar absorptivity / DMSO
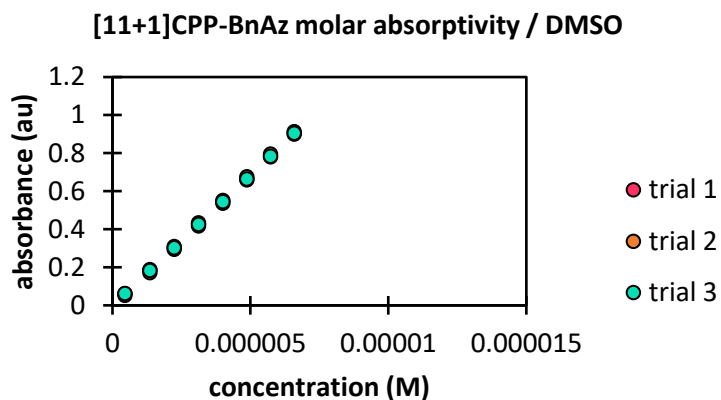
$\lambda_{max,abs}$ = 338 nm	
trial	slope (M^{-1} cm^{-1})
1	1.4×10^5
2	1.4×10^5
3	1.4×10^5
avg.	1.4×10^5
std. dev.	0.0070×10^5

Figure S48. Beer's law plot for [11+1]CPP-BnAz in DMSO.

m[9+1]CPP molar absorptivity / DMSO
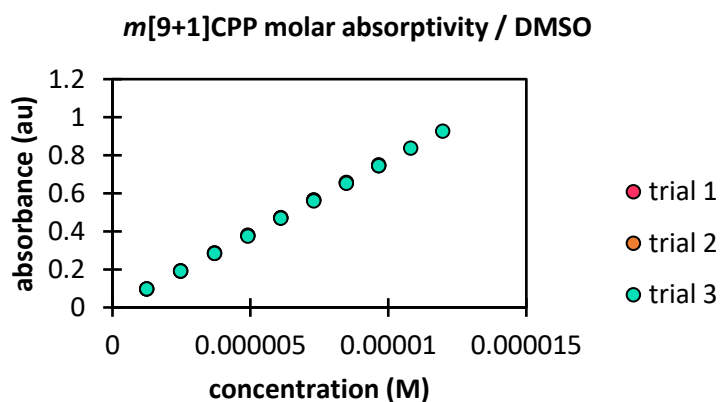
$\lambda_{max,abs}$ = 333 nm	
trial	slope (M^{-1} cm^{-1})
1	7.8×10^4
2	7.8×10^4
3	7.7×10^4
avg.	7.8×10^4
std. dev.	0.039×10^4

Figure S49. Beer's law plot for *m*[9+1]CPP in DMSO.

m[9+1]CPP-BnAz molar absorptivity / DMSO
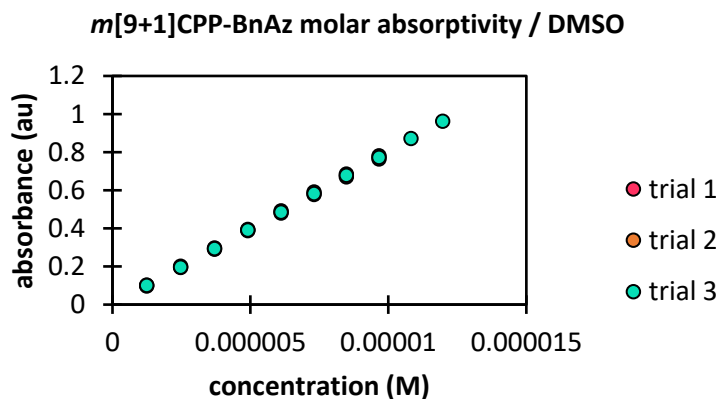
$\lambda_{max,abs}$ = 323 nm	
trial	slope (M^{-1} cm^{-1})
1	7.9×10^4
2	8.1×10^4
3	8.1×10^4
avg.	8.0×10^4
std. dev.	0.082×10^4

Figure S50. Beer's law plot for *m*[9+1]CPP-BnAz in DMSO.

fluor[11+1]CPP molar absorptivity / DCM
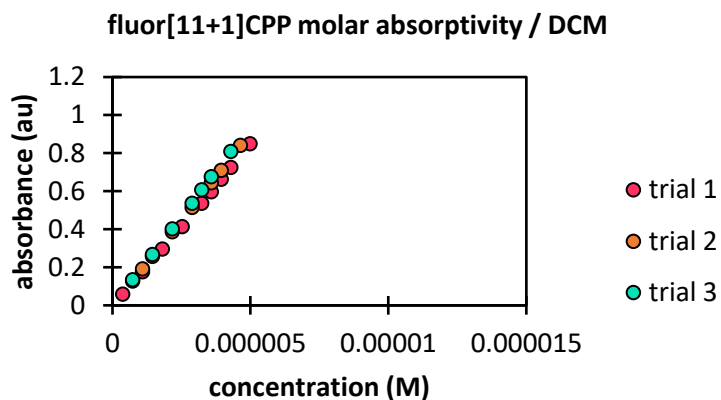
λ_{max,abs} = 337 nm	
trial	**slope (M⁻¹ cm⁻¹)**
1	1.7×10^5
2	1.8×10^5
3	1.9×10^5
avg.	1.8×10^5
std. dev.	0.097×10^5

Figure S51. Beer's law plot for **fluor[11+1]CPP** in DCM.

fluor[11+1]CPP molar absorptivity / DMSO
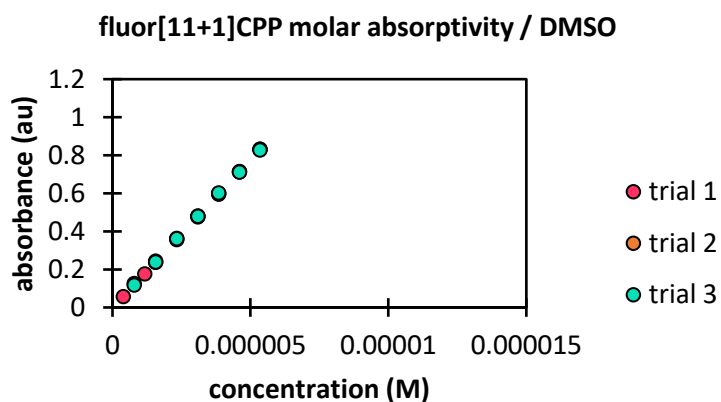
λ_{max,abs} = 343 nm	
trial	**slope (M⁻¹ cm⁻¹)**
1	1.6×10^5
2	1.6×10^5
3	1.6×10^5
avg.	1.6×10^5
std. dev.	0.0073×10^5

Figure S52. Beer's law plot for **fluor[11+1]CPP** in DMSO.

fluor[11+1]CPP-BnAz molar absorptivity / DCM
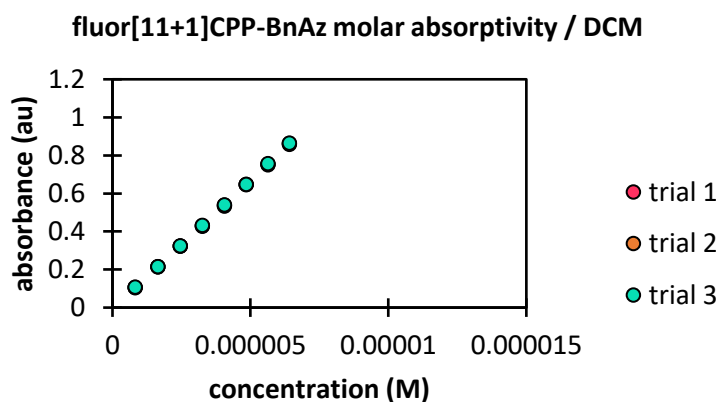
λ_{max,abs} = 328 nm	
trial	**slope (M⁻¹ cm⁻¹)**
1	1.4×10^5
2	1.3×10^5
3	1.4×10^5
avg.	1.4×10^5
std. dev.	0.0052×10^5

Figure S53. Beer's law plot for **fluor[11+1]CPP-BnAz** in DCM.

fluor[11+1]CPP-BnAz molar absorptivity / DMSO
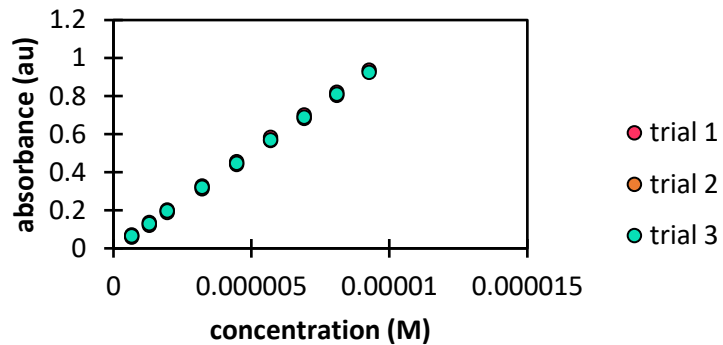
$\lambda_{max,abs}$ = 336 nm	
trial	**slope (M^{-1} cm^{-1})**
1	1.0×10^5
2	1.0×10^5
3	1.0×10^5
avg.	1.0×10^5
std. dev.	0.0045×10^5

Figure S54. Beer's law plot for **fluor[11+1]CPP-BnAz** in DMSO.

Quantum yield measurements were performed using the method described in "A Guide to Recording Fluorescence Quantum Yields" by Horiba Scientific.[5] The internal standards used were quinine sulfate (0.1 M H_2SO_4, aqueous, lit. value Φ = 0.60, fluorescence signal integrated from 400-600 nm) and anthracene (ethanol, lit. value Φ = 0.27, fluorescence signal integrated from 360-480 nm). For fluorescence measurements, all compounds were excited at a wavelength of 340 nm with consistent excitation and emission slit widths of 1 nm. Absorbance values plotted below were as measured at 340 nm. Fluorescence signal integrations for compounds of interest are listed below:

Table S1: Compound integration ranges for each [n+1]CPP and [n+1]CPP-BnAz in DMSO and DCM.

compound of interest	integration range (DCM, nm)	integration range (DMSO, nm)
[9+1]CPP	400 – 600	400 – 600
[9+1]CPP-BnAz	400 – 600	400 – 600
[11+1]CPP	measured previously[2]	400 – 600
[11+1]CPP-BnAz	400 – 600	400 – 600
m[9+1]CPP	390 – 590	390 – 590
m[9+1]CPP-BnAz	350 – 550	350 – 550
fluor[11+1]CPP	390 – 600	390 – 700
fluor[11+1]CPP-BnAz	390 – 600	400 – 600

Figure S55. Quantum yield plot for **[9+1]CPP**.

Table S2: Quantum yield data for **[9+1]CPP**.

compound	solvent	slope	Φ w.r.t. quinine	Φ w.r.t. anthracene	avg. Φ	std. dev.
quinine	0.1 M H_2SO_4 (aq)	2.32×10^8	0.60 (lit)	0.63	0.62	0.011
anthracene	ethanol	9.48×10^7	0.26	0.27 (lit)	0.26	0.0049
[9+1]CPP	DCM	2.50×10^8	0.74	0.78	0.76	0.014
[9+1]CPP	DMSO	2.06×10^8	0.66	0.69	0.67	0.013

Figure S56. Quantum yield plot for **[9+1]CPP-BnAz**.

Table S3: Quantum yield data for **[9+1]CPP-BnAz**.

compound	solvent	slope	Φ w.r.t. quinine	Φ w.r.t. anthracene	avg. Φ	std. dev.
quinine	0.1 M H_2SO_4 (*aq*)	2.32×10^8	0.60 (lit)	0.63	0.62	0.011
anthracene	ethanol	9.48×10^7	0.26	0.27 (lit)	0.26	0.0049
[9+1]BnAz	DCM	2.14×10^8	0.63	0.67	0.65	0.012
[9+1]BnAz	DMSO	2.13×10^8	0.68	0.72	0.70	0.013
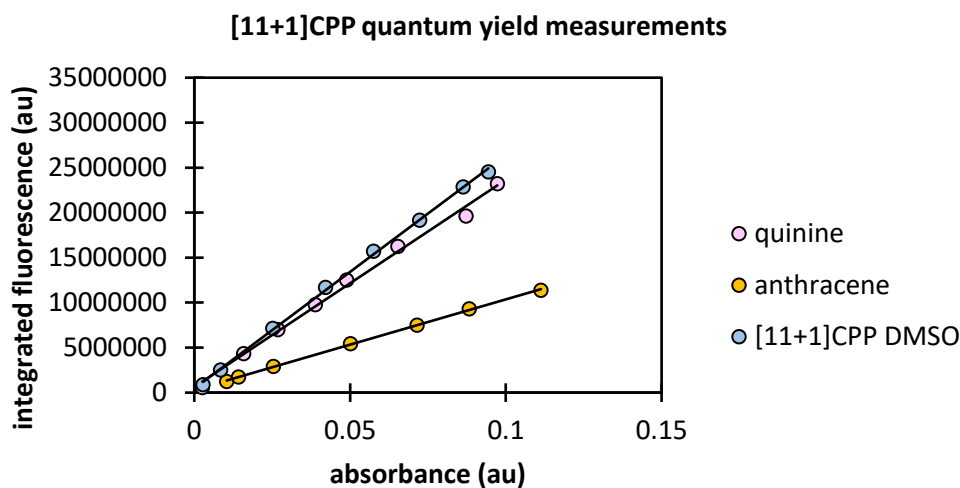
Figure S57. Quantum yield plot for **[11+1]CPP**.

Table S4: Quantum yield data for **[11+1]CPP**.

compound	solvent	slope	Φ w.r.t. quinine	Φ w.r.t. anthracene	avg. Φ	std. dev.
quinine	0.1 M H_2SO_4 (*aq*)	2.30×10^8	0.60 (lit)	0.59	0.60	0.0028
anthracene	ethanol	1.01×10^8	0.27	0.27 (lit)	0.27	0.0013
[11+1]CPP	DMSO	2.59×10^8	0.83	0.82	0.83	0.0038
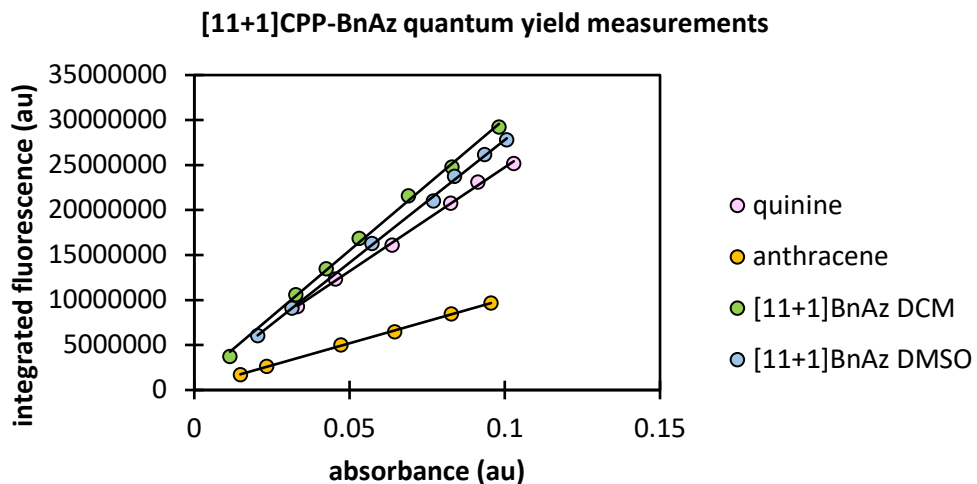
Figure S58. Quantum yield plot for **[11+1]CPP-BnAz**.

Table S5: Quantum yield data for **[11+1]CPP-BnAz**.

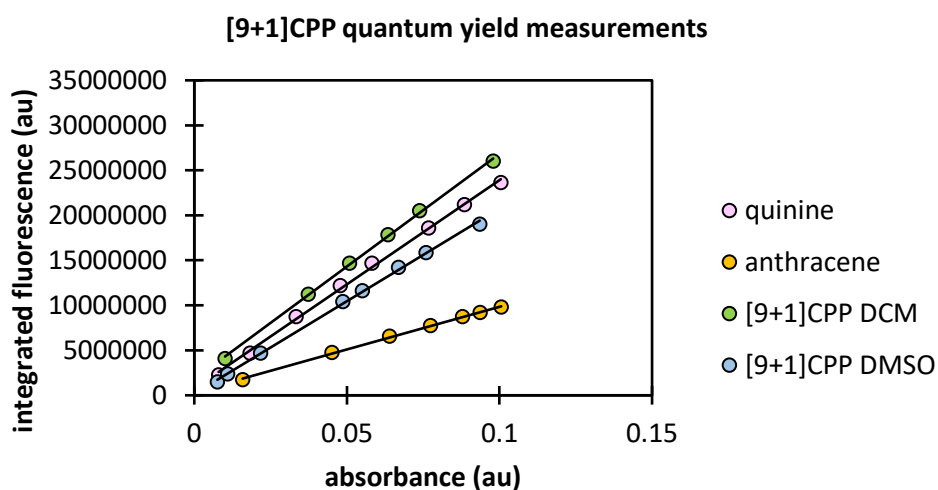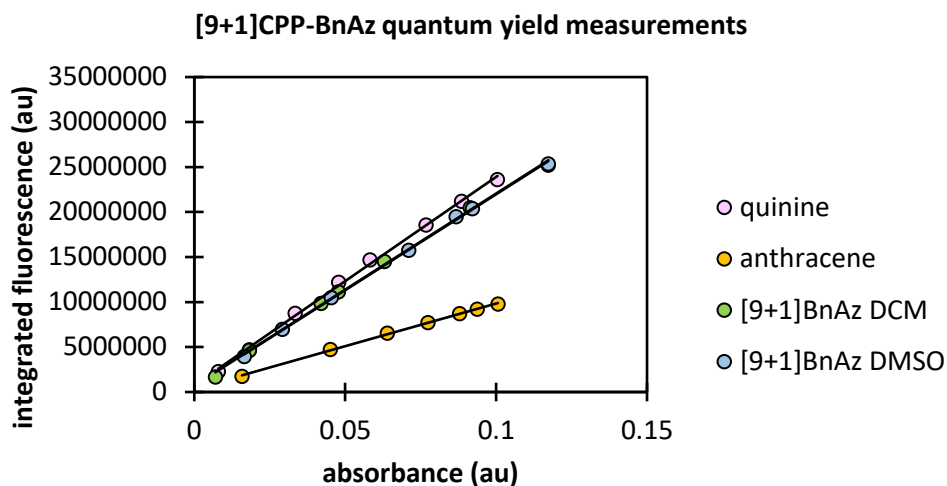| compound	solvent	slope	Φ w.r.t. quinine	Φ w.r.t. anthracene	avg. Φ	std. dev.
quinine	0.1 M H_2SO_4 (*aq*)	2.31×10^8	0.60 (lit)	0.61	0.60	0.0034
anthracene	ethanol	9.81×10^7	0.27	0.27 (lit)	0.27	0.0015
[11+1]BnAz	DCM	2.92×10^8	0.87	0.88	0.87	0.0050
[11+1]BnAz	DMSO	2.73×10^8	0.87	0.88	0.88	0.0049
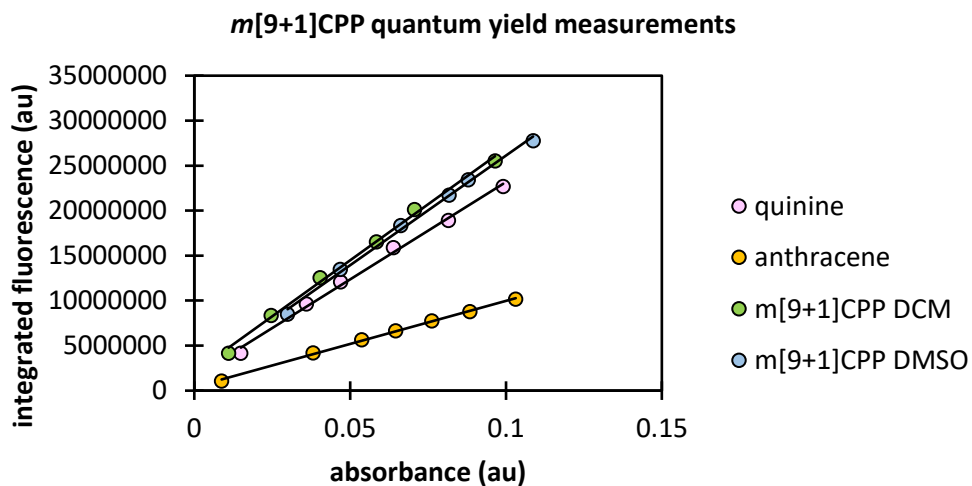
Figure S59. Quantum yield plot for *m*[9+1]CPP.

Table S6: Quantum yield data for *m*[9+1]CPP.

compound	solvent	slope	Φ w.r.t. quinine	Φ w.r.t. anthracene	avg. Φ	std. dev.
quinine	0.1 M H_2SO_4 (*aq*)	2.16×10^8	0.60 (lit)	0.59	0.59	0.0053
anthracene	ethanol	9.57×10^7	0.28	0.27 (lit)	0.27	0.0024
m[9+1]CPP	DCM	2.49×10^8	0.79	0.77	0.78	0.0069
m[9+1]CPP	DMSO	2.44×10^8	0.83	0.81	0.82	0.0073

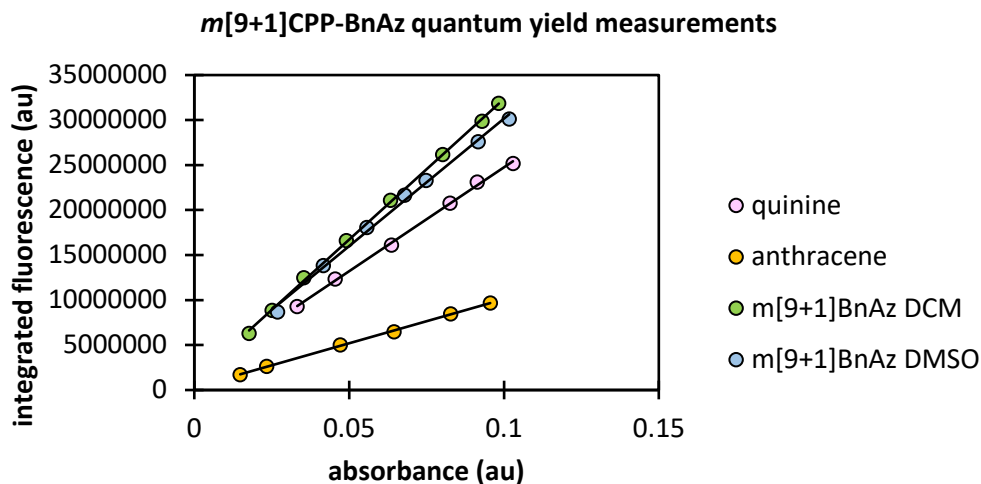**m[9+1]CPP-BnAz quantum yield measurements**

Figure S60. Quantum yield plot for *m*[9+1]CPP-BnAz.

Table S7: Quantum yield data for *m*[9+1]CPP-BnAz.

compound	solvent	slope	Φ w.r.t. quinine	Φ w.r.t. anthracene	avg. Φ	std. dev.
quinine	0.1 M H_2SO_4 (*aq*)	2.31×10^8	0.60 (lit)	0.61	0.60	0.0034
anthracene	ethanol	9.81×10^7	0.27	0.27 (lit)	0.27	0.0015
m[9+1]BnAz	DCM	3.13×10^8	0.93	0.94	0.93	0.0053
m[9+1]BnAz	DMSO	2.83×10^8	0.91	0.92	0.91	0.0052

fluor[11+1]CPP quantum yield measurements
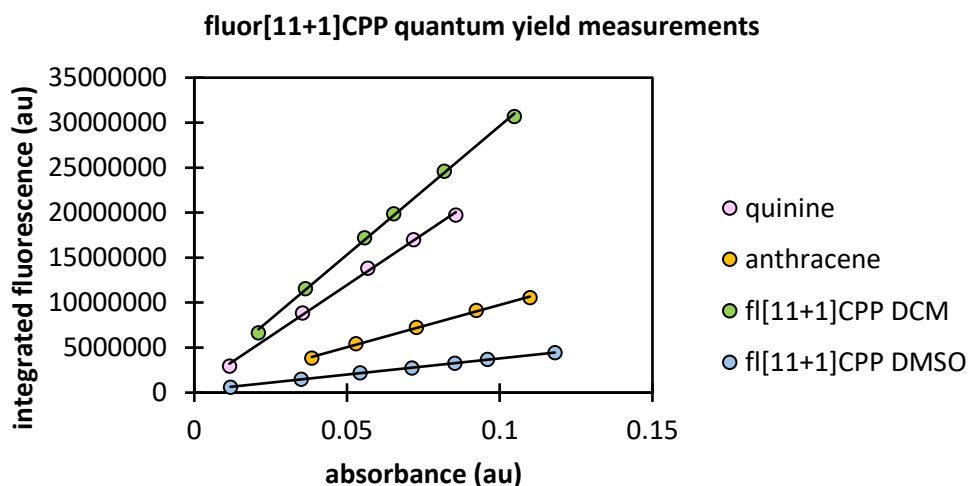
Figure S61. Quantum yield plot for **fluor[11+1]CPP**.

Table S8: Quantum yield data for **fluor[11+1]CPP**.

compound	solvent	slope	Φ w.r.t. quinine	Φ w.r.t. anthracene	avg. Φ	std. dev.
quinine	0.1 M H_2SO_4 (*aq*)	2.27×10^8	0.60 (lit)	0.63	0.61	0.0092
anthracene	ethanol	9.40×10^7	0.26	0.27 (lit)	0.26	0.0040
fluor[11+1]CPP	DCM	2.86×10^8	0.86	0.90	0.88	0.013
fluor[11+1]CPP	DMSO	3.59×10^7	0.12	0.12	0.12	0.0018
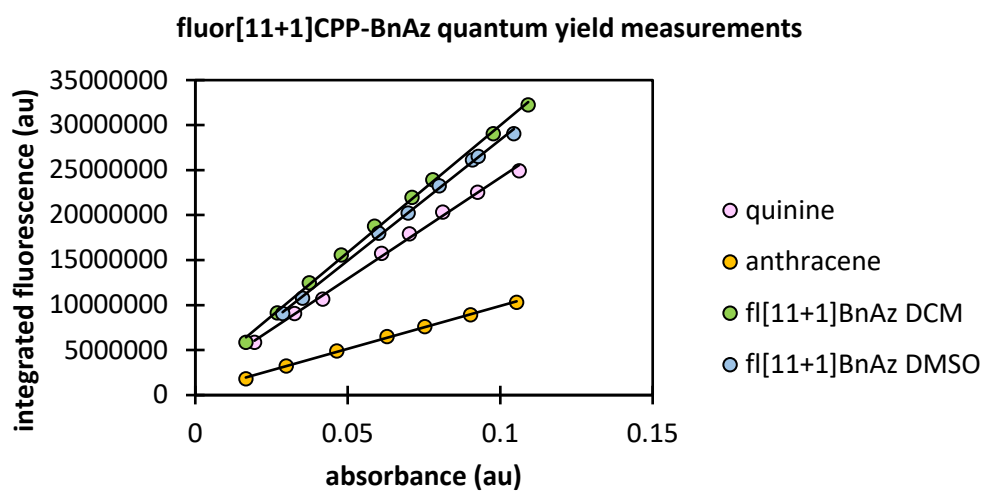
Figure S62. Quantum yield plot for **fluor[11+1]CPP-BnAz**.

Table S9: Quantum yield data for **fluor[11+1]CPP-BnAz**.

compound	solvent	slope	Φ w.r.t. quinine	Φ w.r.t. anthracene	avg. Φ	std. dev.
quinine	0.1 M H_2SO_4 (*aq*)	2.25×10^8	0.60 (lit)	0.61	0.61	0.0038
anthracene	ethanol	9.53×10^7	0.27	0.27 (lit)	0.27	0.0017
fluor[11+1]BnAz	DCM	2.82×10^8	0.86	0.88	0.87	0.0054
fluor[11+1]BnAz	DMSO	2.68×10^8	0.88	0.90	0.89	0.0056

The following absorbance/emission traces show each [*n*+1]CPP and [*n*+1]CPP-BnAz in DCM or DMSO. Each compound of interest was dissolved in the appropriate solvent to an absorbance value of approx. 0.1. This sample was immediately measured in the fluorimeter. For fluorescence measurements, all compounds were excited at a wavelength of 340 nm with consistent excitation and emission slit widths of 1 nm. Absorbance and emission traces for [11+1]CPP were measured previously.[2]
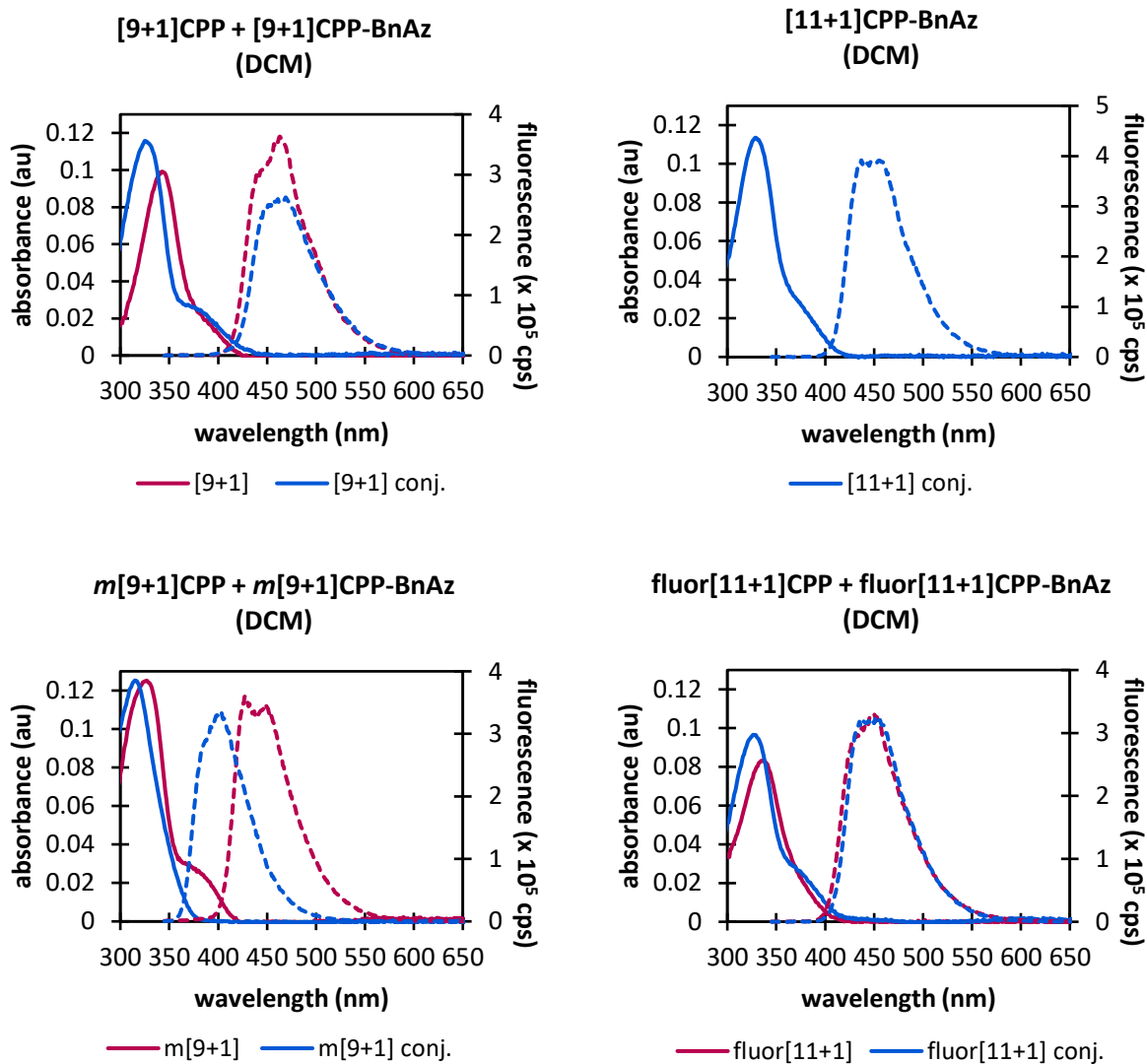

Figure S63. Absorbance and emission traces for [*n*+1]CPPs and their benzyl azide click products in DCM.
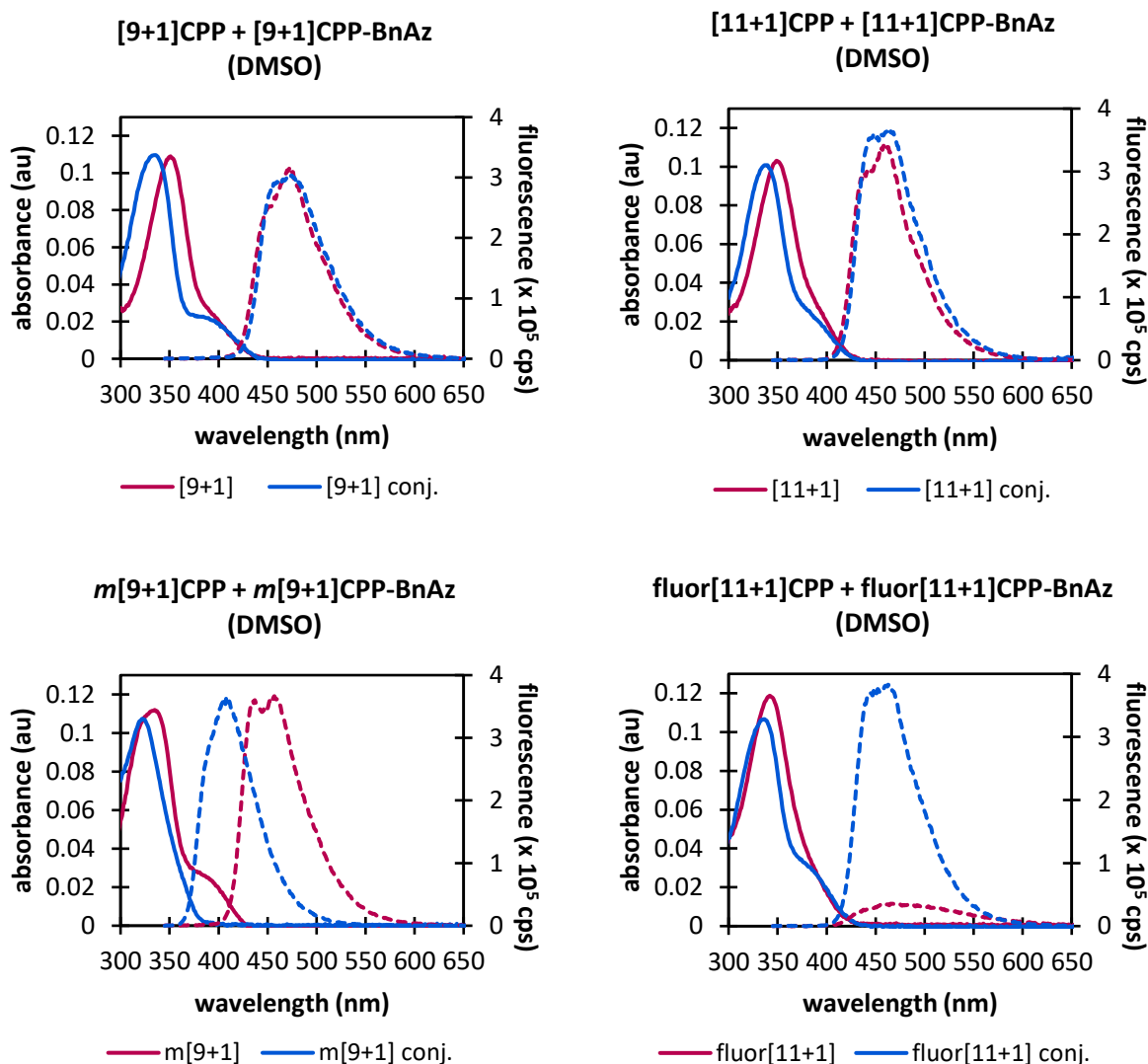
Figure S64. Absorbance and emission traces for [*n*+1]CPPs and their benzyl azide click products in DMSO.

Table S10: wavelengths of maximum absorbance and fluorescence emission for each compound.

compound	$\lambda_{max,abs}$ (nm)		$\lambda_{max,em}$ (nm)	
	DCM	DMSO	DCM	DMSO
[9+1]CPP	343	351	463	473
[9+1]CPP-BnAz	325	335	469	474
[11+1]CPP	341*	350	449*	460
[11+1]CPP-BnAz	329	338	437	464
m[9+1]CPP	327	333	427	457
m[9+1]CPP-BnAz	315	323	403	408
fluor[11+1]CPP	337	343	450	472
fluor[11+1]CPP-BnAz	328	336	451	463

*measured in previous publication.[2]

5. Kinetics Analysis with Benzyl Azide

All kinetics experiments were performed with the same stock of DMSO-d_6 with added dimethyl sulfone as an internal standard (14.5 mM, prepared by dissolving 0.0683 g dimethyl sulfone in 50.0 mL DMSO-d_6 from a fresh bottle with analytical glassware). This solution was kept under inert atmosphere in a Schlenk flask at room temperature. In each experiment, a batch of the [n+1]CPP was dissolved to saturation in the DMSO-d_6 stock solution. The solution was syringe-filtered and then transferred to a clean NMR tube. An initial quantitative ^{1}H NMR (4 scans, pre-scan delay of 25 s, 90° pulse) was collected for the [n+1]CPP. Then, benzyl azide (5-12 equivalents, actual concentration determined by comparison to internal standard) was added to the NMR tube and the solution was thoroughly vortexed to ensure adequate mixing. The tube was placed back in the NMR, the instrument was reshimmed, and set to collect quantitative ^{1}H NMR spectra at specific time increments (longer increments for slower reactions, shorter increments for faster reactions).

At the end of the experiments, the spectra were analyzed with Mestrenova software. Each spectrum was referenced at the DMSO residual solvent peak to 2.50 ppm. Automatic phase correction and baseline correction was applied. The NMRs were stacked and an integrals graph was prepared, with integrations performed over the full width of the peak. Integration widths for each peak were consistent for all experiments for the same [n+1]CPP. The initial concentration for each [n+1]CPP was determined by comparison of its most upfield doublet peak integration to peak integration for the internal standard. Concentration of benzyl azide for all spectra was determined by comparing integration of the benzyl azide peak at approx. 4.44 ppm to the peak integration for the internal standard. Product concentration was determined by comparing integration of the benzylic peak of the [n+1]CPP-BnAz at approx. 5.7 ppm to the peak integration for the internal standard. For all spectra except the initial [n+1]CPP spectrum, the concentration of [n+1]CPP was determined by subtracting the product concentration at that time point from the initial [n+1]CPP concentration.

Having determined the concentrations for each species at each time point, it was possible to plot

$$\frac{1}{[\text{BnAz}]_0 - [\text{CPP}]_0} \times \ln \frac{[\text{CPP}]_0[\text{BnAz}]}{[\text{CPP}][\text{BnAz}]_0}$$

as a function of time. Plotting the reaction until 30% completion* resulted in a linear data curve, the slope of which was taken as the second-order rate constant for the SPAAC reaction between the [n+1]CPP of interest and benzyl azide.

*in two cases, the reaction of **[11+1]CPP** was only monitored until 20% completion due to time constraints on the NMR instrument.
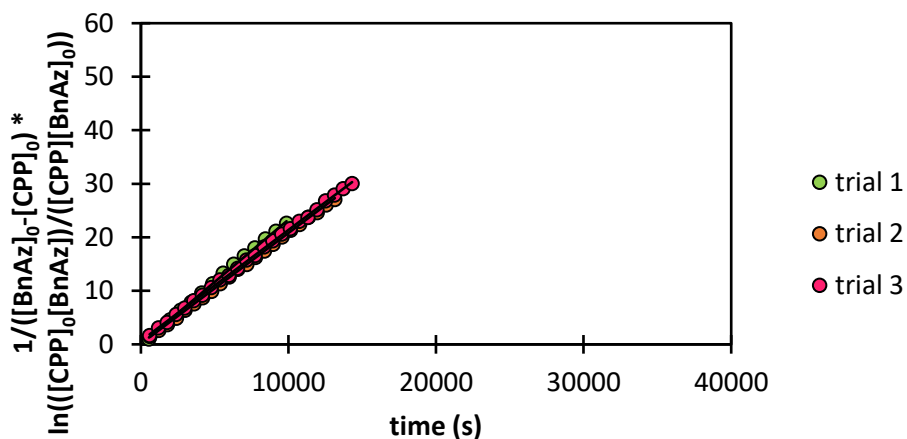
[9+1]CPP + BnAz kinetics analysis

Figure S65. Kinetics analysis for SPAAC reaction of **[9+1]CPP** with benzyl azide in DMSO-d_6.

Table S11: Linear regression and derived second order rate constant for each trial of the SPAAC reaction of **[9+1]CPP** with benzyl azide in DMSO-d_6.

trial	equation of line	second-order rate constant
1	y = 2.33E-03x + 1.21E-02	2.33×10^{-3} M^{-1} s^{-1}
2	y = 2.07E-03x + 1.07E-01	2.07×10^{-3} M^{-1} s^{-1}
3	y = 2.07E-03x + 6.44E-01	2.07×10^{-3} M^{-1} s^{-1}
avg.	-	2.2×10^{-3} M^{-1} s^{-1}
std. dev.	-	0.15×10^{-3} M^{-1} s^{-1}

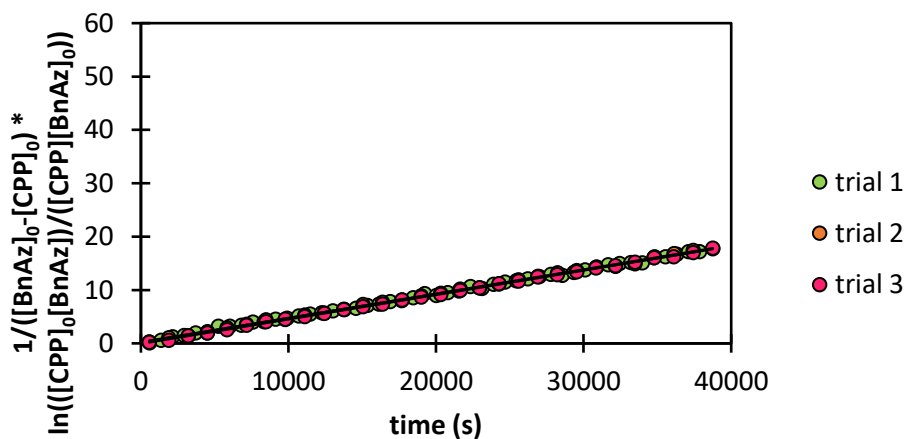## [11+1]CPP + BnAz kinetics analysis

Figure S66. Kinetics analysis for SPAAC reaction of **[11+1]CPP** with benzyl azide in DMSO-d_6.

Table S12: Linear regression and derived second order rate constant for each trial of the SPAAC reaction of **[11+1]CPP** with benzyl azide in DMSO-d_6.

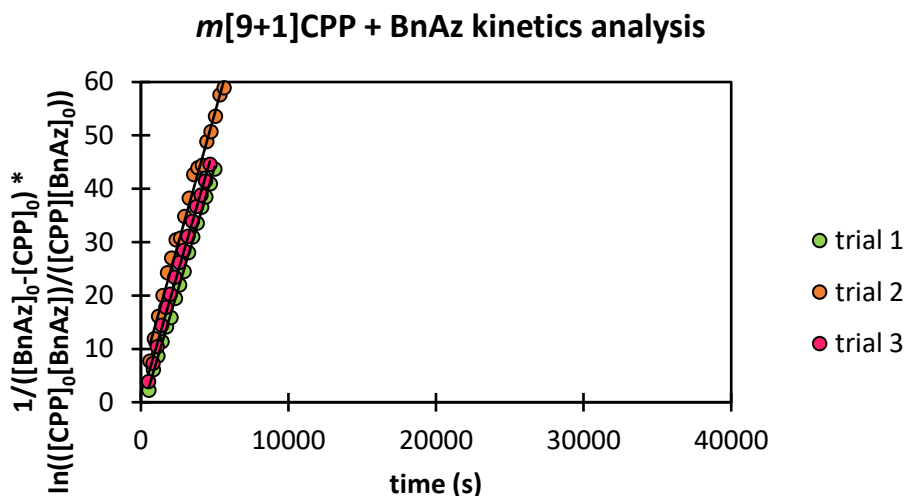| trial	equation of line	second-order rate constant
1	y = 4.50E-04x + 2.32E-01	4.50 x 10^{-4} M^{-1} s^{-1}
2	y = 4.55E-04x + 1.70E-01	4.55 x 10^{-4} M^{-1} s^{-1}
3	y = 4.58E-04x - 4.75E-02	4.58 x 10^{-4} M^{-1} s^{-1}
avg.	-	4.5 x 10^{-4} M^{-1} s^{-1}
std. dev.	-	0.04 x 10^{-4} M^{-1} s^{-1}

Figure S67. Kinetics analysis for SPAAC reaction of *m*[9+1]CPP with benzyl azide in DMSO-d_6.

Table S13: Linear regression and derived second order rate constant for each trial of the SPAAC reaction of *m*[9+1]CPP with benzyl azide in DMSO-d_6.

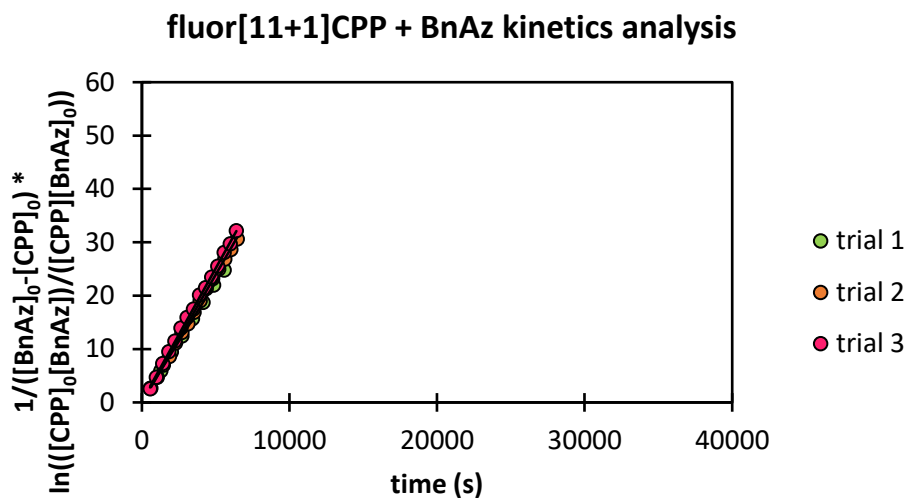| trial	equation of line	second-order rate constant
1	y = 9.26E-03x - 2.19E+00	9.26 x 10^{-3} M^{-1} s^{-1}
2	y = 9.86E-03x + 4.82E+00	9.86 x 10^{-3} M^{-1} s^{-1}
3	y = 9.58E-03x + 3.59E-01	9.58 x 10^{-3} M^{-1} s^{-1}
avg.	-	9.6 x 10^{-3} M^{-1} s^{-1}
std. dev.	-	0.3 x 10^{-3} M^{-1} s^{-1}

fluor[11+1]CPP + BnAz kinetics analysis

Figure S68. Kinetics analysis for SPAAC reaction of **fluor[11+1]CPP** with benzyl azide in DMSO-d_6.

Table S14: Linear regression and derived second order rate constant for each trial of the SPAAC reaction of **fluor[11+1]CPP** with benzyl azide in DMSO-d_6

trial	equation of line	second-order rate constant
1	y = 4.44E-03x + 3.60E-01	4.44×10^{-3} M^{-1} s^{-1}
2	y = 4.80E-03x - 8.65E-02	4.80×10^{-3} M^{-1} s^{-1}
3	y = 4.98E-03x + 2.27E-01	4.98×10^{-3} M^{-1} s^{-1}
avg.	-	4.7×10^{-3} M^{-1} s^{-1}
std. dev.	-	0.3×10^{-3} M^{-1} s^{-1}

6. StrainViz

All input files, fragment geometries, and output files are available for download *via* Figshare at https://figshare.com/projects/Supporting_Information_of_Computational_results_StrainViz_for_Experimental_and_Theoretical_Elucidation_of_SPAAC_Kinetics_for_Strained_Alkyne-Containing_Cycloparaphenylenes/155192. Fragment geometries are shown below and in .xyz format.

Note: one alkyne fragment for each molecule with the smoothest optimization was included to emphasize the local strain between each [*n*+1]CPP and troubleshoot failed optimizations due to linear angles present in alkyne fragments.
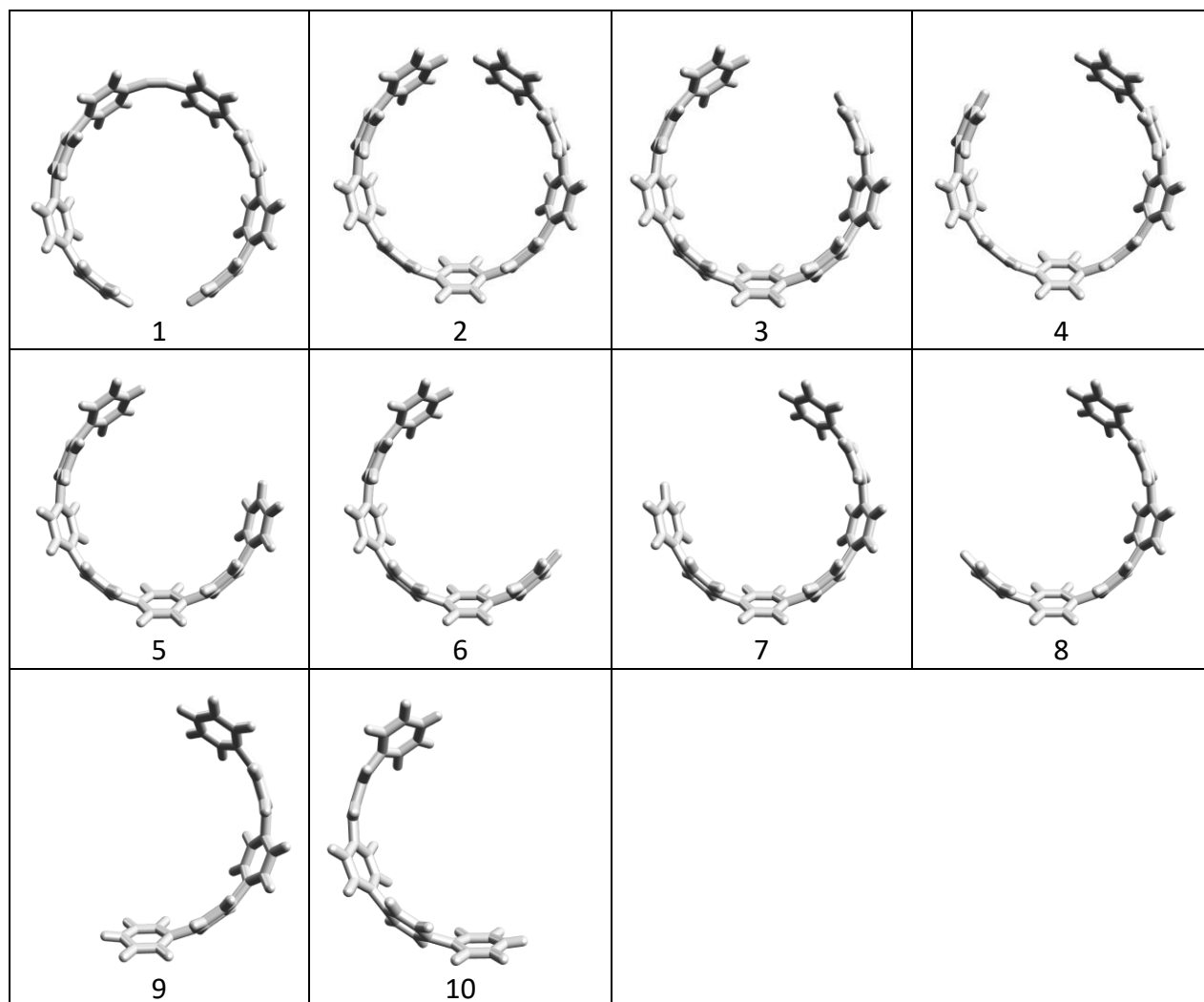

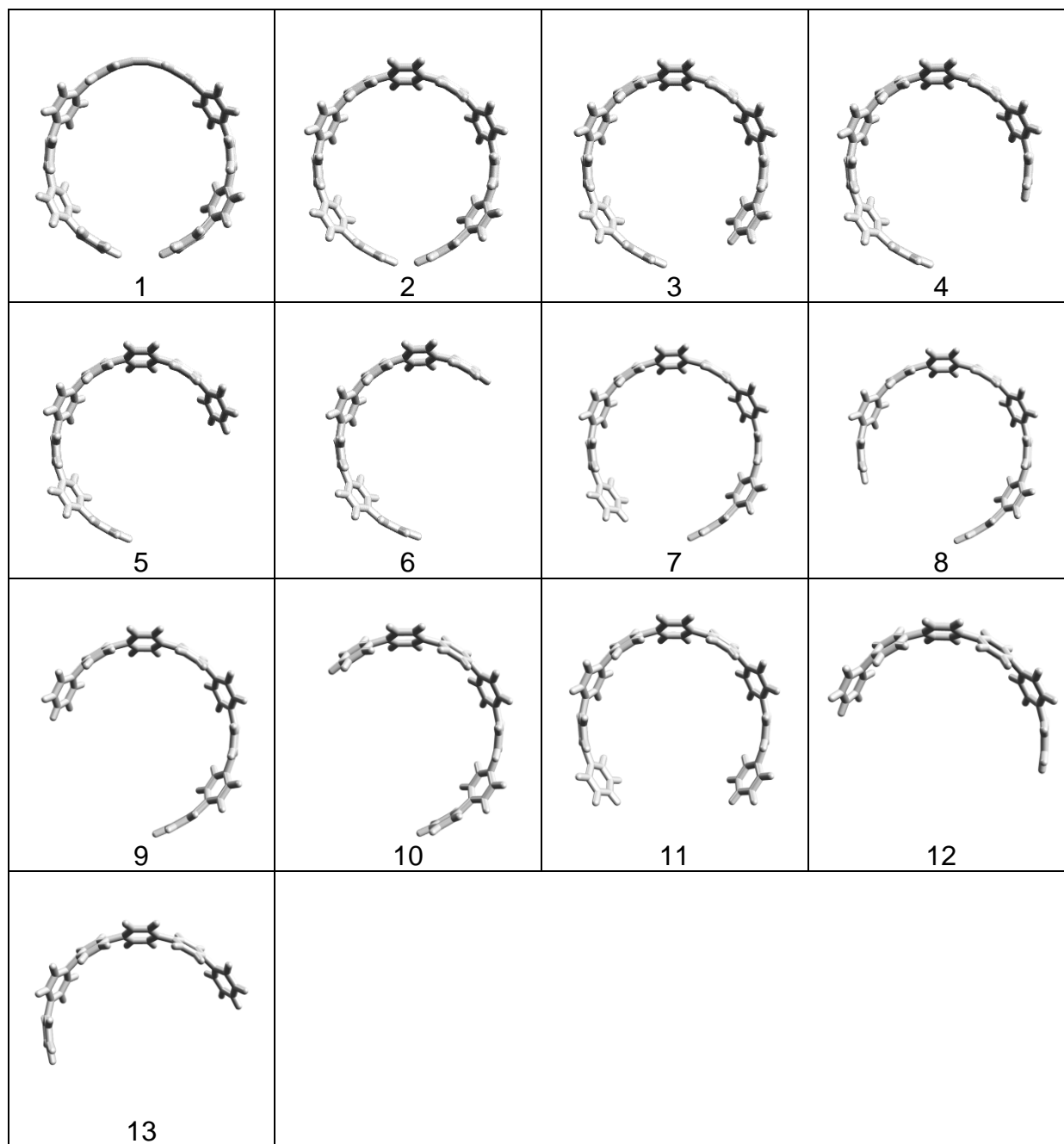**Figure S69**. **[9+1]CPP** molecule fragments used for StrainViz.

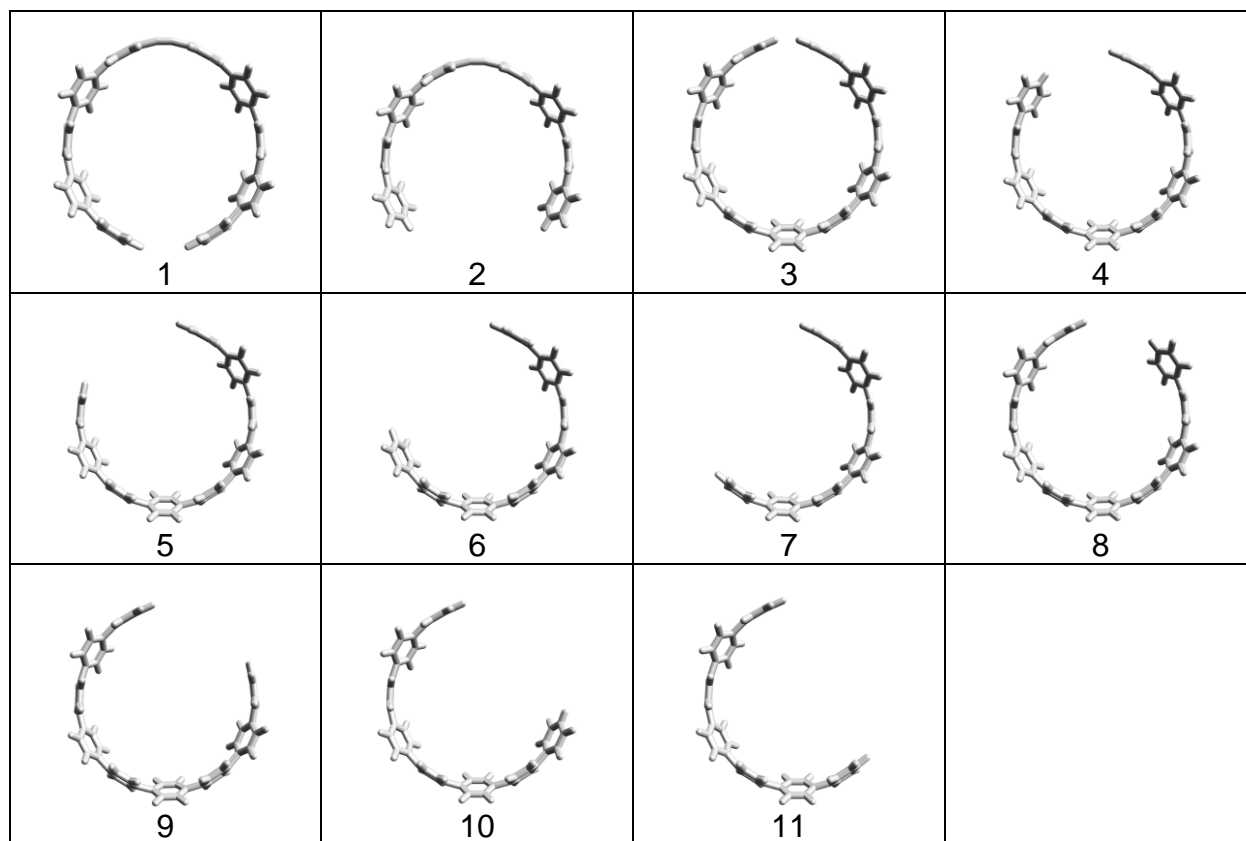**Figure S70**. **[11+1]CPP** molecule fragments used for StrainViz.

Figure S71. **fluor[11+1]CPP** molecule fragments used for StrainViz.
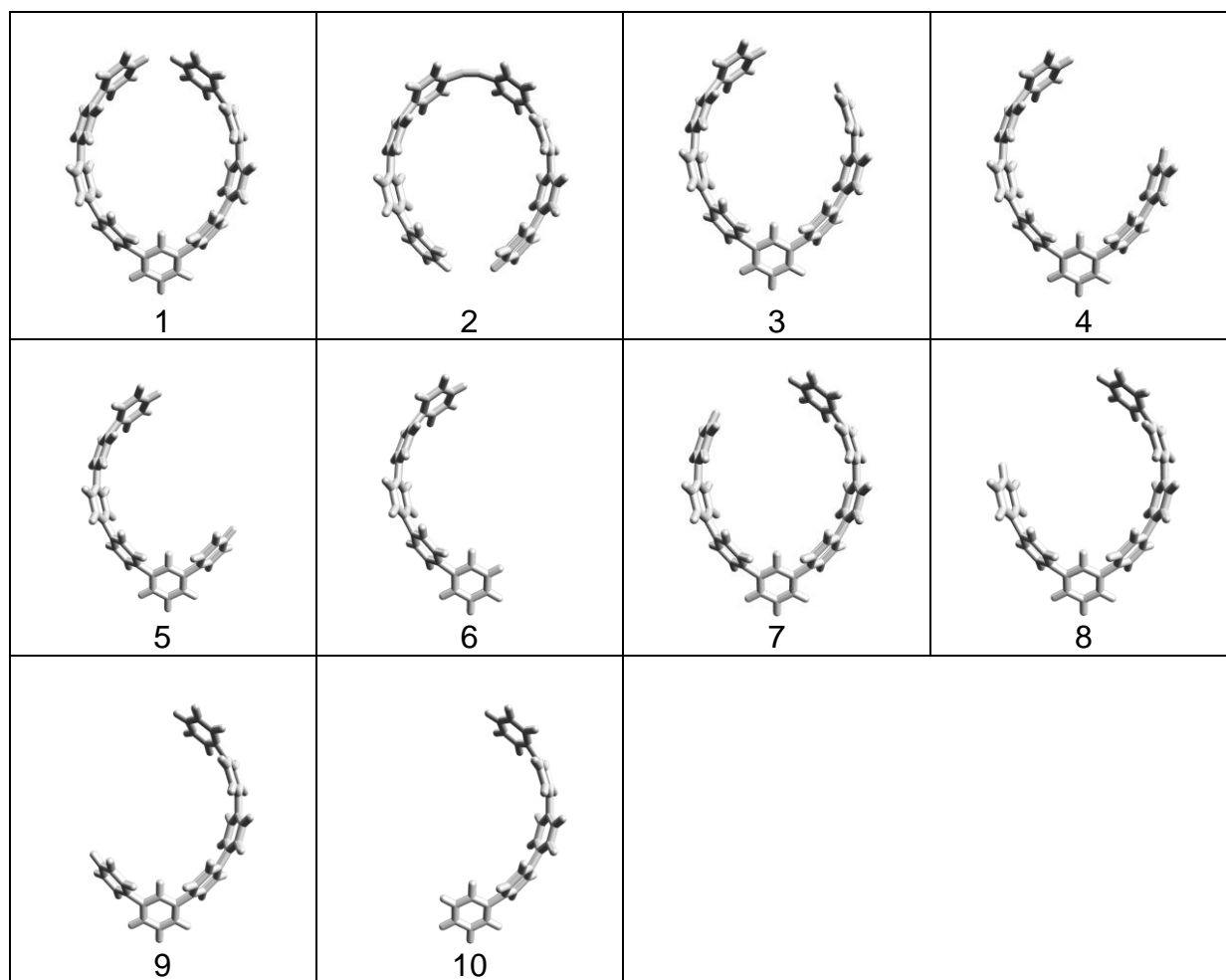
Figure S72. *m*[9+1]CPP molecule fragments used for StrainViz.

7. Transition state and energy calculations

All Gaussian output files for stationary points are available via Figshare with the following link,
https://figshare.com/articles/figure/test/21648506

Table S15: Computed M06-2X/6-31+G(d,p) electronic and free energies, and activation barrier energies for **[11+1]CPP, [9+1]CPP, fluor[11+1]CPP, *m*[9+1]CPP, 13, and 14**, with benzyl azide in DMSO.

	E_{DMSO} (Hartree)	G_{DMSO} (Hartree)	$\Delta G^{\ddagger}_{DMSO}$ (Hartree)	$\Delta G^{\ddagger}_{DMSO}$ (kcal mol^{-1})
Benzyl azide	-434.9815687	-434.884810	---	---
[11+1]CPP	-2616.77369375	-2615.956344	---	---
fluor[11+1]CPP	-3013.60729751	-3012.827492	---	---
[9+1]CPP	-2154.80926912	-2154.142347	---	---
***m*[9+1]CPP**	-2154.82946060	-2154.163188	---	---
13	-2985.63402421	-2984.833285	---	---
14	-2985.63609487	-2984.834431	---	---
[11+1]CPP-TS	-3051.73881391	-3050.800792	0.040362	25.3
[9+1]CPP-TS	-2589.77633131	-2588.988587	0.038273	24.2
fluor[11+1]CPP-TS	-3448.57505364	-3447.674029	0.03857	24.0
***m*[9+1]CPP-TS**	-2589.79813545	-2589.011416	0.036582	23.0
13-TS	-3420.606007	-3419.682297	0.035798	22.5
14-TS	-3420.613547	-3419.687368	0.031873	20.0

Table S16: Computed activation free energies, distortion, and interaction energies for the reactions of **BnAz** with **[11+1]CPP, [9+1]CPP, fluor[11+1]CPP,** and ***m*[9+1]CPP** in DMSO. Energies are in Hartrees.

|	E (TS)	$E_{dist. hoop}$	$E_{dist. azide}$	$E_{int.}$
[11+1]CPP	-3051.73881391	-2616.76428495	-434.957454127	-0.017074833
[9+1]CPP	-2589.77633131	-2154.801036	-434.9586488	-0.016646434
fluor[11+1]CPP	-3448.57505364	-3013.59805123	-434.958366023	-0.018636387
***m*[9+1]CPP**	-2589.79813545	-2154.821985	-434.960042404	-0.016108016
13	-2985.63402421	-2985.62430794	-434.956442407	-0.025256813
14	-3420.613547	-2985.62673930	-434.958292536	-0.028515524
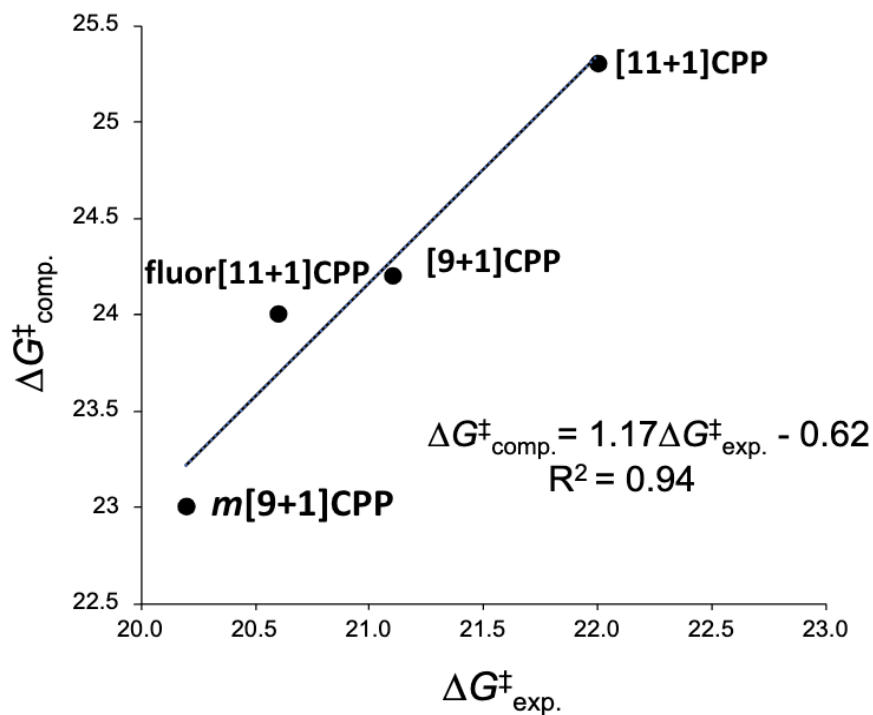
Figure S73. The computed activation free energies for **[11+1]CPP**, **[9+1]CPP**, **fluor[11+1]CPP**, and *m*[9+1]CPP versus the experimentally determined values. The activation free energies were determined in kcal mol^{-1}.
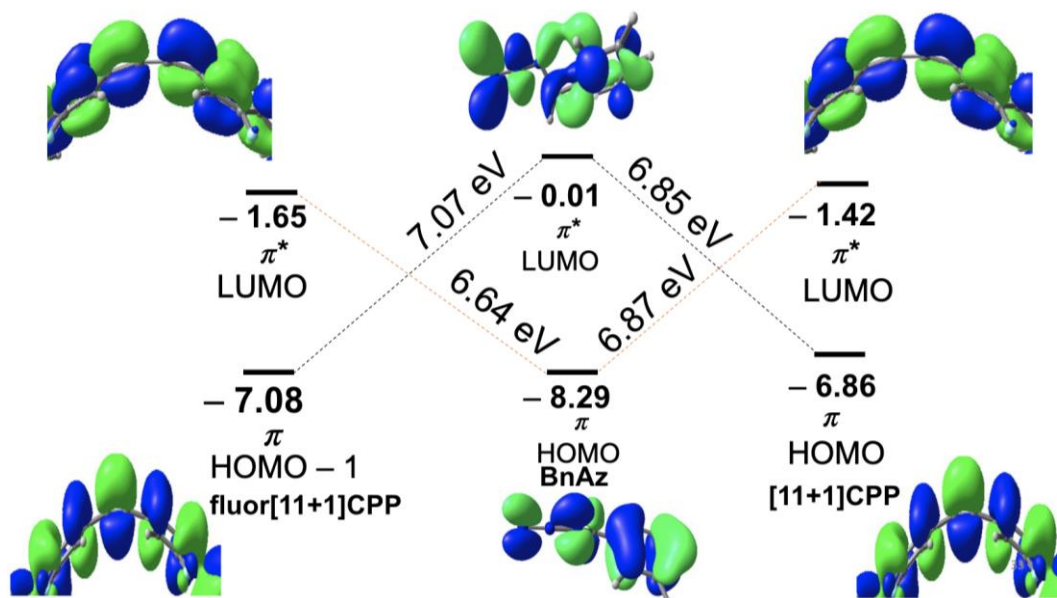

Figure S74. FMO diagram for the cycloaddition of **[11+1]CPP** and **fluor[11+1]CPP** with benzyl azide (**BnAz**) as calculated by M06-2X/6-31+G(d,p) using IEF-PCM: DMSO. Values are reported in eV. The HOMO-LUMO gap energies between the HOMO of **BnAz** and the LUMO of **[11+1]CPP** or **fluor[11+1]CPP** are shown using the dotted orange lines. The black dotted lines are the HOMO-LUMO gap between the HOMO of **[11+1]CPP** or **fluor[11+1]CPP** versus the LUMO of **BnAz**.

References

1   E. P. Jackson, T. J. Sisto, E. R. Darzi, and R. Jasti. *Tetrahedron*, 2016, **72**, 3754–3758.

2   T. A. Schaub, J. T. Margraf, L. Zakharov, K. Reuter, and R. Jasti. *Angew. Chem. Int. Ed.*, 2018, **57**, 16348–16353.

3   N. C. Bruno, M. T. Tudge, and S. L. Buchwald. *Chem. Sci.*, 2013, **4**, 916–920.

4   A. B. Pangborn, M. A. Giardello, R. H. Grubbs, R. K. Rosen, and F. J. Timmers. *Organometallics*, 1996, **15**, 1518–1520.

5   Horiba Scientific: A Guide to Recording Fluorescence Quantum Yields. https://static.horiba.com/fileadmin/Horiba/Application/Materials/Material_Research/Quantum_Dots/quantumyieldstrad.pdf (accessed 2022-10-28).